

INSTITUTO TECNOLÓGICO Y DE ESTUDIOS SUPERIORES DE MONTERREY

**CAMPUS MONTERREY
DIVISIÓN DE BIOTECNOLOGIA Y ALIMENTOS
PROGRAMA DE GRADUADOS EN BIOTECNOLOGIA**



TEC de Monterrey®
DEL SISTEMA TECNOLÓGICO DE MONTERREY

**“ANTI-NEOPLASTIC PROPERTIES OF BLACK BEAN FLAVONOIDS IN
DIFFUSE LARGE B CELL LYMPHOMA”**

TESIS

**PRESENTADA COMO REQUISITO PARCIAL PARA OBTENER EL GRADO
ACADEMICO DE:**

**MAESTRÍA EN CIENCIAS CON
ESPECIALIDAD EN BIOTECNOLOGIA**

POR:

ULISES ALEJANDRO AREGUETA ROBLES

MONTERREY, N.L.

MAYO DE 2011

DEDICATORIA

A mis padres,

María de la Luz Robles Hernández

Álvaro Arequeta Villegas

A mis hermanos,

Génesis Arequeta Robles

Álvaro Tercero Arequeta Robles

*No existen palabras ni
trabajo alguno que
describan el agradecimiento
hacia mi familia. Merecen
más de lo que pudiera
lograr en vida.*

AGRADECIMIENTOS

A mi mamá, por ser siempre motor y razón de mis éxitos y a mi papá por enseñarme a nunca ceder.

A mis hermanos, por su gran amor y apoyo.

A mi Tía Irma por su cariño, apoyo y confianza.

A mi asesor, el Dr. Luis Villela, por las enseñanzas, los consejos, la paciencia y la confianza de poner en mis manos un proyecto tan importante. Por exigir siempre lo mejor de mí. Le estoy muy agradecido Dr.

A mi sinodal, La Dra. Janet Gutiérrez, por su invaluable apoyo y por compartirme su indudable experiencia y conocimiento. Gracias por la paciencia y una disculpa por las innumerables consultas a su oficina.

A mi sinodal, el Dr. Sergio Serna, por el gran apoyo, confianza y todo el respaldo.

Al Dr. Jose Lui Vazquez por entrenarme y por su conocimiento en el manejo de los ratones.

A Oscar Fajardo, amigo y maestro, muchas gracias por instruirme en las técnicas de laboratorio y muchas gracias por toda la ayuda que me prestaste durante toda la maestría.

A mis amigos Enrique, Marco y Victor que me apoyaron y me soportaron en el desarrollo de la tesis. Gracias kike por ser un buen amigo y aguantarme la mitad de la maestría.

A Laura, muchas gracias por estar a mi lado y permitirme estar al tuyo, por el gran apoyo en los tiempos difíciles y por no dejarme caer.

Muchas gracias a Manuel y a José Luis por no olvidarse de su amigo y por seguir apoyándome.

A Bianca, muchas gracias por toda tu ayuda, me facilitaste mucho el trabajo.

A Isabel García, su dedicación a su trabajo permitió que siempre trabajáramos en un laboratorio de calidad.

A todos mis amigos y compañeros de laboratorio que facilitaron el trabajo en un ambiente agradable.

A los ratoncitos que perdieron su vida por el avance de la ciencia y el conocimiento

GENERAL INDEX

INDEX OF FIGURES	8
INDEX OF TABLES	11
1 INTRODUCTION	13
2 BACKGROUND	15
2.1 IMMUNE SYSTEM AND LYMPHOMA	15
2.2 NUTRACEUTICS AND PHENOLIC COMPOUNDS	16
2.2.1 FUNCTIONALITY AND APPLICATIONS	17
2.2.2 SOURCES	18
3 MATERIALS & METHODS	19
3.1 FRACTION OF FLAVONOIDS FROM BLACK BEAN EXTRACT	20
3.2 IDENTIFICATION OF MYRICETIN, QUERCETIN AND KAEMPFEROL	21
3.2.1 HPLC IDENTIFICATION OF GLYCOSILATED FLAVONOIDS	21
3.2.2 HPLC IDENTIFICATION OF AGLYCONES	22
3.3 PURIFICATION OF MYRICETIN, QUERCETIN AND KAEMPFEROL	23
3.4 QUANTIFICATION OF MYRICETIN, QUERCETIN AND KAEMPFEROL ..	24
3.5 PRESERVATION AND GROWING OF CELL LINES FOR BIOASSAYS	27
3.5.1 CELL GROWING MEDIUM PREPARATION	27
3.5.2 CELL FREEZING MEDIUM PREPARATION	27
3.5.3 CELL THAWING	28
3.5.4 VIABLE CELL COUNTING	28
3.5.5 CELL GROWTH MEDIUM CHANGE	29
3.5.6 CELL FREEZZING	29
3.6 CELL GROWTH KINETIC ASSAY	30
3.7 CYTOTOXICITY ASSAYS AND IC ₅₀ DETERMINATION	30
3.7.1 CYTOTOXICITY CONTROL ASSAY	33
3.7.2 IC ₅₀ CALCULATION	34
3.8 CELLULAR APOPTOSIS ASSAY	35
3.9 BAX PROTEIN ASSAY ANALYSIS	37
3.10 CELL CYCLE ASSAY AND DATA ANALYSIS	38
3.10.1 CONTROLS FOR CELL CYCLE ANALISYS	38
3.10.2 CELL CULTURE	39
3.10.3 STAINING PROCEDURE	39
3.11 CHARACTERIZATION OF ANIMAL MODEL	40

3.11.1	MICE HOUSING	40
3.11.2	DEVELOPMENT OF LYMPHOMA ANIMAL MODEL	40
3.12	DETECTION OF FLAVONOIDS IN PELLETS	43
3.13	IDENTIFICATION OF FLAVONOIDS IN MICE PLASMA	43
3.14	ANIMAL MODEL WITH TREATMENT	48
3.14.1	TREATMENTS ADMINISTRATION	48
3.15	STATISTICAL ANALYSIS	50
3.15.1	GOODNESS-OF-FIT STATISTICS	50
3.15.2	CONFIDENCE AND PREDICTION BOUNDS	50
3.15.3	TWO TAILED T-PAIRED TEST	50
3.15.4	LOG RANK TEST	51
4	RESULTS AND DISCUSSION.....	52
4.1	FRACTION OF FLAVONOIDS FROM BLACK BEAN EXTRACT.....	52
4.2	IDENTIFICATION OF MYRICETIN, QUERCETIN AND KAEMPFEROL	52
4.2.1	HPLC IDENTIFICATION OF GLYCOSILATED FLAVONOIDS	52
4.2.2	HPLC IDENTIFICATION OF AGLYCONES.....	54
4.3	PURIFICATION OF MYRICETIN, QUERCETIN AND KAEMPFEROL	55
4.4	QUANTIFICATION OF MYRICETIN, QUERCETIN AND KAEMPFEROL ..	58
4.5	CYTOTOXICITY ASSAYS AND IC ₅₀ DETERMINATION	61
4.5.1	CYTOTOXIC EFFECTS OF BLACK BEAN EXTRACT	61
4.5.2	CYTOTOXIC EFFECTS OF THE FLAVONOID FRACTION	62
4.5.3	CYTOTOXIC EFFECTS OF MYRICETIN, QUERCETIN AND KAEMPFEROL STANDARDS	64
4.5.4	CYTOTOXIC EFFECTS OF PURIFIED GLYCOSYLATED FLAVONOIDS.....	66
4.5.5	CYTOTOXIC EFFECTS OF FLAVONOIDS COMBINATIONS	68
4.6	CELLULAR APOPTOSIS ASSAY	70
4.7	BAX PROTEIN ASSAY ANALYSIS	74
4.8	CELL CYCLE ANALYSIS.....	77
4.9	CHARACTERIZATION OF ANIMAL MODEL.....	80
4.10	DETECTION OF FLAVONOIDS IN PELLETS	83
4.11	DETECTION OF FLAVONOIDS METABOLITES IN PLASMA	84
4.11.1	MASS SPECTROMETRY FLAVONOIDS DETECTION.....	85
4.12	ANIMAL MODEL WITH TREATMENT	87
5	CONCLUSIONS AND RECOMENDATIONS	93

6	REFERENCES	95
A.	APPENDIX A	101
B.	APPENDIX B.....	103
C.	APPENDIX C.....	113
	CELL GROWTH KINETIC ASSAY	113
D.	APPENDIX D	124
E.	APPENDIX E	129
	QUALITY CONTROLS FOR BAX ASSAY	129
	ADDITIONAL RESULTS OF CELL CYCLE ANALYSIS OF OCI-LY7 CELLS	131
	QUALITY CONTROLS FOR CELL CYCLE ANALYSIS.....	134
	CEN AND CTN SAMPLES PREPARATION	134
	DETERMINATION OF RESOLUTION AND LINEARITY	134
	CEN CONTROL	135
	CTN CONTROL	135
	DNA PLOIDY ANALYSIS	136
F.	APPENDIX F	138
	FLAVONOID STANDARDS DETECTION	138
	GLYCOSYLATED FLAVONOIDS DETECTION	140
G.	APPENDIX G	143

INDEX OF FIGURES

FIGURE 3-1 DECISION FLOW CHART OF THE ANALYSIS IN VITRO AND IN VIVO OF BLACK BEAN EXTRACT.	20
FIGURE 3-2 PROCESS TO FRACTION BLACK BEAN EXTRACT INTO FLAVONOIDS, SAPONINS AND PHENOLIC ACIDS.	21
FIGURE 3-3. DIAGRAM OF CYTOTOXICITY ASSAYS PERFORMED WITH BLACK BEAN EXTRACT, FLAVONOID FRACTION AND GLYCOSYLATED FLAVONOIDS.	31
FIGURE 3-4. DIAGRAM OF CYTOTOXICITY ASSAYS PERFORMED WITH FLAVONOID STANDARDS.	32
FIGURE 3-5. ANNEXIN-V AFFINITY WITH PHOSPHATIDILSERINE.	35
FIGURE 3-6. INTRAPERITONEAL INOCULATION.	42
FIGURE 4-1. CHROMATOGRAM OF FLAVONOID FRACTION ANALYZED AT 1 MG/ML AND ABSORPTION SPECTRA OF THE THREE MAIN FLAVONOIDS GLICOSIDES, MYRICETIN 3-O GLUCOSIDE (M), QUERCETIN 3-O GLUCOSIDE (Q) AND KAEMPFEROL 3-O GLUCOSIDE (K), DETECTED AT 365 NM.	53
FIGURE 4-2. CHROMATOGRAM OF HYDROLYZED FLAVONOID FRACTION ANALYZED AT 1.6 MG/ML. THE BLUE CHROMATOGRAM REPRESENTS THE THREE MAIN FLAVONOIDS, MYRICETIN (M), QUERCETIN (Q), KAEMPFEROL (K).	54
FIGURE 4-3. HPLC PURIFICATION OF MYRICETIN – 3 GLUCOSIDE. DETECTION AT 365 NM.	56
FIGURE 4-4. HPLC PURIFICATION OF QUERCETIN – 3 GLUCOSIDE. DETECTION AT 365 NM.	56
FIGURE 4-5. HPLC PURIFICATION OF KAEMPFEROL – 3 GLUCOSIDE. DETECTION AT 365 NM.	57
FIGURE 4-6. CHROMATOGRAMS OF MYRICETIN, QUERCETIN AND KAEMPFEROL STANDARDS FOR CALIBRATION CURVE.	58
FIGURE 4-7 HPLC IDENTIFICATION OF PURIFIED FLAVONOIDS FROM BLACK BEAN EXTRACT.	60
FIGURE 4-8. CHROMATOGRAM AND QUANTIFICATION OF FLAVONOID FRACTION AT 1 MG/ML. THE THREE MAIN GLYCOSYLATED FLAVONOIDS ARE DETECTED, MYRICETIN – 3 GLUCOSIDE (MYR-3-G), QUERCETIN – 3 GLUCOSIDE (QRC-3-G), KAEMPFEROL – 3 GLUCOSIDE (KMP-3-G).	61
FIGURE 4-9. IC ₅₀ COMPARISON OF SU-DHL-4 (ORANGE BAR) AND OCI-LY7 (GREEN BAR) TREATED WITH BLACK BEAN EXTRACT.	62
FIGURE 4-10. IC ₅₀ COMPARISON OF SU-DHL-4 (ORANGE BAR). AND OCI-LY7 (GREEN BAR) TREATED WITH FLAVONOID FRACTION.	63
FIGURE 4-11. IC ₅₀ VALUES COMPARISON BETWEEN SU-DHL-4 (ORANGE BARS) & OCI-LY7 (GREEN BARS) TREATED WITH AGLYCONES, MYRICETIN (M), QUERCETIN (Q), KAEMPFEROL (K). BARS REPRESENT THE ESTIMATED IC ₅₀ . ERRORS ARE GIVEN AS 95% CONFIDENCE INTERVAL.	65
FIGURE 4-12. IC ₅₀ COMPARISON OF OCI-LY7 TREATED WITH AGLYCONES (A) AND GLYCOSYLATED FLAVONOIDS (G). BARS REPRESENT THE ESTIMATED IC ₅₀ . ERRORS ARE GIVEN AS 95% CONFIDENCE INTERVAL.	67
FIGURE 4-13 CONTOUR PLOT OF THE IC ₅₀ VALUES (μM) OBTAINED FROM FLAVONOIDS COMBINATIONS.	68
FIGURE 4-14. APOPTOSIS ASSAY OF OCI-LY7 CELLS TREATED WITH FLAVONOID FRACTION.	70
FIGURE 4-15. APOPTOSIS ASSAY OF OCI-LY7 CELLS TREATED WITH MYRICETIN.	71
FIGURE 4-16. APOPTOSIS ASSAY OF OCI-LY7 CELLS TREATED WITH QUERCETIN.	72
FIGURE 4-17. APOPTOSIS ASSAY OF OCI-LY7 CELLS TREATED WITH KAEMPFEROL.	73
FIGURE 4-18. FLOW CYTOMETRY CONTOUR PLOT ANALYSIS FOR OCI-LY7 WITH TREATMENT OF FLAVONOIDS FRACTION.	74
FIGURE 4-19. BAX PROTEIN MEAN EXPRESSION OF OCI-LY7 CELLS TREATED WITH FLAVONOID FRACTION. ...	75
FIGURE 4-20. BAX PROTEIN EXPRESSION OF SU-DHL-4 CELLS TREATED WITH FLAVONOID FRACTION.	75
FIGURE 4-21. CELL CYCLE ANALYSIS OF OCI-LY7 CELLS TREATED WITH MYRICETIN (B) IN COMPARISON WITH UNTREATED OCI-LY7 CELLS (A).	77
FIGURE 4-22. COMPARISON OF CELL CYCLE PHASES CHANGES IN OCI-LY7 CELL LINE.	78
FIGURE 4-23 . TUMOR GROWTH OF MICE INOCULATED WITH OCI-LY7 CELLS.	80
FIGURE 4-24. PRESENCE OF TUMORS IN MICE INOCULATED WITH OCI-LY7 CELL LINE IN COMPARISON WITH A CONTROL MOUSE WITHOUT INOCULATION.	81
FIGURE 4-25. AVERAGE WEIGHT OF CONTROL MICE (WITHOUT INOCULATION) IN COMPARISON WITH THE INOCULATED MICE, N=8 . ERRORBARS REPRESENT THE STANDARD DEVIATION.	82
FIGURE 4-26 CHROMATOGRAMS OBTAINED AT 365 NM TO SHOW THE PRESENCE OF FLAVONOLES IN PELLETS.	83

FIGURE 4-27. FLAVONOIDS PROFILE IN PLASMA SAMPLES OBTAINED AT 15, 30, 60 AND 90 MIN COMPARED WITH A MOUSE SIMPLE WITHOUT FLAVONOIDS ADMINISTRATION	84
FIGURE 4-28. A. TOF-MS SPECTRUM OF 60 MINUTES MOUSE PLASMA SAMPLE. FLAVONOIDS DETECTED WERE MYRICETIN, KAEMPFEROL AND A FRACTION OF QUERCETIN.....	85
FIGURE 4-29. MOUSE OF PLACEBO GROUP INOCULATED WITH 10^7 OCI-Ly7 CELLS A. ZONE OF PALPABLE TUMOR AT 20 TH DAY. B. TUMOR EVOLUTION 5 DAYS LATER.	87
FIGURE 4-30. BODY WEIGHT INCREASE IN A MOUSE WHICH WAS ONE OF THE FIRST TO PRESENT PALPABLE TUMOR. THIS WAS A MOUSE OF THE PLACEBO GROUP.	88
FIGURE 4-31. . INCREASE OF BODY WEIGHT IN OCI-Ly7 INOCULATED MICE.....	89
FIGURE 4-32. BOX PLOT TO COMPARE THE INCREASE OF BODY WEIGHT SINCE TREATMENT.....	89
FIGURE 4-33. AVERAGE OF CHANGE IN WEIGHT SINCE ADMINISTRATION OF TREATMENTS.....	90
FIGURE 4-34. MEAN OF TUMOR MASS (G) FOR EACH TREATMENT GROUP.	91
FIGURE 4-35. KAPLAN MEYER SURVIVAL CURVES EVALUATED WITH LOG RANK TEST BETWEEN GROUPS.	92
FIGURE B-1. CHROMATOGRAM OF FLAVONOID FRACTION AT 1 MG/ML	103
FIGURE B-2. ABSORPTION SPECTRA OF MYRICETIN-3-GLYCOSIDE PURIFIED FROM BLACK BEAN EXTRACT. .	103
FIGURE B-3. ABSORPTION SPECTRA OF QUERCETIN-3-GLYCOSIDE PURIFIED FROM BLACK BEAN EXTRACT ..	104
FIGURE B-4. ABSORPTION SPECTRA OF KAEMPFEROL-3-GLYCOSIDE PURIFIED FROM BLACK BEAN EXTRACT	104
FIGURE B-5. CHROMATOGRAM OF HYDROLYZED FLAVONOID FRACTION AT 12.408 MG/ML.....	105
FIGURE B-6. ABSORPTION SPECTRA OF MYRICETIN PURIFIED FROM BLACK BEAN EXTRACT	105
FIGURE B-7. ABSORPTION SPECTRA OF QUERCETIN PURIFIED FROM BLACK BEAN EXTRACT	106
FIGURE B-8. ABSORPTION SPECTRA OF KAEMPFEROL PURIFIED FROM BLACK BEAN EXTRACT	106
FIGURE B-9. ABSORPTION SPECTRA OF MYRICETIN STANDARD.....	107
FIGURE B-10. ABSORPTION SPECTRA OF QUERCETIN STANDARD	107
FIGURE B-11. ABSORPTION SPECTRA OF KAEMPFEROL STANDARD	108
FIGURE B-12. CHROMATOGRAM AND QUANTIFICATION OF HYDROLYZED FLAVONOID FRACTION AT 12.408 MG/ML.....	108
FIGURE B-13. CHROMATOGRAM AND QUANTIFICATION OF FLAVONOID FRACTION AT 1 MG/ML	109
FIGURE B-14. CHROMATOGRAM AND QUANTIFICATION OF BLACK BEAN EXTRACT AT 0.3 MG/ML	109
FIGURE B-15. CHROMATOGRAM AND QUANTIFICATION OF HYDROLYZED BLACK BEAN EXTRACT AT 0.3 MG/ML	110
FIGURE B-16. STANDARD CALIBRATION CURVES OF MYRICETIN, QUERCETIN AND KAEMPFEROL (0.1 TO 5PPM)	110
FIGURE B-17. STANDARDS CALIBRATION CURVES OF OF MYRICETIN, QUERCETIN AND KAEMPFEROL (0.1 TO 100PPM).....	111
FIGURE C-1. CELLULAR DENSITY GROWTH OF OCI-Ly7 CELL LINE IN 5 DAYS.....	113
FIGURE C-2. FIRST DERIVATE OF HILL EQUATION FITTED TO THE OCI-Ly7 CELL GROWTH BEHAVIOR.	114
FIGURE C-3. CELLULAR DENSITY GROWTH OF SU-DHL-4 CELL LINE IN 7 DAYS.....	114
FIGURE C-4. FIRST DERIVATE OF HILL EQUATION FITTED TO THE OCI-Ly7 CELL GROWTH BEHAVIOR.	115
FIGURE C-5. CELLULAR VIABILITY OF SU-DHL-4 TREATED WITH BLACK BEAN EXTRACT.	115
FIGURE C-6. CELLULAR VIABILITY OF OCI-Ly7 TREATED WITH BLACK BEAN EXTRACT.	116
FIGURE C-7. CELLULAR VIABILITY OF SU-DHL-4 TREATED WITH FLAVONOID FRACTION.....	116
FIGURE C-8. CELLULAR VIABILITY OF OCI-Ly7 TREATED WITH FLAVONOID FRACTION.....	117
FIGURE C-9. CELLULAR VIABILITY OF OCI-Ly7 AND SU-DHL-4 CELLS TREATED WITH THE SAPONIN FRACTION.	117
FIGURE C-10 CELLULAR VIABILITY OF OCI-Ly7 AND SU-DHL-4 CELLS TREATED WITH THE PHENOLIC ACIDS FRACTION	118
FIGURE C-11. CELLULAR VIABILITY OF OCI-Ly7 TREATED WITH MYRICETIN STANDARD.	118
FIGURE C-12. CELLULAR VIABILITY OF OCI-Ly7 TREATED WITH QUERCETIN STANDARD.....	119
FIGURE C-13. CELLULAR VIABILITY OF OCI-Ly7 TREATED WITH KAEMPFEROL STANDARD.	119
FIGURE C-14. CELLULAR VIABILITY OF SU-DHL-4 TREATED WITH MYRICETIN STANDARD.	120
FIGURE C-15. CELLULAR VIABILITY OF SU-DHL-4 TREATED WITH QUERCETIN STANDARD.....	120
FIGURE C-16. CELLULAR VIABILITY OF SU-DHL-4 TREATED WITH KAEMPFEROL STANDARD.	121
FIGURE C-17. CELLULAR VIABILITY OF OCI-Ly7 TREATED WITH MYRICETIN-3 GLUCOSIDE..	121

FIGURE C-18. CELLULAR VIABILITY OF OCI-LY7 TREATED WITH QUERCETIN-3 GLUCOSIDE.....	122
FIGURE C-19. CELLULAR VIABILITY OF OCI-LY7 TREATED WITH KAEMPFEROL-3 GLUCOSIDE	122
FIGURE C-20. CELLULAR VIABILITY OF NIH3 CELLS TREATED WITH FLAVONOID FRACTION	123
FIGURE C-21. CELLULAR VIABILITY OF VERO CELLS TREATED WITH FLAVONOID FRACTION.....	123
FIGURE D-1. HISTOGRAM OF UNSTAINED CELLS CONTROL FOR APOPTOSIS DETECTION BY FLOW CYTOMETRY.	124
FIGURE D-2. FLOW CYTOMETRY ANALYSIS OF ANNEXIN-V CONTROL FOR APOPTOSIS DETECTION.....	125
FIGURE D-3. . FLOW CYTOMETRY ANALYSIS OF PROPIDIUM IODIDE (PI) CONTROL FOR APOPTOSIS DETECTION.	125
FIGURE D-4. FLOW CYTOMETRY ANALYSIS OF VIABLE CELLS CONTROL FOR THE IDENTIFICATION OF UNTREATED CELLS.....	126
FIGURE E-1. FLOW CYTOMETRY ANALYSIS OF UNSTAINED CELLS CONTROL FOR PROTEIN BAX DETECTION. ..	129
FIGURE E-2. FLOW CYTOMETRY ANALYSIS OF UNTREATED CELLS CONTROL FOR PROTEIN BAX DETECTION. .	130
FIGURE E-3. FLOW CYTOMETRY CONTOUR PLOT ANALYSIS OF CELLS TREATED WITH DOXORUBICIN IN COMPARISON WITH UNTREATED CELLS.	130
FIGURE E-4. CELL CYCLE ANALYSIS TO OCI-LY7 CELLS TREATED WITH FLAVONOID FRACTION	131
FIGURE E-5. CELL CYCLE ANALYSIS TO OCI-LY7 CELLS TREATED WITH QUERCETIN.....	131
FIGURE E-6. CELL CYCLE ANALYSIS TO OCI-LY7 CELLS TREATED WITH KAEMPFEROL	131
FIGURE E-7. CELL CYCLE ANALYSIS TO OCI-LY7 CELLS TREATED WITH DOXORUBICIN	132
FIGURE E-8. CELL CYCLE ANALYSIS TO UNTREATED SU-DHL-4 CELLS	132
FIGURE E-9. CELL CYCLE ANALYSIS TO SU-DHL-4 CELLS TREATED WITH FLAVONOID FRACTION.....	132
FIGURE E-10. CELL CYCLE ANALYSIS TO SU-DHL-4 CELLS TREATED WITH DOXORUBICIN	132
FIGURE E-11. FLOW CYTOMETRY DOT PLOT ANALYSIS OF CTN (CALF THYMOCYTE NUCLEI) STAINED WITH PI (PROPIDIUM IODIDE) DOT PLOT.	135
FIGURE E-12. GRAPHIC PROCEDURE FOR PERIPHERAL BLOOD MONONUCLEAR CELLS ISOLATION.	137
FIGURE F-1 . A. CHROMATOGRAM OF TOTAL IONS AND EXTRACTED IONS OF FLAVONOIDS STANDARDS FOR MASS SPECTRA ANALYSIS.	138
FIGURE F-2. MASS SPECTRA ANALYSIS OF MYRICETIN, QUERCETIN AND KAEMPFEROL STANDARDS.....	139
FIGURE F-3 . CHROMATOGRAM OF TOTAL IONS AND EXTRACTED IONS OF FLAVONOID FRACTION FOR MASS SPECTRA ANALYSIS.	140
FIGURE F-4 . MASS SPECTRA ANALYSIS OF GLYCOSYLATED MYRICETIN, QUERCETIN AND KAEMPFEROL.....	142
FIGURE G-1. COMPARISON OF SPLEEN MASS OF MICE INOCULATED WITH OCI-LY7 (SQUARES), MICE INOCULATED WITH SU-DHL-4 (RHOMBUS) AND MICE NOT INOCULATED (DOTS).	143
FIGURE G-2. COMPARISON OF SLIVER MASS OF MICE INOCULATED WITH OCI-LY7 (SQUARES), MICE INOCULATED WITH SU-DHL-4 (RHOMBUS) AND MICE NOT INOCULATED (DOTS).	143
FIGURE G-3. . COMPARISON OF RIGHT KIDNEY MASS OF MICE INOCULATED WITH OCI-LY7 (SQUARES), MICE INOCULATED WITH SU-DHL-4 (RHOMBUS) AND MICE NOT INOCULATED (DOTS).	144
FIGURE G-4. COMPARISON OF LEFT KIDNEY MASS OF MICE INOCULATED WITH OCI-LY7 (SQUARES), MICE INOCULATED WITH SU-DHL-4 (RHOMBUS) AND MICE NOT INOCULATED (DOTS).	144

INDEX OF TABLES

TABLE 2-1. MAIN NUTRACEUTICS TESTED OR IN PRESENT RESEARCH.	17
TABLE 3-1. HPLC 1200 SERIES PARAMETERS FOR FLAVONOIDS IDENTIFICATION	22
TABLE 3-2 HPLC 1200 SERIES PARAMETERS FOR FLAVONOIDS FRACTION COLLECTION	24
TABLE 3-3 HPLC PARAMETERS FOR FLAVONOIDS AND STANDARDS QUANTIFICATION	25
TABLE 3-4. HPLC CONCENTRATIONS TESTED FOR STANDARD CALIBRATION CURVES.....	26
TABLE 3-5 SAMPLES TESTED FOR FLAVONOID CONTENT CALCULATION.....	26
TABLE 3-6 FLAVONOIDS COMBINATIONS AND CONCENTRATIONS TESTED ON OCI-Ly7.	32
TABLE 3-7 COMPOUNDS AND CONCENTRATIONS TESTED FOR CYTOTOXICITY ON SU-DHL-4 &OCI-Ly7 CELLS.	33
TABLE 3-8 APOPTOSIS ASSAY. TREATMENTS AND CONCENTRATIONS UTILIZED	37
TABLE 3-9 CELL CYCLE ASSAY. COMPOUNDS AND CONCENTRATIONS UTILIZED	39
TABLE 3-10. MICE GROUPS FOR ANIMAL MODEL.....	41
TABLE 3-11. GROUPS FOR IDENTIFICATION OF FLAVONOIDS IN MICE PLASMA	44
TABLE 3-12 HPLC LC/MSD TOF PARAMETERS FOR METABOLITES OF FLAVONOIDS DETECTION	45
TABLE 3-13 GLYCOSYLATED FLAVONOIDS AND STANDARDS MOLECULAR MASS & M/Z RATIO.....	47
TABLE 3-14 EXPERIMENTAL GROUPS FOR ANIMAL MODEL WITH TREATMENT	48
TABLE 4-1. COMPARISON OF RETENTION TIME AND MAXIMUM ABSORPTION WAVELENGTHS OF AGLYCONE FLAVONOIDS IDENTIFIED AND FLAVONOID STANDARDS.....	55
TABLE 4-2. RETENTION TIME AND MAXIMUM ABSORPTION WAVELENGTHS OF PURIFIED GLYCOSYLATED FLAVONOIDS.	55
TABLE 4-3 AMOUNT OF GLYCOSYLATED FLAVONOIDS OBTAINED BY HPLC PURIFICATION.....	57
TABLE 4-4. PROPORTION OF GYCOSYLATED FLAVONOIDS CONTAINED IN THE IC ₅₀ VALUES REPORTED FOR SU- DHL-4 AND OCI-Ly7 CELL LINES TREATED WITH BBE.	62
TABLE 4-5. PROPORTION OF GYCOSYLATED FLAVONOIDS CONTAINED IN THE IC ₅₀ VALUES REPORTED FOR SU- DHL-4 AND OCI-Ly7 CELL LINES TREATED WITH BBE	63
TABLE 4-6 . IC ₅₀ VALUES DETERMINED FOR DIFFERENT CELL LINES TREATED WITH QUERCETIN. TAKEN FROM [28].....	66
TABLE 4-7. IC ₅₀ VALUES OBTAINED IN THE CYTOTOXIC ASSAY WITH FLAVONOIDS COMBINATIONS WITH OCI- Ly7 CELL LINE.....	69
TABLE 4-8. APOPTOSIS ASSAY. REGISTER OF CELL POPULATION UNDERGOING APOPTOSIS AFTER TREATMENT, 24 H OF INCUBATION.	71
TABLE 4-9 CELL CYCLE ANALYSIS. STATISTICAL DIFFERENCE BETWEEN TREATED AND UNTREATED OCI-Ly7 CELLS.....	80
TABLE 4-10. ION FRAGMENTS DETECTED IN MICE PLASMA SAMPLES.....	86
TABLE 4-11. ONE-WAY ANOVA OF DIFFERENCE IN BODY WEIGHT (20 TH DAY TO 29 TH DAY) ACCORDING TO TREATMENTS.	90
TABLE B-1. LINEAR REGRESSION AND GOODNESS OF FIT FOR STANDARDS CALIBRATION CURVES FROM 0.1 TO 5 PPM	111
TABLE B-2. LINEAR REGRESSION AND GOODNESS OF FIT FOR STANDARDS CALIBRATION CURVES FROM 0.1 TO 100 PPM	112
TABLE D-1 APOPTOSIS ASSAY. OCI-Ly7 CELL POPULATIONS UNDER APOPTOSIS AND NECROSIS	127
TABLE D-2 APOPTOSIS ASSAY. SU-DHL-4 CELL POPULATIONS UNDER APOPTOSIS AND NECROSIS	128
TABLE E-1 CELL CYCLE ANALYSIS DATA OF OCI-Ly7 TREATED WITH FLAVONOID FRACTION, MYRICETIN, QUERCETIN & KAEMPFEROL.	133
TABLE E-2 CONDITIONS OF RESOLUTION AND LINEARITY FOR CELL CYCLE ANALYSIS	134

ABBREVIATIONS USED IN TEXT

μL	Microliter
μM	Micromol
BBE	Methanolic extraction of black bean hulls
CTX	Cyclyphosphamide
DAD	Diode array detector
FF	Flavonoid Fraction
g	Gram
HPLC	High pressure liquid chromatography
IC50	50 percent inhibitory concentration
kg	Kilogram
KMP	Kaempferol
L	Liter
MeOH	Methanol
mg	Milligram
mL	Milliliter
MWD	Multiple wavelength detector
MYR	Myricetin
nm	Nanometer
OCI-Ly7	Ontario cancer institute – burkkit's lymphoma patient # 7
ppm	Parts per million
QRC	Quercetin
rpm	Revolutions per minute
SU-DHL-4	Standford university – diffuse histiocytic lymphoma – patient # 4
ug	Microgram

1 INTRODUCTION

In general terms, lymphoma, is the way of designating the set of tumors that develop in the lymphoreticular system, [1].

The most frequent of the lymphomas is the diffuse large B cell lymphoma B (DLBCL), with a frequency of 30 % in the USA, near 50 % in Mexico [2,3].

Some of the drugs that form part of the chemotherapy to treat the DLBCL come from natural sources as plants i.e. alkaloids of the vinca or from microorganisms like the *estreptomyces peucetyus* where Doxorubicine is obtained. Doxorubicin is an anthracycline and its effect is a direct damage in the DNA helix without possibilities of restoring, Doxorubicin is considered as cornerstone in treatment of lymphoma patients [4]. The chemotherapy without anthracyclines has obtained poor results in the survival [5]. Thus, it is necessary to look for new options that could increase the rates of response and the survival of the patients besides doxorubicin. There are several compounds in plants and fruits of our flora, which have the property of being anticancerous such as flavonoids.

Flavonoids are a series of secondary metabolites of plants with antimicrobial, antiinflammatory, anticancerous properties and effects in the immunological system [6]. They are synthesized from a molecule of fenilalanine and 3 of malonil coenzyme A, from what is known as the route of the flavonoids; whose products are cycled across the isomerase enzyme [6]. The actions of the flavonoids, as mentioned previously, produce different effects; but one of the most important is the antineoplastic, having action against colon cancer, hepatic carcinoma and breast cancer [7-9].

The black bean (*phaseolus vulgaris*) is one legume seed that forms an essential part of the Mexican diet. It is a rich source of phytochemicals and one of the richest sources of flavonoids as well as other compounds such as saponins that have an important activity against neoplastic cells as it was been tested in previous works [10,11] .

The published literature talking about cytotoxic action for flavonoids is wide in lines of solid tumor cell lines [7-9]. In our institution, has been evaluated cytotoxicity action of flavonoids obtained from black bean. Those assays have been performed in breast cancer where its inhibition was observed. Other bioassays have been tested also in colon cancer, and hepatic cancer, [10].

There is no research work or literature published in our knowledge documenting the effects of black bean extract as a potential agent against b cell lymphoma, therefore we studied and evaluated the effect of the black bean extract in vitro with SU-DHL-4 and OCI-Ly7 cell lines and immunosuppressed murine model.

The main goal was to establish the anti-neoplastic effect of the methanolic extract of hulls of black bean in vitro and in vivo using human B cell lymphoma.

Particular objectives were the following:

To determine the cytotoxic and pro-apoptotic capacity of the methanolic extract of hulls of black bean in SU-DHL-4 and OCI-Ly7 cell lines.

- To assess in which step of cell cycle the black bean extract induce arrest.
- To set up and characterize a lymphoma animal model.
 - To evaluate the anti-neoplastic capacity of the black bean extract as a treatment for lymphoma animal model

2 BACKGROUND

2.1 IMMUNE SYSTEM AND LYMPHOMA

The immune system is characterized by a group of cells which protects the host against infections. Two fundamental different types of responses are the mechanism of this protection. The natural response (innate) protects against a wide range of pathogen agents such as virus or intestinal parasites. The second one is the adaptive response which is engineered to improve on repeated exposure to a given infection.

The innate responses take action by neutrophils, monocytes, and macrophages which are named phagocytic cells. A second group of cells that releases cytokines i.e. basophils, mast cells or eosinophils.

There are specialized cells, called antigen-presenting cells, which exhibit the antigen to lymphocytes and collaborate with them in the response against the antigen. In order to eliminate extracellular microorganisms, B cells secrete immunoglobulins, which are antigen-specific antibodies. T cells help B cells to make antibodies and annihilate intracellular pathogens by activating macrophages and by killing virally infected cells.

The lymph nodes, spleen, and mucosa-associated lymphoid tissue are the structures in which adaptive immune response is activated. B cells relies on an impressive morphologic feature, it is the germinal mucosa center where B cell responses happen within a meshwork of follicular dendritic cells [12].

Mucosal surfaces are defended by mucosa-associated lymphoid tissues such as tonsils, adenoids, and Peyer's patches, [12].

The term "Lymphoma" stands for the set of tumors developed into the lymphatic system. There are also known as solid hematologic tumors in order to differentiate them from Leukemia. The WHO classifies the lymphoma in two types according to its cellular origin,

the most frequent known lymphoma is Non-Hodgkin Lymphoma (NHL), where B cell lymphoma is predominant and represents more than 90% of the cases [3].

NHL has several forms of manifestation in the patient, so in a practical classification and in order to facilitate their approach they are divided in two groups, aggressive and indolent. Aggressive lymphoma grows and spread quickly, resulting in special symptoms and a remarkably deterioration of patient health. The most common of this type of cancer is the Diffuse large B Cell Lymphoma (up to 80% of the cases).

NHL may appear at any age, with a higher incidence at reproductive ages in México, being 90% of the cases in patients between 40 and 60 years old [3].

2.2 NUTRACEUTICS AND PHENOLIC COMPOUNDS

The nutraceutic term was introduced in 1989 by Stephen DeFelice and comes from the combination of two words “nutrition” and “pharmaceutical”. Nutraceutic may be defined as a food or part of a food which provide health benefits [13]. In many occasions this functional food comes from organic products, supplements, enriched products or food that has been genetically modified.

It has been stated that a nutraceutic is not precisely a supplement in diet because it does not contain only vitamins and minerals in order to be considered a supplement, but it helps to prevent or treat diseases as well. Besides, nutraceutics may be employed as conventional foods.

The nutraceutic industry shows an annual increase rate between 7 to 10%, whereas the conventional food industry just 3%, the large difference has come into the attention of many different economy sectors.

In the last years many companies have bet their investments in nutraceutic research, looking for therapeutic substitutes with the capability to compete with common medicines, taking in advantage that nutraceutics may have fewer side effects. Several pharmaceutical and biotechnologic companies have turned their efforts and resources to study those agents, The table 2-1 (taken from [48]) shows the main nutraceutics tested or in present research to probe its effectiveness in the prevention and treatment of diseases.

Table 2-1. Main nutraceuticals tested or in present research.

Nutraceutical	Disease/Condition	Tested (y). In process (p)
Soy Protein (genistein)	Coronary diseases (diminish LDL)	y
Esterols/Estanol	Coronary diseases (diminish LDL)	y
Omega-3 oil	Coronary diseases	y
Beta-glucans	Coronary diseases	p
cranberries	Urinary infections	y
Hoodia gordonii	Body weight reduction (action at hypothalamus level)	p
Soy Isoflavones	Breast cancer, prostate cancer and bone cancer	y
Phytoestrogens	PMS	y
Phytoestrogens	Bone metabolism	p
Black cohosh	serotonine Modulation (menopause)	p
Red clover	Hormonal actions	y
Poliphenols	Cancer	p
Isothyocianate	Cancer	p
Lycopene	Cancer	p
Green tea	Cancer	p
Luteine	Cancer	p

Flavonoids are the relatively most important group of the phenolic compounds. These are classified in many groups, among the most distinguished are: Isoflavonoids (divided in glycosides and aglycones). The five most studied are: genistein, daidzein, coumestrol, formononetin and biochanin A, anthocyanins, flavones and flavonols.

2.2.1 FUNCTIONALITY AND APPLICATIONS

It has been demonstrated punctually that these phenolic compounds are secondary metabolites that perform a resistance role in plants against microorganisms.

However, the main research efforts concerning these compounds have been directed to its benefic effects in diverse human pathologies. Among the great variety of studies performed, it has been possible to establish, at least *in vitro* studies.

Anti-inflammatory and antioxidant effects: These compounds are considered oxidative stress inhibitors (related in ischemic damage, cancer, fibrosis, etc.) by inhibiting pro-

oxidant enzymes, stimulating anti-oxidant enzymes (Superoxide Dismutase) and increasing antioxidant proteins such as Glutathione [47].

It has been established that these compounds also help in reducing serum cholesterol [45], which is a risk factor to develop a cardiovascular or cerebral ischemic events, by inhibiting hydroxymethyl CoA reductase (HMGCoA reductase). This enzyme is considered the principal step in hepatic cholesterol synthesis from the mevalonate route [46].

Specifically, flavonols and anthocyanines have been labeled as preventive in coronary diseases and thrombotic events by a direct effect in the foam cells involved in the atheromatous plaque formation.

Tannins have been proposed as anti-nutritional agents because when bound to diverse compounds. They can inhibit intestinal absorption of many molecules. It has also been determined that these compounds, by its potent antioxidant effect can reduce LDL oxidation (first step in a atheromatous plaque formation), hemorrhoid apparition (by its antineovascular effect) and ageing.

2.2.2 SOURCES

Phenolic compounds can be found in a great variety of fruits (grapes, cranberries, blueberries) and vegetables. Legume plants (soy, bean, broad beans, lentil, etc) contain great quantities of phenolic compounds, especially isoflavonoids. Green tea and red wine are also important sources of these compounds (in the case of red wine especially tannins are found).

Despite all the functionalities described above, there is evidence that once ingested, flavonoids suffer a bioconversion during hepatic metabolism (methylation, glucuronidation, sulphation, colonic flora degradation), so further studies are required in order to determine the actual bioavailability of these phenolic compounds.

3 MATERIALS & METHODS

The experiments reported in this thesis are grouped in two phases. In Figure 3-1 both phases are detailed as a flow chart of the strategy followed to achieve the main objective of this thesis.

First, in phase I, flavonoids were purified from black bean extract. Then Black bean extract and all the fractions and flavonoids obtained were evaluated by cytotoxicity assays. If cytotoxicity was confirmed by the identification of the IC_{50} then that treatment was evaluated by apoptosis assay. Moreover, if the treatment led cells to a apoptosis, both bax protein assay and a cell cycle assay were performed to enhance the apoptosis detection. On phase II, lymphoma animal model was characterized. Then experiments to detect flavonoids in mice plasma and in the mice food (pellets) were performed in order to approve the black bean extract as a candidate for oral treatment by means of the pellets.

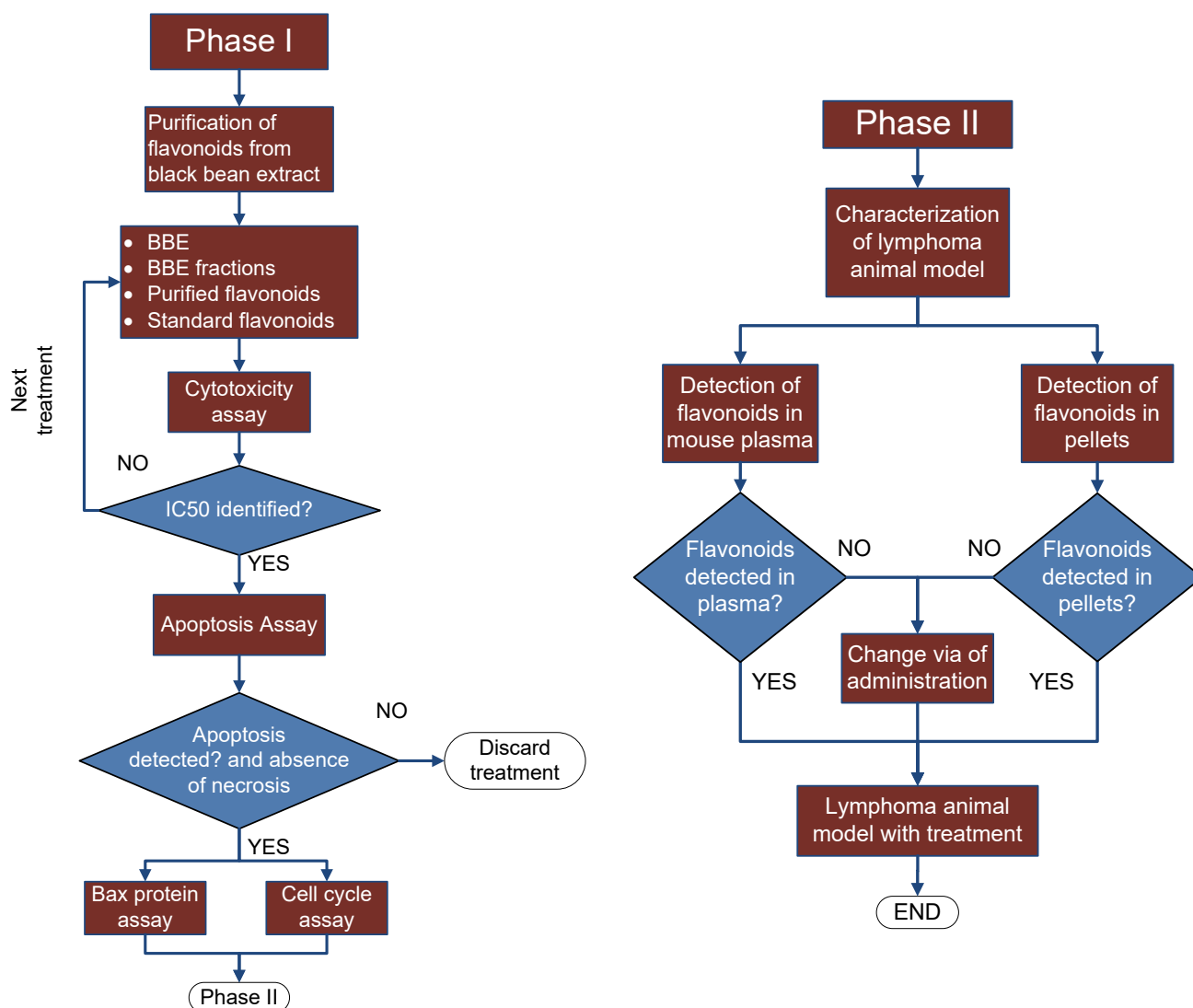


Figure 3-1 Decision flow chart of the analysis in vitro and in vivo of black bean extract.

3.1 FRACTION OF FLAVONOIDS FROM BLACK BEAN EXTRACT

In order to separate flavonoid fraction from BBE, 2 g of lyophilized BBE were diluted in 20 mL of Methanol (Universal Grade high purity solvent, CAS 67-56-1). The mixture was agitated by sonication using an ultrasonic cleaner (Bransonic, Connecticut, USA, SN: RPA060607115E) for 5 minutes and 20 mL of distilled water were added and also agitated by sonication for 5 additional minutes. Then the insoluble phase was separated by centrifugation at 3000 rpm for 5 minutes and supernatant was recovered. This procedure was repeated two more times for the remaining pellet. A C₁₈ – 5g (Waters, Sep-Pak® Vac

20cc, Milford MA, USA) cartridge was equilibrated letting through 10 mL of MeOH and then 10 mL of tri-distilled water. 10 mL of supernatant recovered were passed through the cartridge, which was washed out with 10 mL of 25% MeOH. Finally the flavonoid fraction was eluted with 10 mL of 60% MeOH and then the cartridge was washed with 10 mL of 100% MeOH. The flavonoid fraction solution as well as the other fractions recovered were concentrated by rotatory evaporation and then dried by lyophilization. The separation process is detailed in figure 3-2.

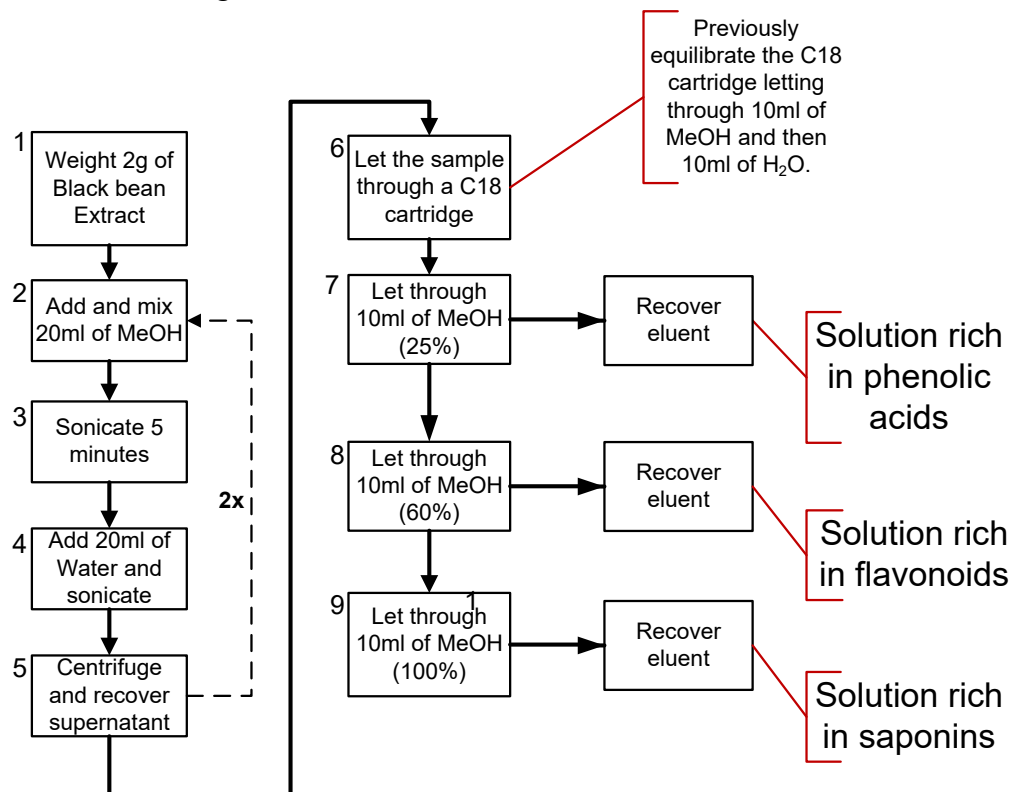


Figure 3-2 Process to fraction black bean extract into flavonoids, saponins and phenolic acids.

3.2 IDENTIFICATION OF MYRICETIN, QUERCETIN AND KAEMPFEROL

3.2.1 HPLC IDENTIFICATION OF GLYCOSILATED FLAVONOIDS

The flavonoid fraction was analyzed by HPLC with diode array detector Agilent Series 1200, (Agilent Technologies, Waldbrunn Germany) modules and serial numbers are listed on appendix A). This procedure was performed according to the method described by [10] which is detailed in Table 3-1. The solvents employed were HPLC grade water (Tedia

Company, OH, USA, Part No. WS2211-001, CAS: 7732-18.5) and Methanol for liquid chromatography (LiChrosolv, Merck, Darmstadt, Germany, Part. No. JB017818). The HPLC was equipped with a Zorbax SB-C18 (Agilent, USA, Part No. 861954-302, Serial: USDD001295) with dimensions of 3 x 100 mm, 3.5 μ m of diameter. 2 μ L of the flavonoid fraction was injected at a concentration of 1 mg/mL.

Table 3-1. HPLC 1200 Series parameters for flavonoids identification

Device	Parameter	Value	
Pump	Flow Rate	0.4 mL/min	
	Channel A (H ₂ O+ Formic	60%	
	Channel B(MeOH)	40%	
	Solvent Gradient	T	%B
		0	40
		15	60
		20	60
		25	90
Column Thermostat	Column Temperature	25 °C	
Detector	Wavelength	360/16 nm	
Fraction Collector	Fraction Trigger Mode	off	

3.2.2 HPLC IDENTIFICATION OF AGLYCONES

The flavonoid fraction was hydrolyzed in order to identify the aglycone compounds myricetin, quercetin and kaempferol. The hydrolysis procedure was performed as follows; 1.6 mL of the flavonoid fraction at 1 mg/mL was mixed with 0.4 mL of HCl. The concentration of the 0.4 mL of HCl was 6 M. so the final concentration of this mixture was 1.2 M. This mixture was heated up to 85 °C for 20 minutes. Then a C18-E Strata cartridge (Phenomenex, Torrance, CA, USA) was equilibrated letting through 1 mL of MeOH and then 1 mL of tri-distilled water. After the 20 minutes period, the complete mixture of flavonoid fraction with HCl was filtered through the equilibrated cartridge, which was

washed out with 1 mL of 25% MeOH. The eluent was dismissed and the hydrolyzed flavonoid fraction was recovered with 1 mL of 100% MeOH.

3.3 PURIFICATION OF MYRICETIN, QUERCETIN AND KAEMPFEROL GLYCOSIDES

Flavonoid compounds, myricetin-3-glycoside, quercetin-3-glycoside and kaempferol-3-glycoside were purified out of flavonoid fraction by means of HPLC with DAD and Fraction Collector module, (Agilent Series 1200, Agilent Technologies, Waldbrunn Germany, modules and serial numbers are listed on appendix A). The method is detailed in Table 3-3. The HPLC column utilized was Zorbax SB-C18 with dimensions of 9.4 x 250 mm, diameter of 5 μ m an injection volume of 50 μ L with a flow of 1.5 mL/min.

Table 3-2 HPLC 1200 Series parameters for flavonoids fraction collection

Device	Parameter	Value		
Pump	Flow Rate	1.5 mL/min		
	Channel A (H ₂ O)	60%		
	Channel B(MeOH)	40%		
	Solvent Gradient	t	%B	
		0	40	
		15	60	
		20	60	
		25	90	
Column Thermostat	Column Temperature	25 °C		
Detector	Wavelength (DAD/MWD)	360/16 nm		
	Spectrum	200-600 nm		
Fraction Collector	Fraction Trigger Mode	Time-based		
	Time Table	Trigger mode	Start (min)	End (min)
		Time-based	15	17
		Off	17	--
		Time-based	17.5	19.5
		Off	19.5	--
		Time-based	19.6	22.6
		Off	22.6	--

3.4 QUANTIFICATION OF MYRICETIN, QUERCETIN AND KAEMPFEROL

In order to determine the concentration of these compounds in the flavonoid fraction purified from of BBE, myricetin, quercetin and kaempferol standards were identified with the HPLC method depicted in table 3-4.

Table 3-3 HPLC parameters for flavonoids and standards quantification

Device	Parameter	Value	
Pump	Flow Rate	0.4 mL/min	
	Channel A (H ₂ O+ Formic Acid 0.1%)	60%	
	Channel B(MeOH)	40%	
	Solvent Gradient	t	%B
		0	40
		15	60
		20	60
		25	90
Column Thermostat	Column Temperature	25 °C	
Detector	Wavelength	360/16 nm	
Fraction Collector	Fraction Trigger Mode	off	

We used semi-preparative HPLC (Hewlett Packard series 1100, Palo Alto CA, USA) and the same column utilized for flavonoid identification to run standards and flavonoid fractions. The following samples were tested.

Myricetin, quercetin and kaempferol standards from Sigma Chemical Co. (Saint Louis, MO, USA) were analyzed by triplicate from 0.1 ppm to 100 ppm as it is detailed in Table 3-5, two calibration curves were calculated however, the first calibration curve embraces concentrations from 0.1 ppm to 5 ppm and the second one from 0.1 ppm to 100 ppm. It was proceeded this way to ensure accuracy in the estimation of small amounts.

Table 3-4. HPLC Concentrations tested for standard calibration curves

Sample	Concentrations tested (ppm)
Myricetin standard	0.1, 1, 5, 10, 50 & 100
Quercetin standard	0.1, 1, 5, 10, 50 & 100
Kaempferol standard	0.1, 1, 5, 10, 50 & 100

Calibration curves were calculated by means of linear regression with the concentrations as the independent variable and the area under curve as the dependent variable. Parameters of goodness of fit were SSE, R-square, adjusted R-square, RMSE. Also 95% confidence bounds were plotted to show the possible range of error in the estimation of new observations. Calculations are detailed in the Statistical Analysis section.

Once linear regressions were calculated we were able to find out an estimate of the concentration of each flavonoid in the following samples:

Table 3-5 Samples tested for flavonoid content calculation

Sample	Concentration
Myricetin purified from BBE	2.752 mg/mL
Quercetin purified from BBE	2.688 mg/mL
Kaempferol purified from BBE	2.368 mg/mL
Glycosylated Flavonoid Fraction	1 mg/mL
Hydrolyzed Flavonoid Fraction	12.408 mg/mL
Black Bean Extract	0.3 mg/mL

The milligrams mentioned in table 3-5 are based on the weight of each dry sample.

3.5 PRESERVATION AND GROWING OF CELL LINES FOR BIOASSAYS

SU-DHL-4 and OCI-Ly7 cell lines were kindly donated by University of Columbia, (NY, USA).

SU-DHL-4 stands for Stanford University – Diffuse Histiocytic Lymphoma – Patient # 4. The cell type of SU-DHL-4 is classified as human B cell lymphoma transformed into indolent lymphoma.

OCI-Ly7 stands for Ontario Cancer Institute – Lymphoma patient # 4. The cell type of OCI-Ly7 is classified as a Burkitt's lymphoma

Both cell lines aggressive lymphomas (DLBCL).

3.5.1 CELL GROWING MEDIUM PREPARATION

The medium used for SU-DHL-4 and OCI-Ly7 cell growth was Iscove's Modified Dulbecco's Medium (IMDM) (GIBCO, NY, USA) which is a highly enriched synthetic media for mammalian cells for rapidly proliferating, high-density cell cultures, with 10% of fetal bovine serum (FBS) (GIBCO, Invitrogen corp., California, USA).

For 1 L of growing medium preparation, 1 package (17.7 g) of IMDM was slowly dissolved in 950 mL distilled water (5% less of total volume) with 3.024 g of NaHCO₃ (Research Organics, Cleveland, USA), pH of 7.2, 100 mL of FBS(10% of total volume) was added to the solution and immediately filtered by vacuum at -70 kPa using a 0.22 µm corning filter (corning, NY, USA) system growing medium was kept at 4 °C.

3.5.2 CELL FREEZING MEDIUM PREPARATION

For 1 L of freezing medium preparation, 1 package (17.7 g) of IMDM was slowly dissolved in 950 mL of distilled water (5% less of total volume) with 3.024 g of NaHCO₃ (Research Organics, Cleveland, USA), and 100 mL of dimethyl sulfoxide (DMSO, Hybri-Max, Sigma-Aldrich, USA), 200 mL of FBS(10% of total volume) was added to the solution and immediately filtered by vacuum at -70 kPa using a 0.22 µm corning filter (corning, NY, USA), freezing medium was kept at -20 °C.

3.5.3 CELL THAWING

Cryopreserved cells are kept in Corning cryogenic vials (Corning, NY, USA). The most recent registered tube was thawed quickly, putting it under 37 °C water bath and immediately diluted into 10 mL of cell growing medium (gently mixed using sterile pipette) in a 15 mL centrifuge tubes (Corning, Massachusetts, USA). Cells were pelleted by centrifugation at 1000 rpm for 5 minutes in a Beckman centrifuge (GS-15R, Serial: GYB94B44) and the medium was slowly removed from above. Cells were gently mixed in 5 mL of cell growing medium, already warmed up at 37°C and passed into a sterile 125 mL Erlenmeyer Flask, baffled with ventilated cap (Corning, COSTAR, MA, USA), 15 mL more of cell growing medium were added to get a final volume of 20 mL. 200 µL of antibiotic/antimycotic solution (1% of total volume) were added, (GIBCO, Invitrogen corp., California, USA, Exp. Date: Aug-27-2012). Cells were kept into a CO₂ incubator (Fisher 1168751H, Pittsburg, PA) regulated at 37 °C, 5% of CO₂ and 80% moisture. Cell count was performed to determine viability.

3.5.4 VIABLE CELL COUNTING

10 µL of Trypan Blue reagent (stain 0.4%, 0.85% saline, GIBCO NY) was added to 10 µL of cells in suspension in 1:1 rate in a micro-centrifuge tube (Corning, NY) and using sterile pipettes, cell samples were always taken from a previous 1 mL aliquot taken from the cell culture flask, always taken from the center of the solution after a gentle shake of the flask. The reagent was allowed to stain for 5 – 15 minutes. 10 µL of the mixed solution was placed in both hemocytometer chambers making sure that the entire surface of the rectangular grid was covered. 5 out of 9 sub-squares were counted using 10x objective lens, cells on the center were counted, cells on the border outline were not counted. Stained cells (non-viable cells) and not stained cells (viable cells) were counted and cellular concentration was calculated as follows:

$$\frac{\# \text{ of cells}}{\text{ml of suspension}} = \frac{\frac{\sum \text{Cells}_1}{5} + \frac{\sum \text{cells}_2}{5}}{2} * \frac{10000}{df} \quad (\text{Eq. 1})$$

$$df = \frac{\text{volume of cells in suspension}}{\text{volume of cells in suspension} + \text{volume of Trypan Blue}} \quad (\text{Eq. 2})$$

df stands for dilution factor. Mean viability was calculated as the rate of viable cells over total of cells.

3.5.5 CELL GROWTH MEDIUM CHANGE

To change the cell growth medium cells in suspension were passed from the Erlenmeyer flask to a 50 mL corning tube (Corning, NY, USA) and pelleted in a Beckman centrifuge (GS-15R, Serial: GYB94B44) at 1000 rpm for 5 minutes, then medium was gently removed from above. Cells were gently mixed in 5 mL of cell growing medium, already warmed up at 37°C and passed into a sterile 125 mL Erlenmeyer Flask adding 15 mL more of cell growing medium were added to get a final volume of 20 mL plus 200 µL of antibiotic/antimycotic solution (1% of total volume). Whenever cell lines were undergoing several procedures cell growth medium change was performed every three days and the number of medium pass was recorded in the flask otherwise cells were frozen.

3.5.6 CELL FREEZING

For cell freezing, cell viability was determined to check if they were in late log phase, in order to determine this, a kinetic growth analysis was performed (this experiment is detailed in next method). Cells in suspension were passed from the Erlenmeyer flask to a 50 mL corning tube (Corning, NY, USA) and pelleted in a Beckman centrifuge (GS-15R, Serial: GYB94B44) at 1000 rpm for 5 minutes, then medium was gently removed from above. Cells were diluted with cell freezing medium fixing cell density at 1×10^7 cells/mL then cryogenic storage vials were filled up to 1.8 mL. Data as date, number of cell growth medium pass, number of vial and operator was labeled over the cryogenic vials. Right away vials were taken into a -20 °C freezer for 30 minutes and then passed into a -80°C freezer.

3.6 CELL GROWTH KINETIC ASSAY

The aim of this assay was to determine the period in which SU-DHL-4 and OCI-Ly7 cells remains in log phase due to it is indicated in the cell titer blue assay manufacturer's instructions as a condition for the reagent to work. 20 mL of cells in suspension (both SU-DHL-4 and OCI-Ly7 lines) were set to grow with three different cell densities. Several cell counts were performed by means of neubauer hemocytometer. These results are included in appendix C.

3.7 CYTOTOXICITY ASSAYS AND IC50 DETERMINATION

The Figure 3-2 describes the steps in which we proceeded to determine whether or not the black bean extract was toxic to SU-DHL-4 and OCI-Ly7 cell lines. Since black bean extract was fractionated into phenolic acids fraction, flavonoids fraction and saponins fraction, these fractions were tested individually in order to identify which one of them was the most cytotoxic. As it is described in Figure 3-2 the flavonoid fraction was the one with the highest cytotoxicity. Then glycosylated flavonoids were tested after purification by HPLC. The flavonoid standards myricetin, quercetin and kaempferol were tested too as it is detailed in Figure 3-3.

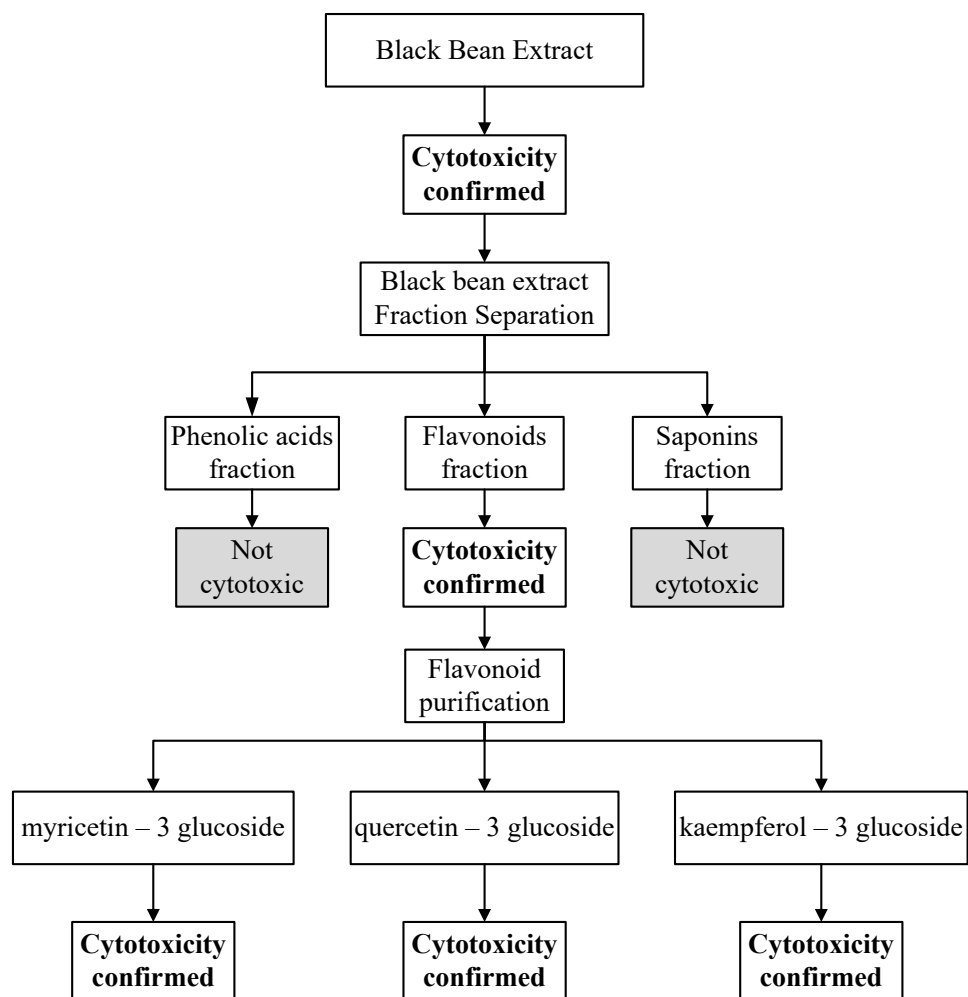


Figure 3-3. Diagram of cytotoxicity assays performed with black bean extract, flavonoid fraction and glycosylated flavonoids.

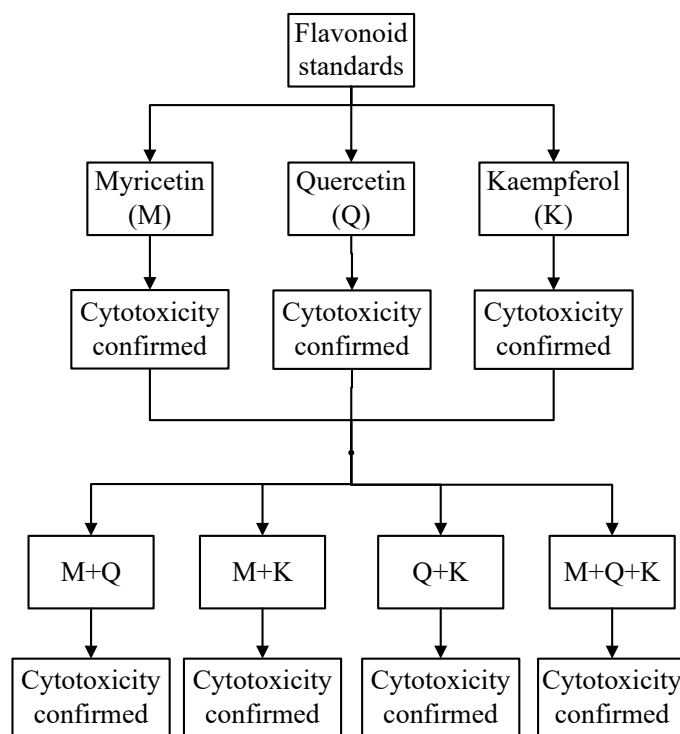


Figure 3-4. Diagram of cytotoxicity assays performed with flavonoid standards.

Combinations of flavonoids standards were tested in order to identify a possible synergistic interaction. The solutions of combinations were prepared in 1:1 proportion for groups of two, and 1:1:1 for the group of three as it is described in Table 3-6. For instance, for the combination of myricetin–quercetin, one of the concentrations tested was 50 µg/mL and the volume of the combination was 100 µL so 50 µL of myricetin at 100 µg/mL and were mixed with 50 µL of quercetin at 100 µg/mL.

Table 3-6 Flavonoids combinations and concentrations tested on OCI-Ly7.

Combinations	Concentration of single compound	Proportion, v/v
Myricetin + quercetin	0.5 µg/mL – 50 µg /mL	1:1
Myricetin + kaempferol	0.5 µg /mL – 50 µg /mL	1:1
Quercetin + kaempferol	0.5 µg /mL – 50 µg /mL	1:1
Myricetin + quercetin + kaempferol	0.5 µg /mL – 50 µg /mL	1:1:1

For each cytotoxicity assay, a sterile, polystyrene, white opaque wall, 96 wells plate (Corning, NY, USA) was used and cellular viability assay was performed using Cell-titer Blue reagent (Promega, Madison, USA. Exp. Date: Aug-27-2012). Sample wells (S) contained 100 μ L of cells in suspension plus 100 μ L of treatment at 6 different dilutions. Sample control wells (SC) contained 100 μ L of cell growth medium plus 100 μ L of treatment at the same 6 different dilutions. Assay Control wells (AC) contained 100 μ L of cells in suspension plus 100 μ L of cell growth medium. Blank wells (B) contained 200 μ L of cell growth medium. 20 μ L of CellTiter blue were added to each well after 24 h of incubation.

Several compounds were tested in SU-DHL-4 and OCI-Ly7 cell lines by means of cell titer Blue protocol for viability assay. An initial range of dilutions from 1:10 to 1:10⁶ were tested in each compound and using hill equation fit we reduced the range to get a smoother response. Compounds tested in OCI-Ly7 and SU-DHL-4 cell lines are detailed in Table 3-7 and the range of concentrations in which we were able to get a smooth response.

Table 3-7 Compounds and concentrations tested for cytotoxicity on SU-DHL-4 &OCI-Ly7 cells.

Treatment/Cell line	OCI-Ly7	SU-DHL-4
Black bean extract	0.025 mg/mL – 1 mg/mL	3 mg/mL – 0.025 mg/mL
Flavonoid fraction	0.0132 mg/mL – 1.45 mg/mL	0.0132 mg/mL – 1.32 mg/mL
Saponin fraction	0.333 mg/mL – 6.666 mg/mL	0.333 mg/mL – 6.666 mg/mL
Phenolic aids fraction	0.333 mg/mL – 6.666 mg/mL	0.333 mg/mL – 6.666 mg/mL
Myricetin glycoside	10 μ g/mL – 90 μ g /mL	10 μ g /mL – 90 μ g /mL
Quercetin glycoside	10 μ g /mL – 90 μ g /mL	10 μ g /mL – 90 μ g /mL
Kaempferol glycoside	10 μ g /mL – 90 μ g /mL	10 μ g /mL – 90 μ g /mL
Myricetin aglycone	10 μ g /mL – 50 μ g /mL	1 μ g /mL – 100 μ g /mL
Quercetin aglycone	1 μ g/mL – 40 μ g/mL	1 μ g /mL – 50 μ g/mL
Kaempferol aglycone	1 μ g /mL – 50 μ g/mL	1 μ g /mL – 100 μ g/mL

3.7.1 CYTOTOXICITY CONTROL ASSAY

A cytotoxic control assay was performed in NIH-3T3 and VERO cell lines testing flavonoid fraction in the same concentrations used for the IC₅₀ values determined for OCI-

Ly7 and SU-DHL-4 cell lines. These assays were done by triplicate and results were presented as the mean viability \pm 1 standard deviation.

3.7.2 IC₅₀ CALCULATION

A variant of Hill equation (Eq. 3), was used to determine the 50% inhibitory concentration

$$v = Vmax \frac{\left(\frac{[s]}{[s]_{0.5}}\right)^h}{1 + \left(\frac{[s]}{[s]_{0.5}}\right)^h} \quad (\text{Eq. 3})$$

$$\widehat{f(x)} = a + \frac{b - a}{1 + \left(\frac{x}{c}\right)^{-h}} \quad (\text{Eq. 4})$$

Eq. 4 was the one used for calculations, where a is the minimum cellular viability, b is the maximum cellular viability, c stands for the concentration where $f(x)$ is 50% of maximum response “b”, h is hill coefficient and x is the concentration tested.

Data was processed and plotted using the curve fitting toolboxTM of Matlab R2008b software which performs goodness of fit statistics for parametric models. For each cytotoxicity assay performed the following statistical parameters were calculated:

- The sum of squares due to error (SSE)
- R-square
- Adjusted R-square
- Root mean squared error (RMSE)

3.8 CELLULAR APOPTOSIS ASSAY

The purpose of this assay was to determine whether or not flavonoids are able to lead cells to a natural programmed cell death, i.e., apoptosis or produced necrosis. This was evaluated by the Annexin-FITC apoptosis Assay kit (Miltenyi Biotech, Auburn CA, USA).

One of the two principles of the apoptosis evaluation is based on the detection of a phospholipid called phosphatidylserine (PS). When a cell is undergoing apoptosis, PS turns from inner cell membrane to the outer side of the cell membrane as it is depicted in Figure 3-5 [18]. Figure was taken from [19]. The presence of PS on the surface of plasma membrane is one of the specific signals for recognition and removal of apoptotic cells by macrophages. The anticoagulant, Annexin V, has a high affinity for binding to PS. In the Apoptosis assay kit, the Annexin V is attached to a fluorescent chemical called fluorescein isothiocyanate or FITC. FITC will fluorescence at 525/40 nm after excitation with a 494 nm wavelength Laser.

The second principle of the apoptosis evaluation is based on the detection of iodide propidium (PI). PI binds to DNA, and as the apoptotic process progresses, cell membrane integrity is lost and according to the stage of cell apoptosis it is possible to distinguish between early apoptotic, late apoptotic, and dead cells PI will fluorescence and can be detected with a 562 – 588 nm band pass filter after excitation with a 488 nm wavelength Laser.

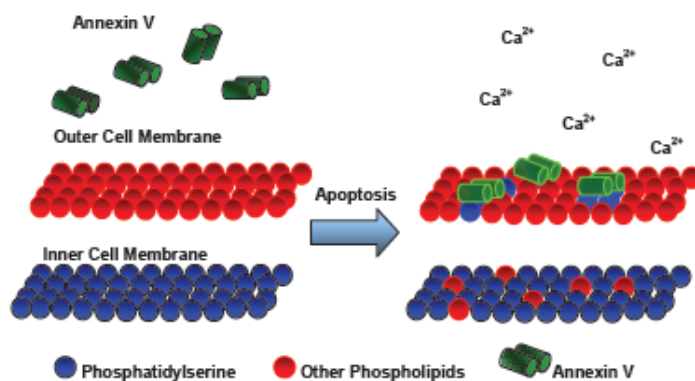


Figure 3-5. Annexin-V affinity with phosphatidilserine.

A sterile, polystyrene, clear, 12 wells plate (Corning, NY, USA) was employed, a cellular density of 400,000 cells/mL was fixed and 500 μ L of cells in suspension were added to each plate. Sample wells (S) contained 500 μ L of cells in suspension plus treatment by triplicate. Assay Control wells (AC) contained 500 μ L of cells in suspension plus 1000 μ L of cell growth medium. For each plate three different treatments were tested.

After 24 h of incubation, cells in suspension were washed in 1 mL of 1X Binding Buffer and immediately centrifuged at 300 g for 10 minutes. Then supernatant was aspirated completely. Cell's pellet was re-suspended in 100 μ L of 1X Binding Buffer per 10^6 cells. 10 μ L of Annexin V-FITC per 10^6 cells was added and well mixed, incubation in the dark at room temperature was done.

Cells were washed by adding 1 mL of 1X Binding Buffer and centrifuged at 300 g for 10 minutes. Supernatant was aspirated completely. Cells pellet was re-suspended in 500 μ L of 1X Binding Buffer per 10^6 cells. 5 μ L of PI solution was added immediately prior to analysis by flow cytometry.

Compounds tested in OCI-Ly7 and SU-DHL-4 cell lines are shown in Table 3-8. These concentrations were used based on the IC₅₀'s values determined by the cytotoxicity assays. Doxorubicin was used as a positive control to identify apoptotic cells.

In order to distinguish from false positives and false negatives, it is required to run four control assays. An Annexin-V control, a PI control, an unstained cells control and a no-treated cells control these control assays are included in appendix D.

With these controls we detected if treated cells were in apoptosis (early or late), necrosis or remain viable after 24 h of exposure to treatment. The treatments utilized for the apoptosis assay are detailed in Table 3-8. The concentrations utilized correspond to the IC₅₀ values determined by the cytotoxicity assays.

Table 3-8 Apoptosis Assay. Treatments and concentrations utilized

Treatment/Cell line	OCI-Ly7	SU-DHL-4
Black bean extract	132 µg/mL	618 µg/mL
Flavonoid fraction	161 µg/mL	273 µg/mL
Myricetin Aglycone	98 µM	119 µM
Quercetin Aglycone	33 µM	37 µM
Kaempferol Aglycone	62 µM	59 µM
Doxorubicin	3.44 µg/mL	3.44 µg/mL

3.9 BAX PROTEIN ASSAY ANALYSIS

As well as the apoptosis assay, a sterile, polystyrene, clear, 12 wells plate (Corning, NY, USA) was employed, a cellular density of 400,000 cells/mL was fixed and 500 µL of cells in suspension were added to each plate. Sample wells (S) contained 500 µL of cells in suspension plus treatment by triplicate. Assay Control wells (AC) contained 500 µL of cells in suspension plus 1000 µL of cell growth medium. For each plate three different treatments were tested.

Polystyrene round-bottom 12x75 mm Falcon tubes were utilized for the intracellular staining procedure. Each well's content was placed in a Falcon tube. 100 µL of fixative were added to each tube. Then cells were incubated for 10 minutes at room temperature followed by 100 µL detergent based permeabilising agent and then incubated in the dark at room temperature for 15 minutes. Cells were washed by adding 2 mL of PBS (containing 0.1% triton), centrifuged at 2000 rpm for 5 minutes, supernatant was discarded and the pellet was re-suspended in 400 µL of ice cold PBS, 10%FCS, 1% sodium azide. 100 µL of cell suspension were added to each tube then 1 µL of the primary monoclonal mouse antibody BAX [6A7] (ab5714, 1/10 dilution in 3% BSA/PBS) was added to each tube (but one that was used as no staining control) followed by 30 minutes incubation at 4°C in the dark. After incubation cells were washed by centrifugation at 400 g for 5 min and re-suspended in ice cold PBS. secondary antibody used was DyLight® 488 goat anti-mouse IgG (H+L) (ab96879), 10 µL at 1/500 dilution in 3% BSA/PBS were added to each tube except control, and then incubated for 30 min at 4°C in the dark. Then cells were washed by centrifugation at 400 g for 5 min and re-suspended in ice cold PBS, 3% BSA, 1% sodium azide. Cells were analyzed right after.

In order to distinguish from false positives and false negatives, it is required to run two control assays. The first control, is a Dylight stain control assay which consists of cells with no treatment but incubated at the same conditions and stained with the Dylight dye. The second control consists of cells treated with doxorubicin but this group of cells was not stained. These controls are detailed in Appendix E.

In order to detect different levels of protein Bax expression, we left cells in incubation with treatment at three different periods, 12, 24 and 48 h and flow cytometer analysis was performed right after each period was over.

For data analysis, two tailed t-paired test was used to infer statistical difference between populations. Calculations are detailed in the Statistical Analysis section

3.10 CELL CYCLE ASSAY AND DATA ANALYSIS

3.10.1 CONTROLS FOR CELL CYCLE ANALYSIS

Cell cycle analysis is the study for the identification of cell cycle phases and detection of aneuploidy of cells samples either healthy cells, neoplastic cells or cells under stress conditions.

Quality control assays such as instrument linearity, resolution and the ability to identify aggregates and discriminate between G₀/G₁ doublets and G₂/M singlets for an accurate estimation of DNA content must be performed in order to ensure accurate results. These quality controls are included in Appendix E. With the quality control tests performed the cell cycle assay was able to detect G₀/G₁, S and G₂/M phases for new observations, and also was able to compare how populations of cells changes when treatment was applied.

3.10.2 CELL CULTURE

As well as the apoptosis assay, a sterile, polystyrene, clear, 12 wells plate (Corning, NY, USA) was employed, a cellular density of 400,000 cells/mL was fixed and 500 μ L of cells in suspension were added to each plate. Sample wells (S) contained 500 μ L of cells in suspension plus treatment by triplicate. Assay Control wells (AC) contained 500 μ L of cells in suspension plus 1000 μ L of cell growth medium. For each plate three different treatments were tested. After 24 h of incubation.

Compounds tested in OCI-Ly7 and SU-DHL-4 cell lines are shown in Table 3-9, the concentration tested was the IC₅₀ determined for each compound in the cytotoxic assays.

Table 3-9 Cell Cycle Assay. Compounds and concentrations utilized

Treatment/Cell line	OCI-Ly7	SU-DHL-4
Black bean extract	132 μ g/mL	618 μ g/mL
Flavonoid fraction	161 μ g/mL	273 μ g/mL
Myricetin Aglycone	98 μ M	119 μ M
Quercetin Aglycone	33 μ M	37 μ M
Kaempferol Aglycone	62 μ M	59 μ M
Doxorubicin	3.44 μ g/mL	3.44 μ g/mL

3.10.3 STAINING PROCEDURE

Polystyrene round-bottom 12x75 mm Falcon tubes were utilized for the intracellular staining procedure. Each well's content was placed in a Falcon tube. Cells in suspension were centrifuged at 400 g for 5 minutes at room temperature (20° to 25°C). 250 μ L of Solution A (trypsin buffer) were added to each tube and gently mixed by tapping the tube by hand. Solution A was allowed to react for 10 minutes at room temperature (20° to 25°C). Then 200 μ L of Solution B (trypsin inhibitor and RNase buffer) was added to each tube and gently mixed by tapping the tube by hand. This mix was allowed to incubate for 10 minutes at room temperature (20° to 25°C). 200 μ L of cold (2° to 8°C) Solution C (propidium iodide stain solution) was added to each tube. It was gently mixed as above and incubated for 10 minutes in the dark in the refrigerator (2° to 8°C). Then samples were analyzed on the flow cytometer.

3.11 CHARACTERIZATION OF ANIMAL MODEL

Before setting up the animal model the facilities where mice were going to stay were disinfected with benzalkonium chloride and then sterilized with Microdacyn 60. This solution has been tested as antiviral, antifungal and wide range antimicrobial, working as super oxidant [37]. Every surface of the room, the change station, rack and cages were sterilized with Mycrodacin 60 (Oculus, Innovative Sciences, Petaluma, California, USA). Then bacteriologic tests were performed, LB medium was prepared in petri dishes then samples were taken rubbing cotton swabs against the surface of walls, floor, ceiling, cages, change station and working station. Petri dishes were incubated 48 hrs at 37°C and CO₂ at 5% and no growing colonies were detected.

3.11.1 MICE HOUSING

Mice were kept in ventilated cages (Part No.1291H, Techniplast, Italy). The ventilated cages are connected into a rack (SEALSAFE RACK Part No. 2H30MAC20CA, Techniplast, Italy). The main unit of the rack supplies the inlet air of cages with filtered air by HEPA filters and release air 75 times per hour keeping a positive pressure. The cages counted with a 0.2 µm round filter which ensure the safety of animals in case of power failure of the rack, the filter is located on the top of the cage as it is show in figure. The structure of the cage ensures a noise level below 50 dBA to reduce stressing conditions.

3.11.2 DEVELOPMENT OF LYMPHOMA ANIMAL MODEL

The mouse chosen for the study was severe combined immune deficiency C.B-17 Prkdc* (scid) (Fox Chase Cancer Center, Philadelphia, Pennsylvania, USA) which is recommended for xenograft transplantations [36] due to its engineered characteristic of being deficient in function and/or number of T Cells and B cells and normal function of NK cells.

Mice were 6-8 weeks old, recommended age at [36]. 30 mice were purchased at Harlan Laboratories. Mice were acclimated for one week with free access to food and water before inoculation. Food was autoclavable Global 19% Protein Extruded Rodent Diet (Teklad

Diets, Madison WI, USA). Animal protocol was approved by the “Comite Institucional para el cuidado y uso de los animales de laboratorio”. Registered as protocol No. 2010-011.

Drinking water, water bottles, food and bed were sterilized by autoclave 120 °C for 30 minutes and cages along with every other accessory were sterilized with Mycrodacyn 60 letting the solution to be in contact for at least 15 minutes. Aseptic procedures were used routinely. Room temperature was controlled at 22°C, relative humidity at 45%, dark and light periods of 12 h and free access to feed and water.

In Table 3-10 it is described the experimental groups in which mice were randomly divided.

Table 3-10. Mice groups for animal model

Group	n
Control	8
Inoculated with SU-DHL-4	11
Inoculated with OCI-Ly7	11

3.11.2.1 PROPHYLAXIS

The mice were kept on trimethoprim and sulfamethoxazole (Bactinver) administered in water for prophylaxis. Dosage of antibiotic was 15 mg per Kg of mouse body weight, statistically a mouse consumes 15 mL for each 100 g of body weight per day [39]. The antibiotic concentration is 200mg/40mg/5ml and the mean weight of mice is 20 g this gives 25 mL of antibiotic diluted in 1 L of drinking water.

3.11.2.2 ANESTHESIA

The anesthesia used was a mixture of Ketamine (100 mg/mL, Ketamin-Pet, Laboratorios Aranda, Qro. México, Batch No. 905014, Exp. Date: May 2012) and Xylazine (procin 2% or 20 mg/mL, 25 mL)

The Recommended dose for Ketamine is 100-200 mg per Kg of body weight and for xylazine is 5 – 16 mg per Kg of body weight, taking the highest dose of both ranges, i.e. 200 mg of Ketamine and 16 mg of Xylazine, a mouse of 20 g will receive 40 µL of Ketamine and 16 µL of Xylazine. Injection is administered into the anterolateral region of

any caudal limb muscle. 1 mL insulin syringe (31 G) are used for this procedure. Anesthesia dose information was taken from [38].

3.11.2.3 EUTHANASIA

Mice were sacrificed by means of cervical dislocation always previously anesthetized as described above. Handling and injection procedures were taken from [39].

3.11.2.4 INOCULATION OF LYMPHOMA CELLS

Lymphoma cells inoculation was performed one week after mice arrival.

For Intraperitoneal inoculation, 1 mL insulin syringes of 25 – 27 G of small bevel were used. Mouse was hold and immobilized with one hand and positioned with his head facing downwards in order to displace down intraperitoneal organs as it is illustrated in Figure 3-6. Then syringe is inserted into the skin over left iliac fossa, syringe is leaded in the direction of cranium and introduced into the peritoneal cavity. It was carefully raised against abdominal wall to avoid puncturing into organs, and then cells in solution were administered slowly.

Inoculation was done with a shot of approximate 4 million of cells in 300 μ L of PBS. Cells were prepared with anticipation to be in log phase, previous work recommended from 3 to 10 million of cells [36].



Figure 3-6. Intraperitoneal inoculation

3.11.2.5 Characterization of Lymphoma

Several parameters were measured every week, body weight was measured twice a week, daily food intake was registered and every week one mouse of each group was sacrificed by cervical dislocation previously anesthetized.

During autopsies liver, spleen, kidneys, bowels and tumors were extracted and the measures length, width, weight and volume were taken.

3.12 DETECTION OF FLAVONOIDS IN PELLETS

The purpose of this experiment was to identify if the flavonoids were not modified as a result of being in contact with the pellet. Four pellets of the extruded rodent food used for the animal models were sterilized. 300 μ L of FF at 20 mg/mL were embedded within the pellet by triplicate. Nothing was added to the fourth pellet, this pellet was used as a control. Pellets were left inside a mouse cage for one day with the FF embedded. The next day all the pellets were processed as follows. Each pellet was placed into a mortar with 80% MeOH (proportion 1:10, m/v). The pellet was smashed and then agitated by vortex at 900 rpm for 30 min. Then the solution was filtered using Whatman paper filters grade no. 1 and concentrated by rotatory evaporation. Then each solution was hydrolyzed and filtered with a C18 cartridge into HPLC vials. The HPLC analysis was performed with the HPLC parameters listed in Table 3-1.

3.13 IDENTIFICATION OF FLAVONOIDS IN MICE PLASMA

26 adult male mice CD1 were utilized for this study. After 12 h overnight fast the flavonoid fraction was administered using an intragastric feeding needle, working with two groups of 12 mice each, one group was fed with 500 μ L of flavonoid fraction at 1 mg/ml and the second one with 500 μ L of flavonoid fraction at 2 mg/ml.

Blood samples were taken at 15 min, 30 min, 60 min and 90 min since the flavonoid fraction was administered.

In Table 3-11 it is detailed the groups of mice and the times in which blood samples were taken. 3 mice of each group were anesthetized via intramuscular at each time mentioned above and the largest possible amount of blood was drawn and then they were sacrificed immediately by cervical dislocation. 2 mice were sacrificed at the beginning of the experiment and their blood samples were taken also. These two mice were labeled as basal.

Table 3-11. Experimental groups for identification of flavonoids in mice plasma

Time/Groups	1 mg/ml	2 mg/ml	BASAL
0 min	0	0	2
15 min	3	3	--
30 min	3	3	--
60 min	3	3	--
90 min	3	3	--

Samples were processed according to previous studies [40]. Blood was poured into EDTA tubes and centrifuged immediately at 800 g for 10 min at room temperature. Plasma was pipetted away from red globules. Ascorbic acid was added (final concentration 1 mM). NOTE: In this part 10 μ L of quercetin were added to a basal mouse sample as an internal control. Then plasma was acidified to a pH de 5 with acetic acid (0.65 mM; 0.1 Vol.), this was done to stabilize samples during the process. Acetonitrile (2.5 Vol.) was used to precipitate plasma proteins and then extract flavonoid metabolites from remaining solution. All samples were shaken by means of vortex for 30 s every 2 min for 10 min. Then samples were centrifuged at 13600 g at 4 °C for 10 min. Supernatant was concentrated up to 75 μ L by means of the eppendorf concentrator. 75 μ l de MeOH were added to get a final volume of 150 μ L. Samples were centrifuged at 13600 g, 4 °C for 2 min and filtered into HPLC vials.

The HPLC parameters detailed in Table 3-12 were set at the HPLC LC/MSD TOF (Part No. G1969A, Serial: U55470072).

Table 3-12 HPLC LC/MSD TOF parameters for Metabolites of flavonoids detection

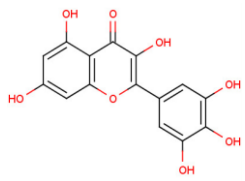
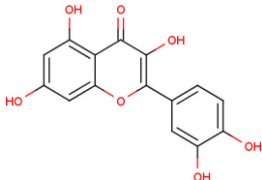
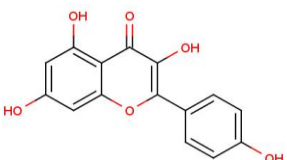
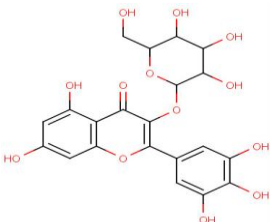
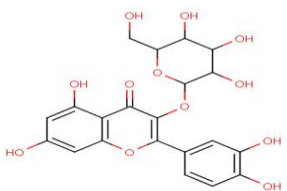
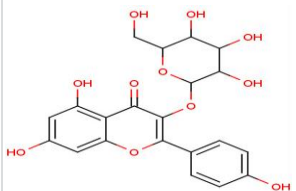
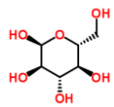
Device	Parameter	Value	
Injector	Injection Volume	10 µL	
Pump	Flow Rate	0.4 mL/min	
	Channel A (H ₂ O+ Formic Acid 0.1%)	60%	
	Channel B (MeOH)	40%	
	Solvent Gradient	t	%B
		0	40
		15	60
		20	60
		25	90
Column Thermostat	Column Temperature	25 °C	
Detector	Wavelength	360/16 nm	
ESI(Seg.)	Ion polarity	Positive	
	Gas Temperature	350 °C	
	Drying Gas	12 L/min	
	Nebulizer	35 psig	
MSD TOF	Fragmentor	225 V	
	Skimmer	60 V	
	OCT RFV	25 V	
ESI(Scan)	Capillary	3000 V	
	Ion Energy	33.50 V	
	Ion Focus	-150 V	
	Slicer	-12 V	
TOF	Pusher	1250 V	
	Puller	-800 V	
	Puller Offset	32 V	
	Acc. Focus	-1950 V	
	Mirror Mid	-13295.50 V	
Detector	PMT	634 V	

All samples were run into HPLC Hewlett Packard Series 1100 and also in the HPLC Series 1200 DAD/MWD with all storage spectrum software in order to detect Myricetin, Quercetin, & Kaempferol either Glycosylated or in aglycone form, employing the method of Table 3-1 with 10 μ L of injection volume.

In order to detect the masses

For mass spectrometry detection we had to define the masses we were looking for. In Table 3-13 it is detailed the masses of the compounds of interest, since we are working with positive ionization 1 unit of m/z must be added to each mass and these will be the masses of interest. The mass spectra analysis of the flavonoid fraction and myricetin, quercetin and kaempferol standards are included in appendix F.

Table 3-13 Glycosylated flavonoids and standards molecular mass & m/z ratio

Compound	Molecular mass, g/mol	[X+H]	Structure
Myricetin	318.2351	319.2351	
Quercetin	302.2357	303.2357	
Kaempferol	286.2363	287.2363	
Myricetin-3-Glucoside	480.3757	481.3757	
Quercetin-3-Glucoside	464.3763	465.3763	
Kaempferol-3-Glucoside	448.3769	449.3769	
Glucoside	162.1406	163.1406	

3.14 ANIMAL MODEL WITH TREATMENT

45C.B-17 Prkdc* (scid) mice were purchased at Harlan Laboratories. Mice were allowed to acclimate for one week with free access to food and water before inoculation. Food, water, bed, cages and water bottles were sterilized as it was described in the animal model characterization. To inoculate, mice were injected with approximate 10^7 of cells diluted in 300 μ L of PBS were injected at right iliac fossa. Cells were prepared with anticipation to be in log phase.

3.14.1 TREATMENTS ADMINISTRATION

Mice were randomly divided into the experimental groups detailed in Table 3-14.

Table 3-14 Experimental groups for animal model with treatment

Treatments	N	Via of administration	Dose
Cyclophosphamide	9	I.P.	150 mg/Kg
Placebo	9	P.O.	--
Quercetin	9	I.P.	300 μ M
FF	9	P.O.	15 mg/mL
BBE	9	P.O.	20 mg/mL

Mice were weighed every day since experimental groups were divided.

BBE and FF were administered Orally (P.O.) by embedding the treatments directly into the pellets. 300 μ L at 20 mg/mL of the BBE was injected into the pellet. This way mice were receiving BBE and FF treatments every day.

Cyclophosphamide (Hydrofosmin®, 200 mg, Laboratorios Sanfer, S.A. de C.V.) was selected as a positive treatment. The administration of cyclophosphamide was i.p. The content of CTX vial was dissolved in 10 ml of CS solution (PiSA farmaceutica Mexicana) and stored at 4° C. The dose of the cyclophosphamide was 150 mg/kg. The schedule of administration was one i.p. injection every three days for 21 days [41].

Quercetin was administered i.p., the dose was calculated as 10-times the IC₅₀ value determined in the cytotoxic assays.

The administration of treatments started two weeks later since mice were inoculated, when the first mouse showed signs of tumor.

Autopsies were performed whenever any subject deceased. Tumors were extracted and measured.

At the end of the experiment a Kaplan Meyer - survival curve was plotted and the statistical difference between treatments was evaluated using the log rank test. Calculations were performed based on [42]. To determine whether the treatments were different, tumor masses were compared using the one-way ANOVA test. The Kruskal-Wallis test was utilized to compare which treatment was significantly different in comparison with the placebo group, calculations were performed based on [43].

3.15 STATISTICAL ANALYSIS

The Matlab ®2010 software was used for the statistical analysis of all the results mentioned in this work.

3.15.1 GOODNESS-OF-FIT STATISTICS

Curve Fitting Toolbox software supports these goodness-of-fit statistics for parametric models:

- The sum of squares due to error (SSE)
- R-square
- Adjusted R-square
- Root mean squared error (RMSE)

3.15.2 CONFIDENCE AND PREDICTION BOUNDS

Curve Fitting Toolbox software calculates confidence bounds for the fitted coefficients, and prediction bounds for new observations or for the fitted function. The coefficient confidence bounds are presented numerically, while the prediction bounds are displayed graphically and are also available numerically. The confidence intervals presented in this thesis are calculated with level of significance of 5%.

3.15.3 TWO TAILED T-PAIRED TEST

For flow Cytometer analysis viable cells group and treatment cells group are random samples, both with unknown and different population variances, so we can statistically compare differences between sample group means using the two tailed t-test which is

Let be $H_0: \Delta_x = 0, \mu_0 = 0$; and $H_1: \Delta_x \neq 0, \mu_0 = 0$, the statistic test is:

$$t = \frac{\bar{\Delta_x} - \mu_0}{S / \sqrt{n}} \quad (\text{Eq. 6})$$

Where $\Delta x = |\overline{X}_1 - \overline{X}_2|$, S is the standard deviation of Δ_x . Degrees of freedom are determined as $n - 1$. H_0 is rejected with an α significance level if $|t| > t_{\alpha/2, n-1}$.

3.15.4 LOG RANK TEST

The statistic employed was chi-square test:

$$\chi^2 = \frac{(O - E)^2}{E} \quad (\text{Eq. 7})$$

Where O and E are the totals of the observed and expected events respectively. Since the comparison between groups was always by pairs, i.e, one of the treatment groups against the placebo group, chi-square was calculated with 1 degree of freedom.

4 RESULTS AND DISCUSSION

4.1 FRACTION OF FLAVONOIDS FROM BLACK BEAN EXTRACT

The raw black bean extract was made from the methanolic extraction from hulls obtained after decortication of black beans (*Phaseolus vulgaris*). This black bean extract was processed in the Biotechnology Center from the Tecnológico de Monterrey according to the procedure detailed by [10] and the extract was provided freeze dried as a lyophilized powder. This experiment was performed to isolate the flavonoid fraction that comes from the methanolic extraction mentioned above. We were able to obtain 1.1604 g of flavonoid fraction out of 20.4 g of lyophilized raw black bean extract. We obtained a yield of the first fraction of 5.6% (w/w). This yield is far less than it is reported in [11], this loss could be happening in the 25% MeOH washing, since this step is required to eliminate most of the part of the tannins and to ease the isolation of myricetin, quercetin and kaempferol.

As it detailed in Figure 3-1 in Materials & Methods section, tannin's fraction and saponin's fraction were recovered, concentrated and lyophilized, these fractions were utilized for the cytotoxicity assays.

The dried flavonoid fraction was utilized for cytotoxic assays, apoptosis assay, animal model and for the purification of Myricetin, Quercetin and Kaempferol.

4.2 IDENTIFICATION OF MYRICETIN, QUERCETIN AND KAEMPFEROL

The main objective of this identification was to confirm the presence of the flavonols, Myricetin-3-Glycoside, Quercetin-3-Glycoside and Kaempferol-3-Glycoside, which has been reported previously by [10] as the flavonols contained in that black bean extract.

4.2.1 HPLC IDENTIFICATION OF GLYCOSILATED FLAVONOIDS

The chromatograms depict the peaks corresponding to glycosylated Myricetin, Quercetin and Kaempferol. Retention time and maximum absorption wavelengths for each peak is reported in table 4-1. The absorption spectrum of each peak is shown in Appendix B, figures B-2 to B-4. Comparing Figure 4-1 with Figure 4-2, glycosylated flavonoids have a

shorter retention time than the hydrolyzed flavonoids, perhaps the glucoside structure increases the polarity index of the molecule this information was useful in order to identify flavonoids and/or flavonols in mice plasma.

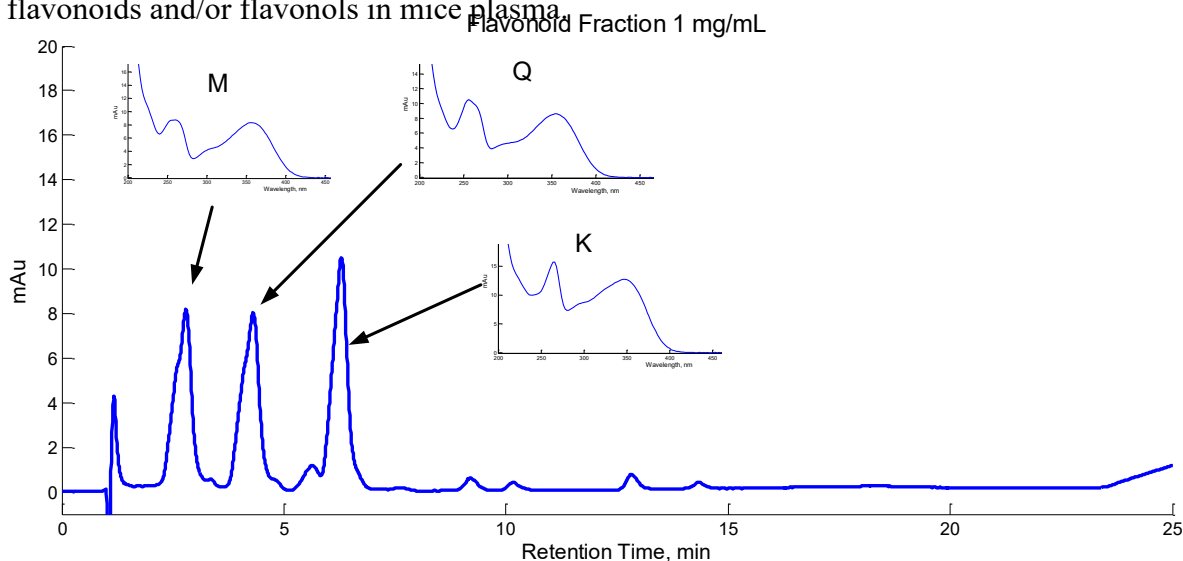


Figure 4-1. Chromatogram of flavonoid fraction analyzed at 1 mg/mL and absorption spectra of the three main flavonols glucosides, miricetin 3-o glucoside (M), quercetin 3-o glucoside (Q) and kaempferol 3-o glucoside (K), detected at 365 nm.

As it has been described in previous research [14], the two maximum absorption wavelength reported of myricetin-3-glucoside, quercetin-3-glucoside and kaempferol-3-glucoside purified from black bean were (260, 358), (258,356), (266, 348) respectively. [14] compared the flavonols purified from black bean with standards flavonols in order to confirm the identity. In table 4-2 it is compared the two maximum absorption wavelengths of the flavonoid fraction of the chromatogram of Figure 4-1 and the two maximum absorption wavelengths reported in [14]. With the information presented on Table 4-1 we were able to confirm that the glycosylated flavonoids were identified as Myricetin – 3 Glucoside, Quercetin – 3 Glucoside, Kaempferol – 3 Glucoside, the wavelengths difference presented was result of the solvent utilized for HPLC run.

4.2.2 HPLC IDENTIFICATION OF AGLYCONES

As it was mentioned in last section the flavonoid fraction was hydrolyzed and then analyzed by the same HPLC method used for the analysis of glycosylated flavonoid fraction described in section 4.1.2.1 above.

In order to confirm the identity of these flavonoids, the retention time and maximum absorption wavelengths were compared between the chromatogram of the hydrolyzed flavonoid fraction (blue chromatogram, Figure 4-2) and the control chromatogram. This control contained myricetin, quercetin and kaempferol standards at 5 ppm. The blue chromatogram of the Figure 4-2 depicts the hydrolyzed flavonoid fraction and the red chromatogram depicts the standard control flavonoid fraction. Both were compared, the retention time and the two maximum absorption wavelengths for each peak, this is reported in table 4-1, where we can confirm that the hydrolyzed flavonoids are identified as myricetin, quercetin and kaempferol. The absorption spectrum of each peak is shown in Appendix B, from figure B-6 to figure B-11.

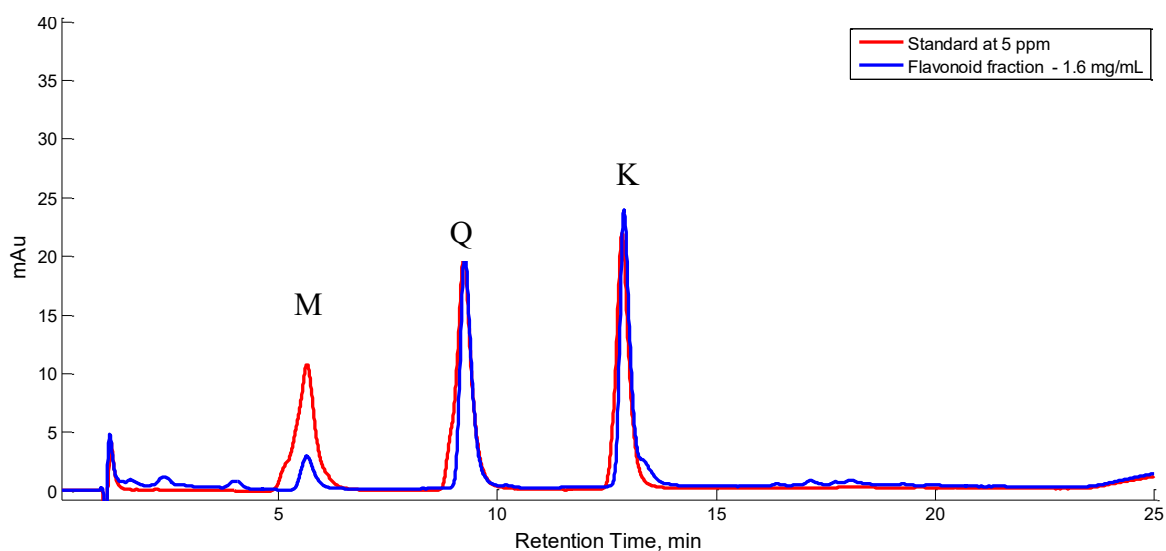


Figure 4-2. Chromatogram of hydrolyzed flavonoid fraction analyzed at 1.6 mg/mL. The blue chromatogram represents the three main flavonoids, myricetin (M), quercetin (Q), kaempferol (K).

Chromatogram of flavonoid fraction analyzed at 1 mg/mL and absorption spectra of the three main flavonols glycosides, miricetin 3-o glucoside (M), quercetin 3-o glucoside (Q) and kaempferol 3-o glucoside (K), detected at 365 nm.

Table 4-1. Comparison of retention time and maximum absorption wavelengths of aglycone flavonoids identified and flavonoid standards.

Hydrolized Flavonoids			Standards			
Retention Time, min	$\lambda 1, \text{nm}$	$\lambda 2, \text{nm}$	Retention Time, min	$\lambda 1, \text{nm}$	$\lambda 2, \text{nm}$	Compound
5.656	253	372	5.656	253.1	371.8	Myricetin
9.269	254	370	9.236	254.5	369.5	Quercetin
12.889	264	366	12.846	264.54	365.45	Kaempferol

4.3 PURIFICATION OF MYRICETIN, QUERCETIN AND KAEMPFEROL

Once glycosylated flavonoids were identified we purify them according to the retention time and the maximum absorption wavelengths. The HPLC used for purification was not equipped with the all spectra storage software that allows presenting the absorption spectrum at any time, instead the online spectra was used to identify the peaks corresponding to myricetin-3 glucoside, quercetin- 3 glucoside, kaempferol – 3 glucoside. In figures 4-3, 4-4 and 4-5 is shown the online spectra which exhibits the two maximum absorption wavelengths by the time the peak is at its maximum absorption units. Retention time and maximum absorption wavelengths for each peak are reported in table 4-2. Different retention times are reported because for this HPLC purification process we used a larger HPLC column and the flow rate was higher too, however we identified and purified glycosylated flavonoids.

Table 4-2. Retention time and maximum absorption wavelengths of purified glycosylated flavonoids.

Retention Time, min	$\lambda 1, \text{nm}$	$\lambda 2, \text{nm}$	Compound Identified
13	260	358	Myricetin – 3 – Glucoside
16.5	256	356	Quercetin – 3 – Glucoside
19.1	265	348	Kaempferol – 3 – Glucoside

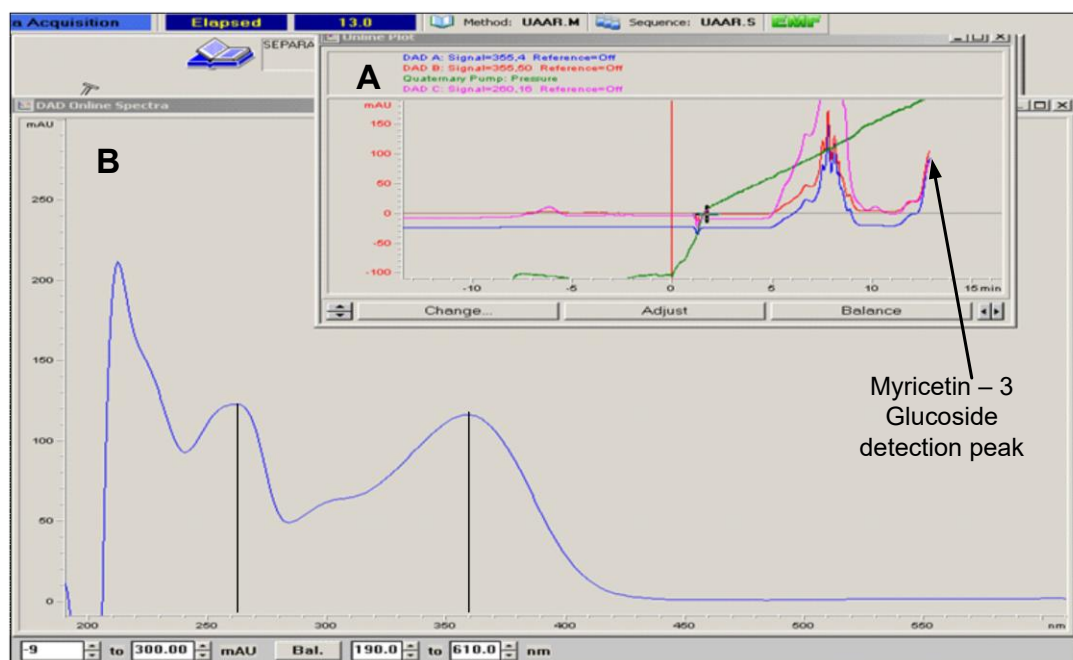


Figure 4-3. HPLC purification of Myricetin – 3 Glucoside. Detection at 365 nm.

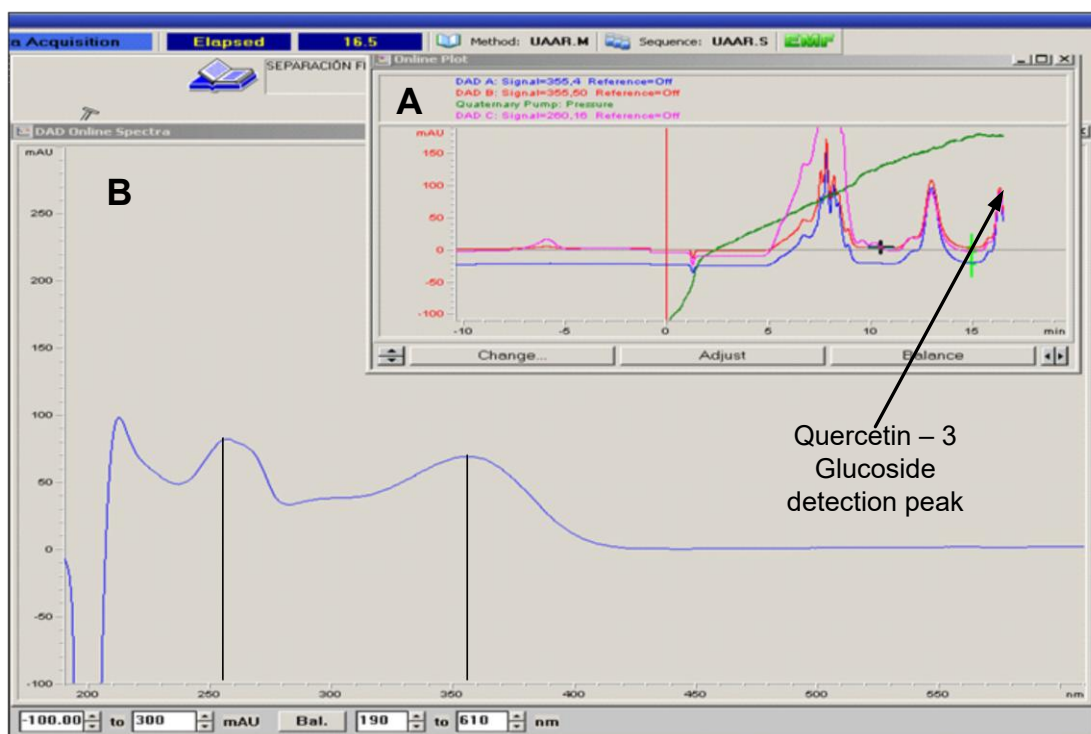


Figure 4-4. HPLC purification of Quercetin – 3 Glucoside. Detection at 365 nm.

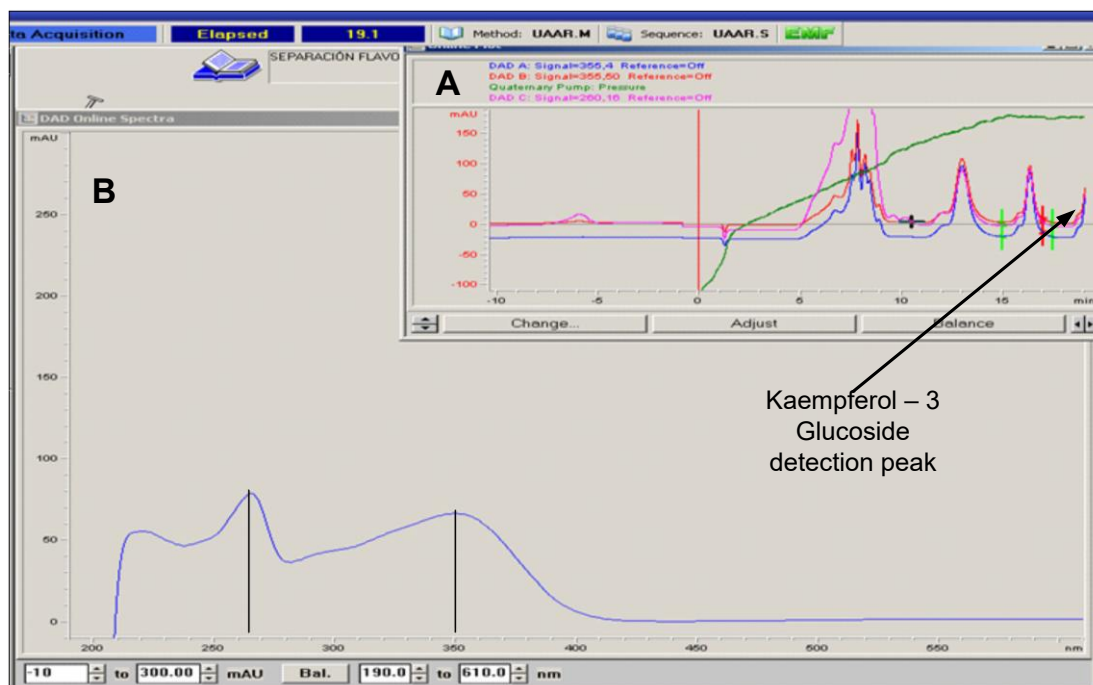


Figure 4-5. HPLC purification of Kaempferol – 3 Glucoside. Detection at 365 nm.

For every HPLC run, 2.5 mL of each fraction was obtained, several runs had to be performed in order to obtain approximately 450 mL of each of the three collections. Each one of them were concentrated through rotatory evaporation and dried by lyophilization. Once dried they were weighed getting the amounts described in Table 4-3:

Table 4-3 Amount of glycosylated flavonoids obtained by HPLC purification

Glycosilated Flavonoid purified	Weigth, mg
Myricetin- 3 Glucoside	25.8
Quercetin- 3 Glucoside	25.3
Kaempferol- 3 Glucoside	7.4

4.4 QUANTIFICATION OF MYRICETIN, QUERCETIN AND KAEMPFEROL

The figure shown below, Figure 4-6, illustrates the chromatograms for Myricetin, Quercetin and Kaempferol standards, identified at 0.1 ppm, 1 ppm, 5 ppm and 10 ppm. Z-axis (depth) separates each chromatogram according to their different concentrations. For each concentration was identified by triplicate, which can be slightly appreciated as the red, green and blue chromatograms presented at each concentrations.

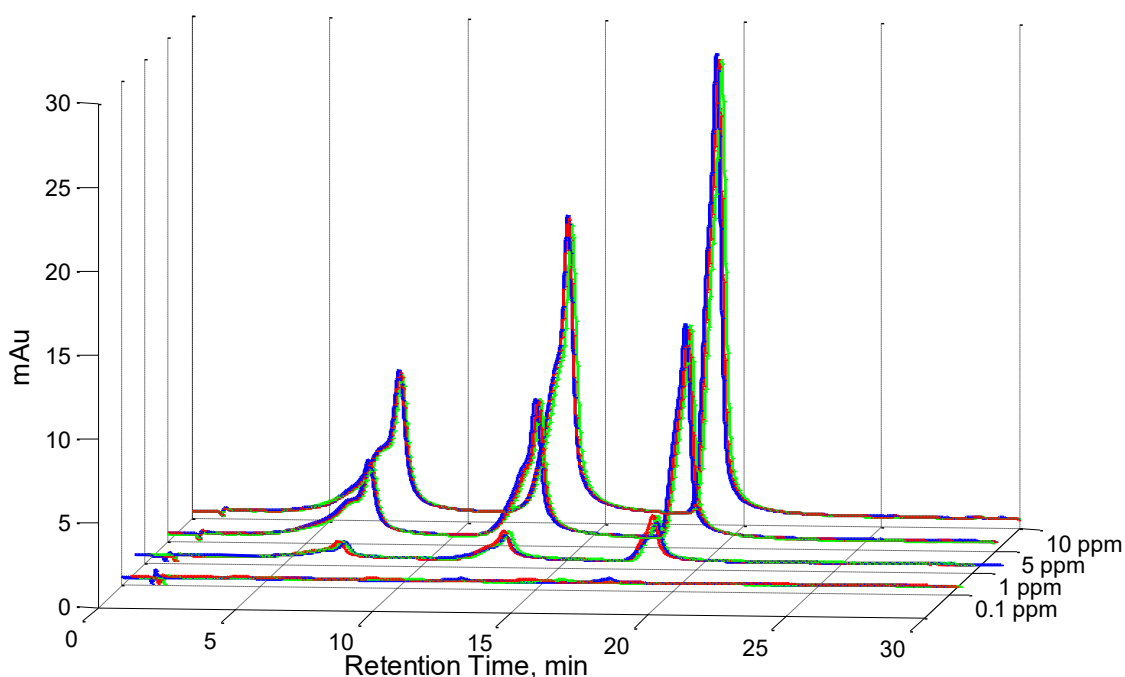


Figure 4-6. Chromatograms of myricetin, quercetin and kaempferol standards for calibration curve.

The calibration curve utilized to estimate the concentration of Myricetin, Quercetin and Kaempferol was calculated using the area under curve of the chromatograms from 0.1 to 5 ppm. Linear regressions calculated for Myricetin, Quercetin & Kaempferol are shown in Appendix B, Figures B-16 & B-17, the goodness of fit is detailed in Tables B-1 & B-2. On Table B-2 it is detailed that square sum of error is 10^3 times greater when higher concentrations are included to the regression, despite of the goodness of fit of the R-square. This was the reason to perform a calibration curve embracing a rank of concentrations from 0.1 to 5 ppm. The linear regressions of the calibration curves were calculated using the

linear model $f(x) = p_1x + p_0$, where x is the concentration of interest and $f(x)$ stands for the area under curve. Isolating the variable of interest we obtain the Equations 8, 9 & 10 which determine the concentration of myricetin, quercetin and kaempferol respectively. These relationships were utilized to estimate the concentration on the purified flavonoids chromatograms of Figure 4-8 as well as the flavonoids tested on ,

$$\widehat{x}_M = \frac{AUC_M + 4.745}{39.73} \quad (\text{Eq. 8})$$

$$\widehat{x}_Q = \frac{AUC_Q + 11.06}{80.76} \quad (\text{Eq. 9})$$

$$\widehat{x}_K = \frac{AUC_K + 0.5946}{93.41} \quad (\text{Eq. 10})$$

In the Figure 4-7, the chromatograms of myricetin, quercetin and kaempferol are depicted as the blue, green and red chromatograms respectively. Flavonoid samples were the glycosylated flavonoids purified from Black Bean Extract described in section 3.1.3, and therefore each one of them has been hydrolyzed previous to HPLC identification. The chromatogram colored in blue represents myricetin aglycone with a retention time of 5.61, an area under curve of 1481.02 and the estimated concentration of 21.53 $\mu\text{g/mL}$ which corresponds to 67.65 μM . The green chromatogram represents quercetin aglycone with a retention time of 9.28, an area of 3238.54 and the estimated concentration of 30.98 $\mu\text{g/mL}$ corresponding to 102.5 μM . And the red chromatogram represents kaempferol aglycone with a retention time of 12.92, an AUC of 934.35 and the estimated concentration of 9.63 $\mu\text{g/mL}$ corresponding to 33.64 μM .

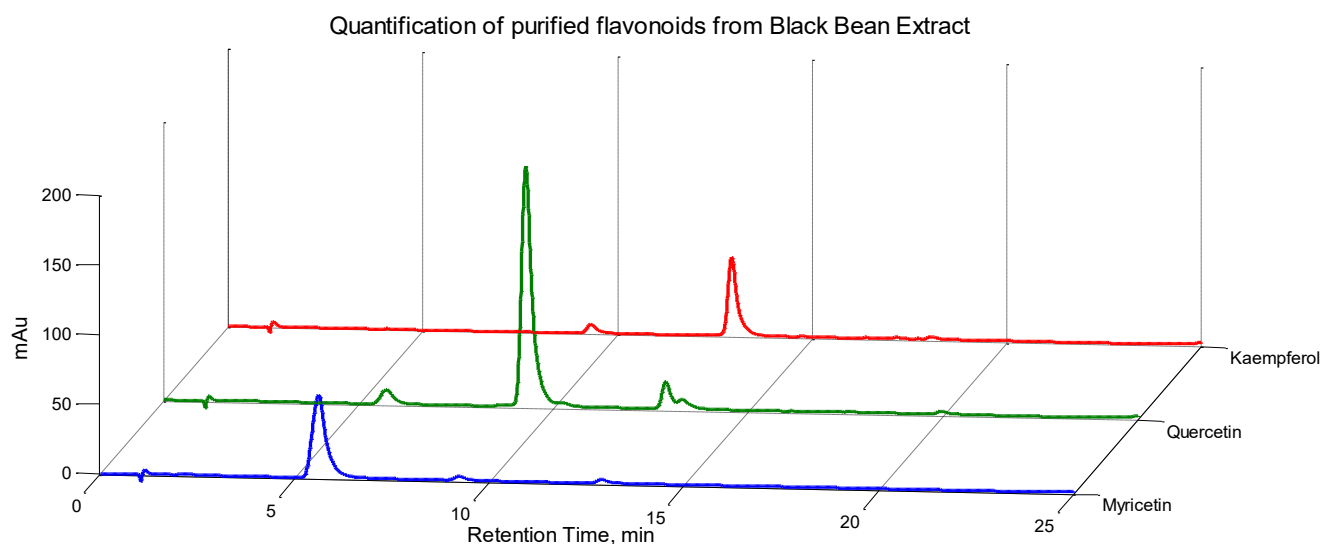


Figure 4-7 HPLC identification of purified flavonoids from black bean extract.

The equations 8, 9 & 10 were employed to calculate concentrations in “ $\mu\text{g/mL}$ ”. The molar units were calculated as the rate of the concentration (g/L) over the molecular mass of the flavonoid of interest (mol/L), the molecular weights of glycosylated flavonoids and aglycones were consulted in the database of dictionary of natural products [15]. These equations were also used to calculate the proportion of flavonoids present in the Black Bean extract and in the flavonoid fraction used in the cytotoxic assays according to the IC_{50} determined.

These linear regressions and equations determines the concentration of the aglycone flavonoid, however, since the detection of flavonoids is based on the UV excitation of the pi electrons of the C rings and it does not interact with the glycoside structure we can make an estimation of the concentration of glycosylated flavonoids using the linear models calculated for aglycone standards. In Figure 4-8 it is detailed the chromatogram of the flavonoid fraction at 1 mg/mL and it is illustrated that myricetin-3-glucoside, quercetin-3-glucoside and kaempferol-3-glucoside are contained in the flavonoid fraction at the concentrations of $5.4 \text{ }\mu\text{g/mL}$, $2.82 \text{ }\mu\text{g/mL}$ & $2.42 \text{ }\mu\text{g/mL}$ respectively. And the corresponding molar concentrations are $9.36 \text{ }\mu\text{M}$, $6.56 \text{ }\mu\text{M}$ & $5.44 \text{ }\mu\text{M}$. In the same way the proportion of glycosylated flavonoids was calculated for a sample of black bean extract at a concentration of $300 \text{ }\mu\text{g/mL}$, and the resultant concentrations were $47.08 \text{ }\mu\text{M}$, $20.34 \text{ }\mu\text{M}$ &

21.2 μM for myricetin-3-glucoside, quercetin-3-glucoside and kaempferol-3-glucoside respectively. The BBE chromatogram at 300 $\mu\text{g/mL}$ has been included in Appendix B, Figure B-14. As an additional note, the proportion of glycosylated flavonoids contained in 10 μL of a Black bean extract solution at 300 $\mu\text{g/mL}$ is near 10 times larger than the proportion of glycosylated flavonoids contained in 10 μL of a flavonoid fraction solution at 1 mg/mL .

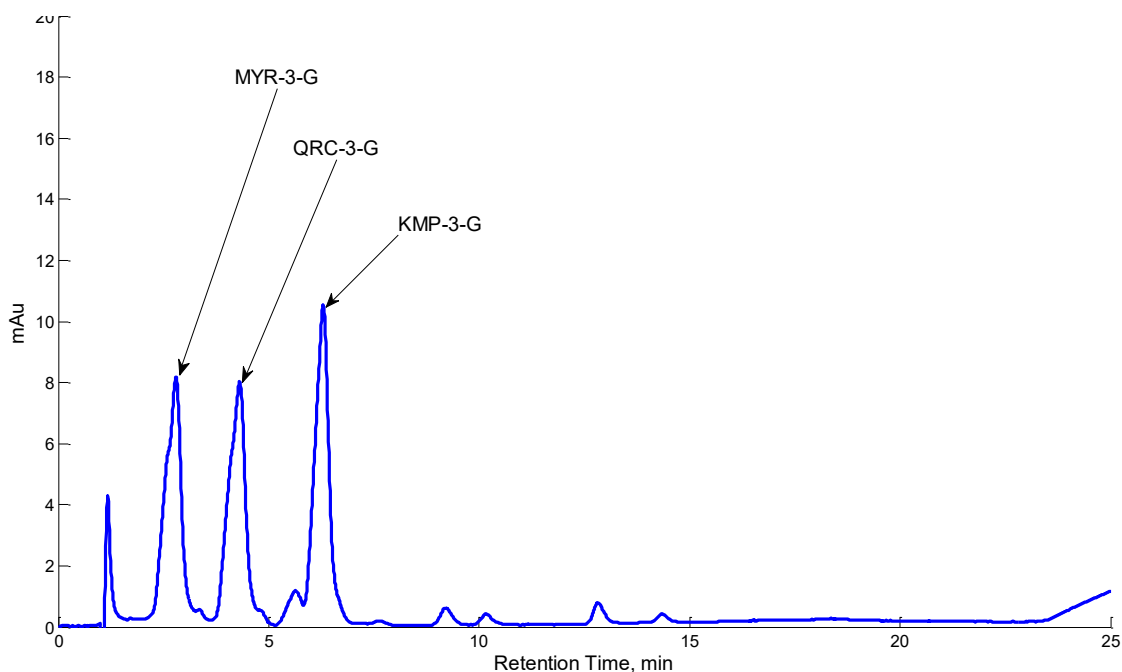


Figure 4-8. Chromatogram and quantification of flavonoid fraction at 1 mg/mL . The three main glycosylated flavonoids are detected, myricetin – 3 glucoside (MYR-3-G), quercetin – 3 glucoside (QRC-3-G), kaempferol – 3 glucoside (KMP-3-G).

4.5 CYTOTOXICITY ASSAYS AND IC_{50} DETERMINATION

4.5.1 CYTOTOXIC EFFECTS OF BLACK BEAN EXTRACT

The Figure 4-9 depicts a comparison of the IC_{50} values determined for OCI-Ly7 cell line and SU-DHL-4 cell line using the BBE as a treatment. The cytotoxicity waveforms are reported in Appendix C, Figures C-1 and C-2. There is not research reported in which black

bean extract were tested as a treatment in OCI-Ly7 cell line and SU-DHL-4, not even on B-lymphoma cell lines.

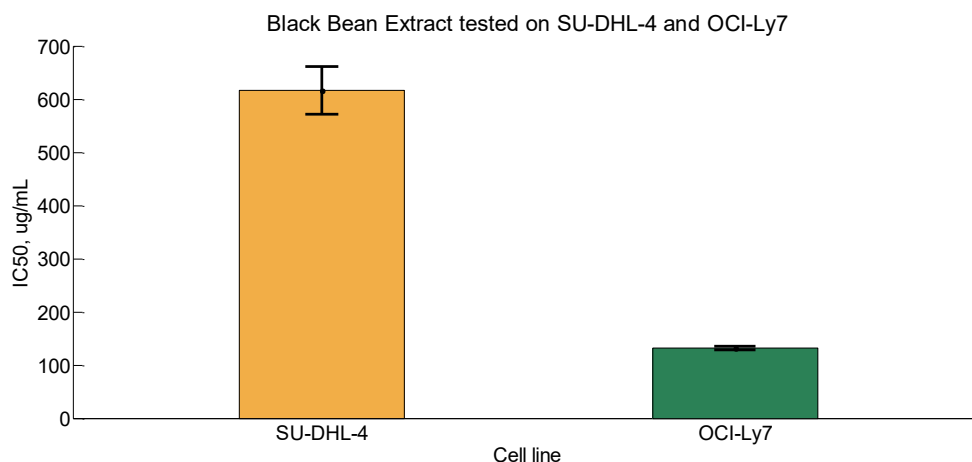


Figure 4-9. IC₅₀ comparison of SU-DHL-4 (orange bar) and OCI-Ly7 (green bar) treated with Black bean extract.

The IC₅₀ values determined for BBE were 131 ± 3.9 µg/mL for OCI-Ly7 cell line and 617.7 ± 45 µg/mL for SU-DHL-4 cell line.

In Table 4-4 it is described the proportion of glycosylated flavonoids contained in the IC₅₀ values reported for SU-DHL-4 and OCI-Ly7 cell lines. In order to calculate these proportions BBE and FF were analyzed by HPLC at their respective IC₅₀ values, and then areas under each peak were extracted from the chromatogram analysis and then substituted in Equations 8, 9 and 10 mentioned in section 4.1.4.

Table 4-4. Proportion of glycosylated flavonoids contained in the IC₅₀ values reported for SU-DHL-4 and OCI-Ly7 cell lines treated with BBE.

Cell line	IC ₅₀ , µg/mL	Myricetin - 3 glucoside, µM (equivalents of myricetin)	Quercetin - 3 glucoside , µM. (equivalents of quercetin)	Kaempferol - 3 glucoside, µM (equivalents of kaempferol)
SU-DHL-4	617	82.71	50.77	65.33
OCI-Ly7	131	21.76	13.51	14.16

4.5.2 CYTOTOXIC EFFECTS OF THE FLAVONOID FRACTION

The Figure 4-10 depicts a comparison of the IC₅₀ values determined for OCI-Ly7 cell line and SU-DHL-4 cell line using the FF as a treatment. The IC₅₀ values determined for the FF were 153.9 ± 7.1 µg/mL for OCI-Ly7 cell line and 272.5 ± 18.2 µg/mL for SU-DHL-4 cell line.

In Table 4-5 it is detailed the proportion of glycosylated flavonoids contained in the IC₅₀ values reported for SU-DHL-4 and OCI-Ly7 cell lines. The proportions were calculated in the same way as BBE.

Table 4-5. Proportion of glycosylated flavonoids contained in the IC₅₀ values reported for SU-DHL-4 and OCI-Ly7 cell lines treated with BBE

Cell line	IC ₅₀ , μg/mL	Myricetin - 3 glucoside, μM (equivalents of myricetin)	Quercetin - 3 glucoside , μM. (equivalents of quercetin)	Kaempferol - 3 glucoside, μM (equivalents of kaempferol)
SU-DHL-4	617	4.8	2.8	2.3
OCI-Ly7	131	2.9	1.8	1.3

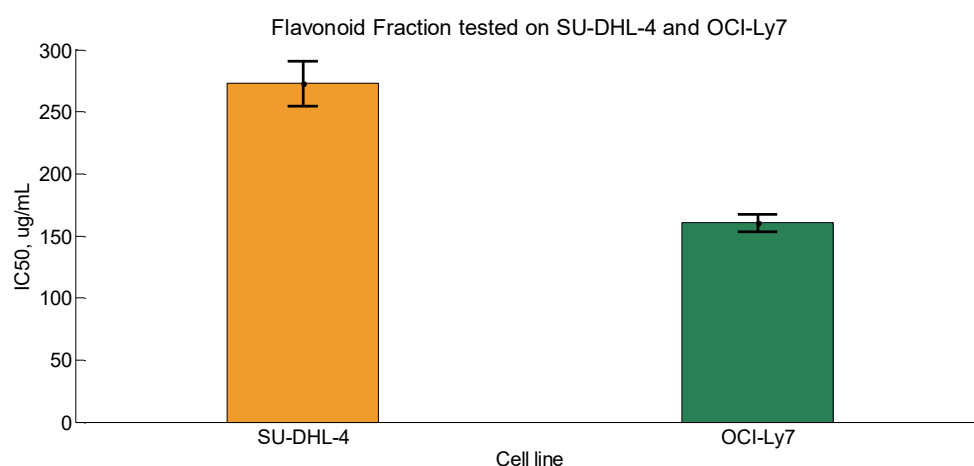


Figure 4-10. IC₅₀ comparison of SU-DHL-4 (orange bar). and OCI-Ly7 (green bar) treated with flavonoid fraction.

Among the three fractions obtained from BBE (phenolic acids, FF and SF), the FF was the most effective fraction to inhibit cell proliferation SU-DHL-4 and OCI-Ly7 cell lines. The phenolic acids fraction was ruled out due because it presented the highest cytotoxic activity at concentrations of 3.3 mg/mL resulting in 80% of viable cells after treatment in both cell lines, this cytotoxicity assay is included in Appendix C, Figure C-5.

It was also tested that the FF is not as toxic to healthy cells such as NIH3T3 and VERO cells as it is to SU-DHL-4 and OCI-Ly7 lymphoma cells. In the cytotoxic assays performed in NIH3-T3 and VERO cell lines treated with the FF it was determined that the mean viability after 48 hrs of incubation was 65.74 ± 10.25 % and 80.42 ± 4.36 % respectively. These viability assays are included in Appendix C, figures C-14 and C-15.

SF was also discarded because of IC_{50} value obtained was higher than 6 mg/mL for OCI-Ly7 cells. In the case of SU-DHL-4 cells, the SF did not present toxicity at any of the tested concentrations. This cytotoxicity assay is included in Appendix C, Figure C-6.

As well as BBE, FF has not been reported before as a cytotoxic agent on OCI-Ly7 cell line and SU-DHL-4, or any other B-lymphoma cell lines. Cytotoxicity waveforms for each assay are reported on appendix C, Figures C-3 and C-4. In comparison with studies in different cell lines the Black bean extract has demonstrated cytotoxicity in human colon cancer (Caco-2) cells (IC_{50} value = 190 ± 10 μ g/mL), and in human liver cancer (HepG2) cells (IC_{50} value = 508 ± 12 μ g/mL) [10].

4.5.3 CYTOTOXIC EFFECTS OF MYRICETIN, QUERCETIN AND KAEMPFEROL STANDARDS

Figure 4-11 details a comparison of the IC_{50} values obtained for both cell lines treated with myricetin, quercetin and kaempferol. Where quercetin resulted as the most cytotoxic flavonoid for SU-DHL-4 and OCI-Ly7 cell lines (IC_{50} = 37.09 ± 2.75 μ M for SU-DHL-4 and IC_{50} = 33.03 ± 0.74 μ M for OCI-Ly7).

For kaempferol, the IC_{50} value obtained for SU-DHL-4 cell line (58.9 ± 5.22 μ M) was lower than the IC_{50} value obtained for OCI-Ly7 cell line (61.837 ± 0.82 μ M). It must be emphasized that, among all the treatments tested, kaempferol was the only one to be more effective in SU-DHL-4 cell line than in OCI-Ly7. This result was not expected since SU-DHL-4 cell line has been characterized as a resistant cell line among others diffuses histiocytic lymphomas [16].

In the case of myricetin the IC_{50} value obtained for OCI-Ly7 cell line (97.97 ± 0.94 μ M) was lower than the IC_{50} value obtained for SU-DHL-4 cell line (119.35 ± 4.26 μ M).

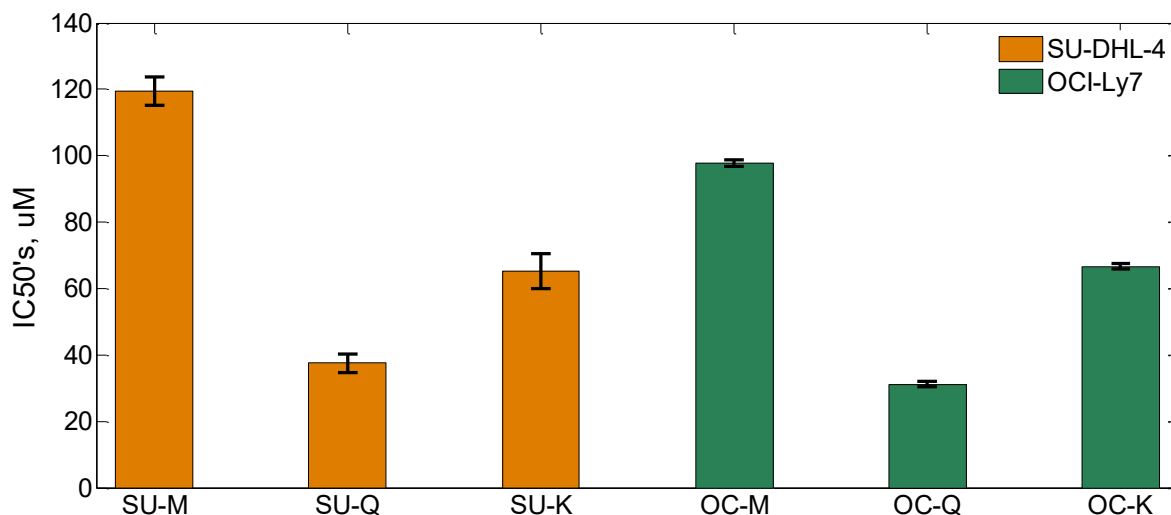


Figure 4-11. IC₅₀ values comparison between SU-DHL-4 (orange bars) & OCI-Ly7 (green bars) treated with aglycones, myricetin (M), quercetin (Q), kaempferol (K). Bars represent the estimated IC₅₀. Errors are given as 95% confidence interval.

For both cell lines (SU-DHL-4 and OCI-Ly7) quercetin resulted as the most cytotoxic treatment, followed by kaempferol and as the less cytotoxic compound, myricetin.

None of these compounds (myricetin, quercetin and kaempferol) have been tested in SU-DHL-4 and OCI-Ly7 cell lines before. However, myricetin and quercetin have shown cytotoxic activity against Daudi cells and against human CEM cells reporting IC₅₀ values among 13-25 μ M [17]. Daudi cells are classified as a Burkitt's lymphoma cell line such as the OCI-Ly7 cell line we are working with. And human CEM line is classified as T cells of acute lymphoblastic leukemia. In both cell lines (Daudi and CEM) quercetin was more cytotoxic than myricetin.

Quercetin has been tested in several cell lines and it has proved to develop cytotoxicity. A comparison of the IC₅₀ values determined in different cell lines treated with quercetin is shown in Table 4-6. Quercetin has also been tested in oral cancer cells (SCC-9) and the IC₅₀ value was determined as 94 μ M at 48 h of incubation [26].

**Table 4-6 . IC₅₀ values determined for different cell lines treated with quercetin.
Taken from [28].**

Malignant Cell line	IC₅₀
Bladder	Not given
Breast (MDA-MB-435)	55 μ M
Breast (MDA-MB-468)	21 μ M
Breast (MDA-MB-435)	31 μ M
Breast (MCF-7)	4.9 μ M
Breast (MCF-7)	15 μ M
Colon (HT29 and Caco-2)	45-50 μ M
Colon (HT29 and Caco-2)	30-40 μ M
Gastric (HGC, NUGC, MKN-7 and MKN-28)	32-55 μ M
Head and neck (HTB43)	Significant Inhibition above 100 μ M
Head and neck (HTB43 and CCL 135)	Significant Inhibition above 100 μ M
Leukemia (14 AML lines and four ALL lines)	Average IC ₅₀ = 2 μ M
Leukemia (CML line K562)	59 μ M
Lung (non-small-cell lines)	0.45 - 2.28 μ M
Melanoma (MNT1, M10, M14)	7 nM, 20 nM, 1-10 μ M
Ovarian (OVCA 433)	10 μ M

Kaempferol has been found as cytotoxic to two human pancreatic cancer cells (PaCa-2 and Panc-1 cells) the IC₅₀ values reported were 35 μ M for PaCa-2 and 70 μ M for Panc-1 [29].

4.5.4 CYTOTOXIC EFFECTS OF PURIFIED GLYCOSYLATED FLAVONOIDS

Figure 4-12 details a comparison of the IC₅₀ values obtained for OCI-Ly7 cell line treated PGF and aglycones. The PGF were no effective against SU-DHL-4 cell line, in the range of concentrations tested. As regards OCI-Ly7 cell line, all IC₅₀ values obtained were greater in comparison with the IC₅₀ values of the aglycones. The IC₅₀ value determined for quercetin – 3 glucoside, was 4-times greater (141.8 ± 2.59 μ M). In the case of kaempferol – 3 glucoside, the IC₅₀ value was 2- times greater (127.3 ± 2.69 μ M). And regarding myricetin – 3 glucoside the IC₅₀ value was 1.6 times greater (163.47 ± 4.39 μ M).

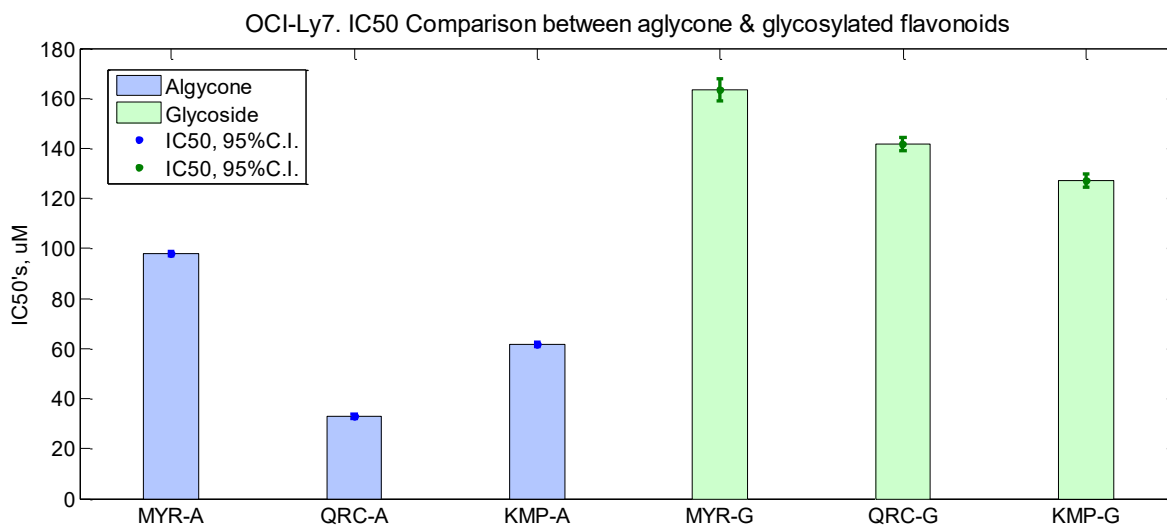


Figure 4-12. IC₅₀ comparison of OCI-Ly7 treated with aglycone (A) and glycosylated flavonoids (G). Bars represent the estimated IC₅₀. Errors are given as 95% confidence interval.

The IC₅₀ values determined for the PGF are 3-times higher compared with the calculated content of glycosylated flavonoids in BBE and at least 100-times higher compared with the calculated content of glycosylated flavonoids in the flavonoid fraction. It is suggested that the three PGF are synergized by them self or some other unidentified components of the extract are interacting too.

In general, myricetin, quercetin and kaempferol presented more cytotoxic activity than the PGF.

4.5.5 CYTOTOXIC EFFECTS OF FLAVONOIDS COMBINATIONS

In figure 4-13 it is described the contour plot of the IC_{50} values obtained in the cytotoxic assays of OCI-Ly7 treated with the combinations of myricetin, quercetin and kaempferol. The best combination was quercetin-kaempferol followed by myricetin-quercetin-kaempferol demonstrating synergistic effects. None of rest of the combinations presented better IC_{50} values than the ones determined for quercetin or for kaempferol as single compounds.

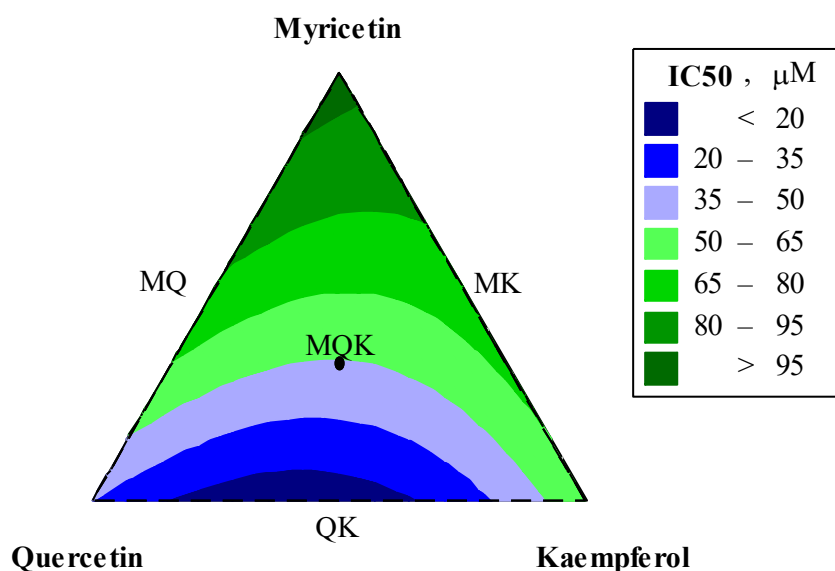


Figure 4-13 Contour plot of the IC_{50} values (μM) obtained from flavonoids combinations.

In Table 4-7 is detailed the estimated concentration of each flavonoid when it was mixed. In the case of the combination quercetin-kaempferol, the cytotoxicity of kaempferol was increased 3-times in combination with quercetin and the cytotoxicity of quercetin was increased 1.7-times in combination with kaempferol.

The combinations of myricetin-quercetin and myricetin-kaempferol showed that myricetin cytotoxicity was enhanced but the cytotoxicity of quercetin or kaempferol was diminished. For the three flavonoid combination, myricetin and kaempferol improved in the presence of quercetin, and quercetin did not show any cytotoxicity change.

Table 4-7. IC₅₀ values obtained in the cytotoxic assay with flavonoids combinations with OCI-Ly7 cell line

Combinations Single Flavonoid	OCI-Ly7 [IC ₅₀ , μ M]		
	Myricetin	Quercetin	Kaempferol
Myricetin & quercetin	41.61	43.82	--
Myricetin & kaempferol	38.79	--	43.12
Quercetin & kaempferol	--	9.53	10.06
Myricetin & quercetin & kaempferol	10.03	10.57	11.16

4.6 CELLULAR APOPTOSIS ASSAY

To determine the capability of a cytotoxic agent to induce apoptosis and also that I does not causes necrosis are the two fundamental conditions to be fulfilled in order to evaluate a treatment as a possible anticancer drug. In this section it is described that BBE, FF, myricetin, quercetin and kaempferol induces apoptosis in both SU-DHL-4 and OCI-Ly7 cell lines and also it is demonstrated that they do not produce necrosis.

In Figure 4-14 depicts OCI-Ly7 cells treated with FF after 24 h of incubation. 51.8% of cells still viable, 44.6% are apoptotic cells (33.4% in early apoptosis, 11.2 % in late apoptosis) and 3.6% cells are undergoing necrosis. Figures 4-13, 4-14 and 4-15 detail population of OCI-Ly7 cells treated with myricetin, quercetin and kaempferol respectively.

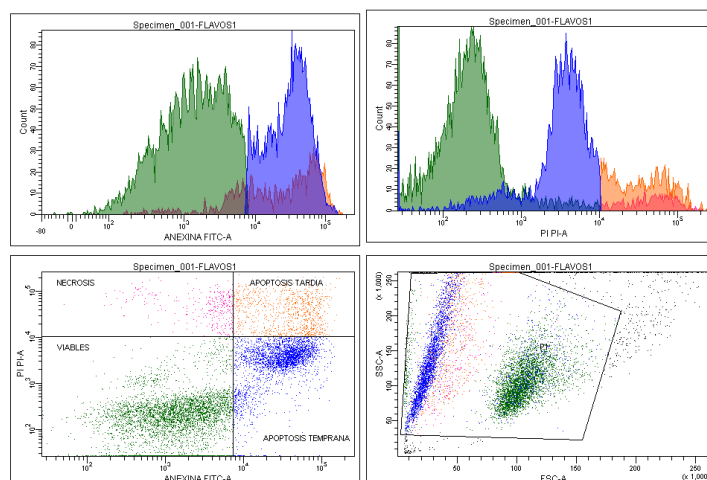


Figure 4-14. Apoptosis Assay of OCI-Ly7 cells treated with flavonoid fraction.

The Table 4-8 details the apoptosis analysis results for SU-DHL-4 and OCI-Ly7 cell lines. In this table it is detailed the percentage of the cellular population undergoing apoptosis as well as necrosis. The no treatment control was included to show that even if cells were no treated some percentage population undergoes necrosis as a consequence of the staining procedure. As well as the cytotoxicity assay there is no literature reported of the BBE or the FF used as treatments to evaluate apoptosis in B-cell lymphomas.

Table 4-8. Apoptosis Assay. Register of cell population undergoing apoptosis after treatment, 24 h of incubation.

Populations	OCI-Ly7			SU-DHL-4		
	Viable Cells	Apoptosis	Necrosis	Viable Cells	Apoptosis	Necrosis
No treatment	90.10 \pm 1.15	8.97 \pm 0.86	0.97 \pm 0.25	86.30 \pm 0.61	12.23 \pm 0.59	1.50 \pm 0.20
Black bean extract	60.13 \pm 11.21	37.23 \pm 10.36	2.63 \pm 1.06	56.20 \pm 6.54	41.23 \pm 7.27	2.57 \pm 0.76
Flavonoid fraction	59.27 \pm 11.86	39.33 \pm 12.51	1.43 \pm 0.83	43.63 \pm 4.56	54.63 \pm 4.88	1.70 \pm 0.46
Myricetin	65.37 \pm 8.36	33.00 \pm 8.05	1.63 \pm 0.50	56.50 \pm 13.46	41.07 \pm 13.07	2.40 \pm 0.70
Quercetin	54.37 \pm 6.26	43.63 \pm 6.31	2.00 \pm 1.44	50.17 \pm 2.20	46.80 \pm 1.47	3.03 \pm 0.86
Kaempferol	55.17 \pm 6.80	43.50 \pm 7.06	1.33 \pm 0.51	55.17 \pm 6.80	43.50 \pm 7.06	1.33 \pm 0.51

Figures 4-15, 4-16 and 4-17 depicts the results of the apoptosis assay for myricetin, quercetin and kaempferol respectively.

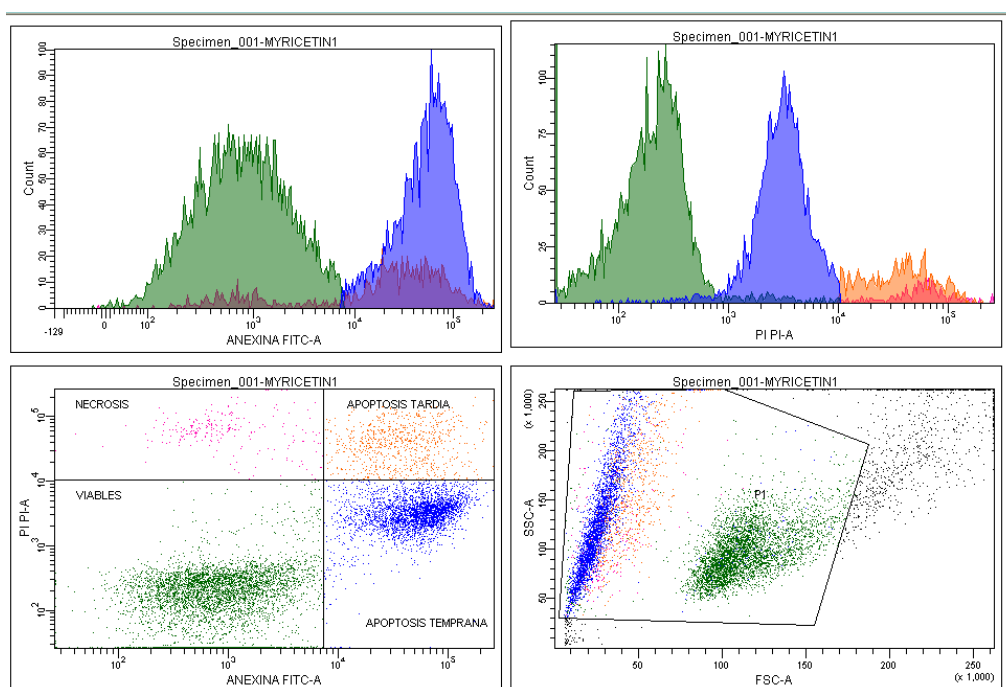


Figure 4-15. Apoptosis Assay of OCI-Ly7 cells treated with Myricetin.

[20] reported that quercetin induce apoptosis if it is administered to cells at concentrations higher than 20 μ M. This was tested in HRC57 cell line (human B-cell line), DoHH2 (diffuse large b cell lymphoma), RPMI-8226 and U266 (both myeloma cell lines). In the case of myricetin and kaempferol [20] reported that both have a similar function as an apoptosis inducers.

It has also been demonstrated that quercetin induces apoptosis at 25 μ M in human chronic myeloid K562 cells and acute lymphoblastic leukemia HSB-2 cells [21].

Comparing with different cell lines myricetin, quercetin and kaempferol induced apoptosis in human esophageal squamous cell carcinoma (KYSE-510 cells) [22].

In comparison with studies in different cell lines, quercetin induced apoptosis in oral cancer cells SCC-9 at 50 μ M [26].

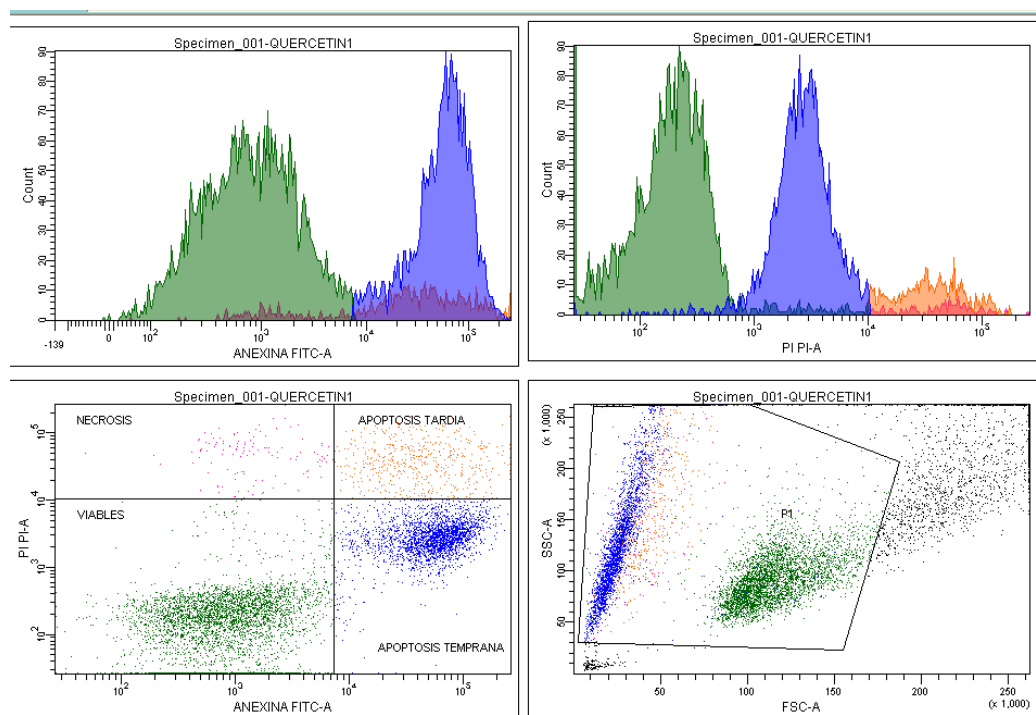


Figure 4-16. Apoptosis Assay of OCI-Ly7 cells treated with Quercetin.

Kaempferol has been found as to induce apoptosis in human pancreatic cancer cells at 35 μ M [29].

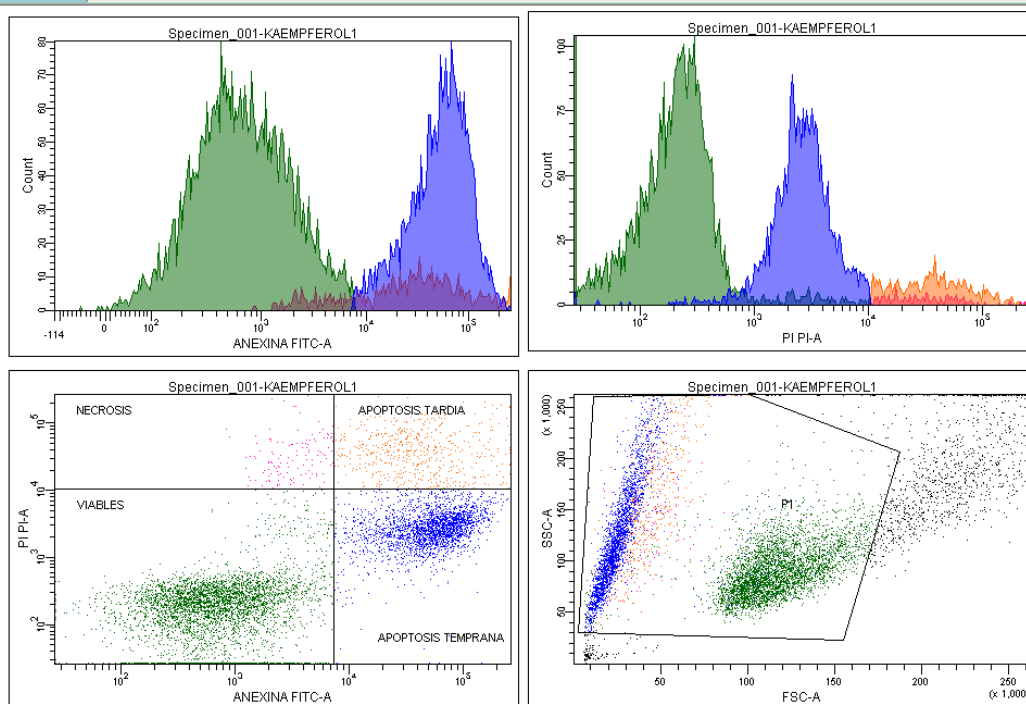


Figure 4-17. Apoptosis Assay of OCI-Ly7 cells treated with Kaempferol.

We demonstrated that BBE and FF, as well as all myricetin, quercetin and kaempferol, lead SU-DHL-4 and OCI-Ly7 cells to Apoptosis which is the primarily act of chemotherapy and radiotherapy. And also it is discarded the induction of necrosis.

4.7 BAX PROTEIN ASSAY ANALYSIS

Figure 4-18 illustrates three populations as a result of the treatment of flavonoids (blue, yellow and purple). Blue population represents cells that remains viable, purple population as well as yellow represents cells undergoing apoptosis. As we mentioned in the apoptosis section, the side scatter help us to identify the displacement of populations. This contour plot indicates that there are three different distributions with three different means of Dyligh signal. Table 4-12 details the statistical difference between groups.

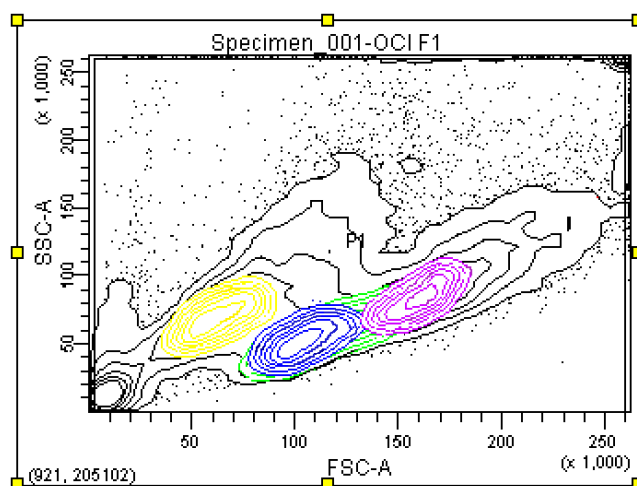


Figure 4-18. Flow Cytometry contour plot analysis for OCI-Ly7 with treatment of flavonoids fraction.

Figures 4-19 & 4-20 depict how Bax expression as incubation time changes. We can see that OCI-Ly7 has a significant increase in the expression of the Bax protein at 48 h of incubation with the flavonoid extract, in contrast with SU-DHL-4 cell line which present the highest expression at 12h of incubation. As we can compare in table 4-11 the blue population (will be the viable group) is not different ($p > 0.05$) to the untreated cells but the blue and yellow populations (which we can say that they are undergoing apoptosis because of the size change and positioning in the plot) they are different with $p < 0.05$.

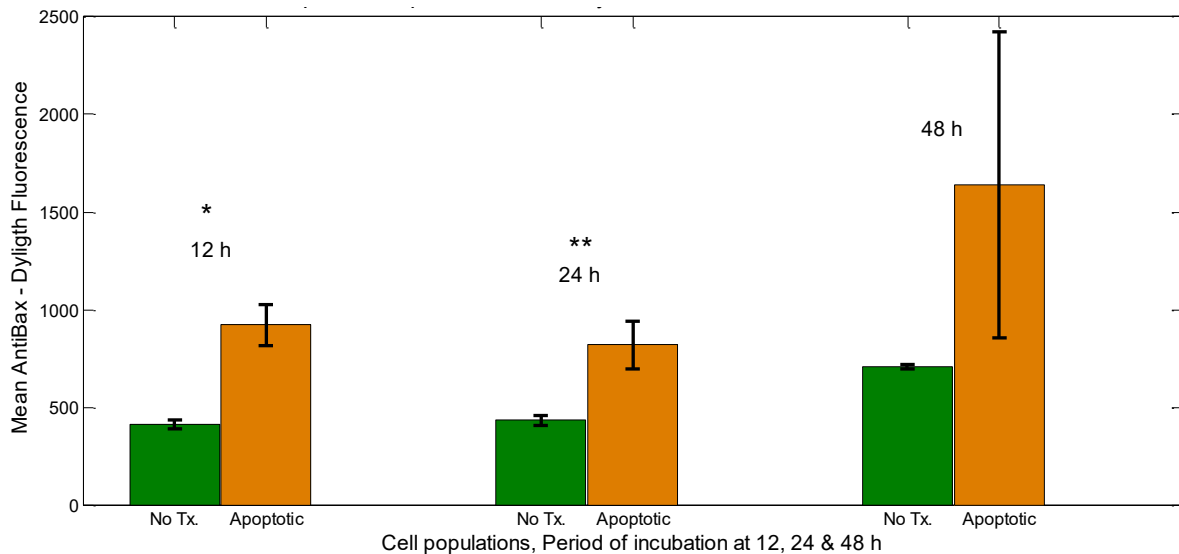


Figure 4-19. Bax protein mean expression of OCI-Ly7 cells treated with flavonoid fraction. Statistical difference between apoptotic cells (orange bars) and no treated cells (green bars) groups with $P=0.021(*)$ and $P = 0.01()$. Bars represent the mean intensity of Anti-Bax-Dylight signal at 12 h, 24 h and 48 h of incubation time. Errors are given as 95% confidence interval.**

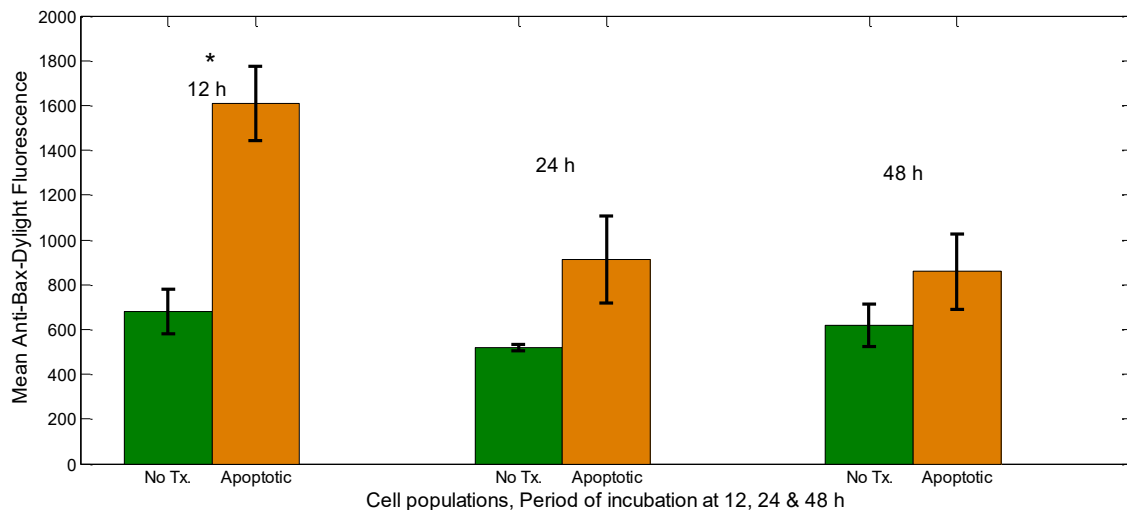


Figure 4-20. Bax protein expression of SU-DHL-4 cells treated with flavonoid fraction. Statistical difference between apoptotic cells (orange bars) and no treated cells (green bars) groups with $P=0.01(*)$. Bars represent the mean intensity of Anti-Bax-Dylight signal at 12 h, 24 h and 48 h of incubation time. Errors are given as 95% confidence interval.

For both untreated cell lines there was an increment in bax expression which could be the result of the stress caused by the conditions and treat received when the 12 well plate was set up.

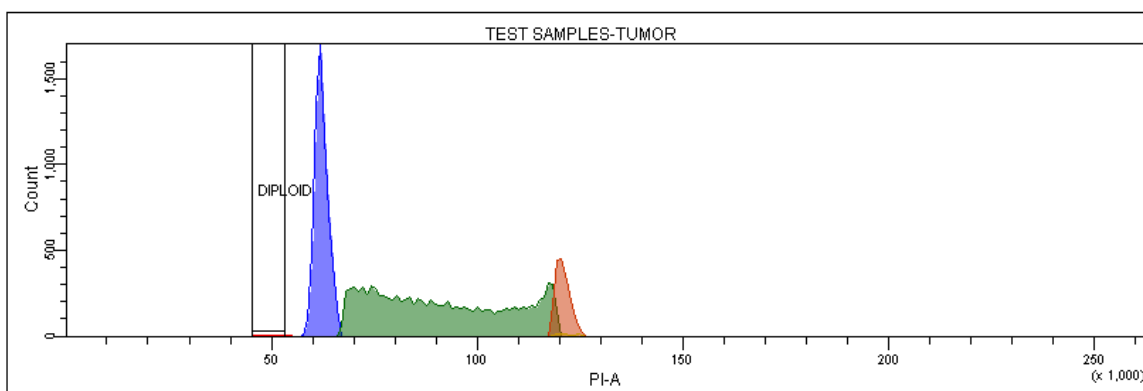
We present statistical information that become the bax protein expression evident, the mechanism of apoptosis activation remains uncertain however. These results are consistent with other studies [33], which reported that quercetin increased Bax levels and reduced the total levels of Bcl-2 protein in HT-29 cells. Pro-apoptotic Bax is one of the direct targets of p53, Bax is an apoptotic protein, and Bcl-2 an antiapoptotic protein.

4.8 CELL CYCLE ANALYSIS

In figure 4-21A, it is depicted a regular set of histograms representing the cell cycle phases of a not treated OCI-Ly7 cells. The percentage of populations for each cell cycle phase was determined as 30.4% for G0/G1 phase, 51.4% for S phase and 9.5% for G2/M phase.

The Figure 4-21B details the histograms representing the cell cycle phases of OCI-Ly7 cells treated with myricetin after 24 h of incubation. All the concentrations tested were at the IC₅₀ determined in the cytotoxicity assays. The percentage of populations for each cell cycle phase was determined as 11.7% for G0/G1 phase, 28.4% for S Phase and 0.4% for G2/M phase. This corresponds to a reduction calculated as 40% for G0/G1 population, 44.7% for S population and a 95% for G2/M population.

A



B

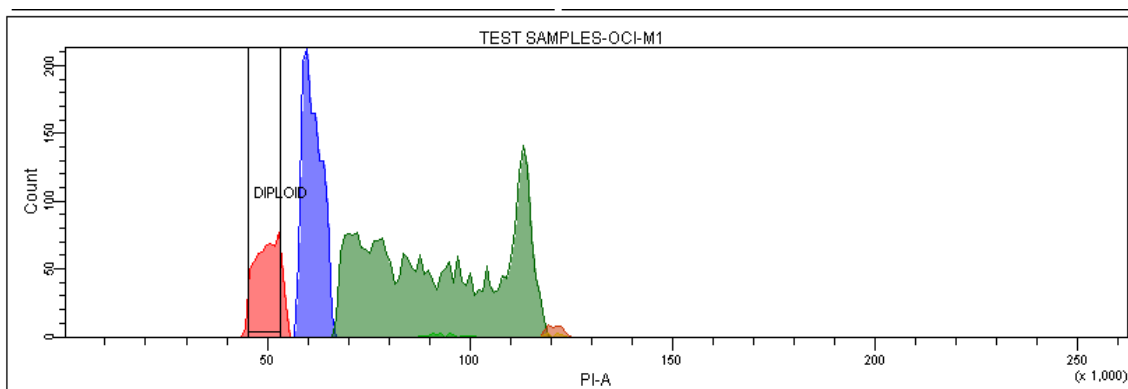


Figure 4-21. Cell Cycle Analysis of OCI-Ly7 cells treated with Myricetin (B) in comparison with untreated OCI-Ly7 cells (A).

On figure 4-22 it is depicted the difference between treatments in comparison with untreated cells at G0/G1 phase, S phase and G2/M phase. Graphic bars represent the mean population of each treatment at the cell cycle phase indicated and the error bars stands for standard deviation.

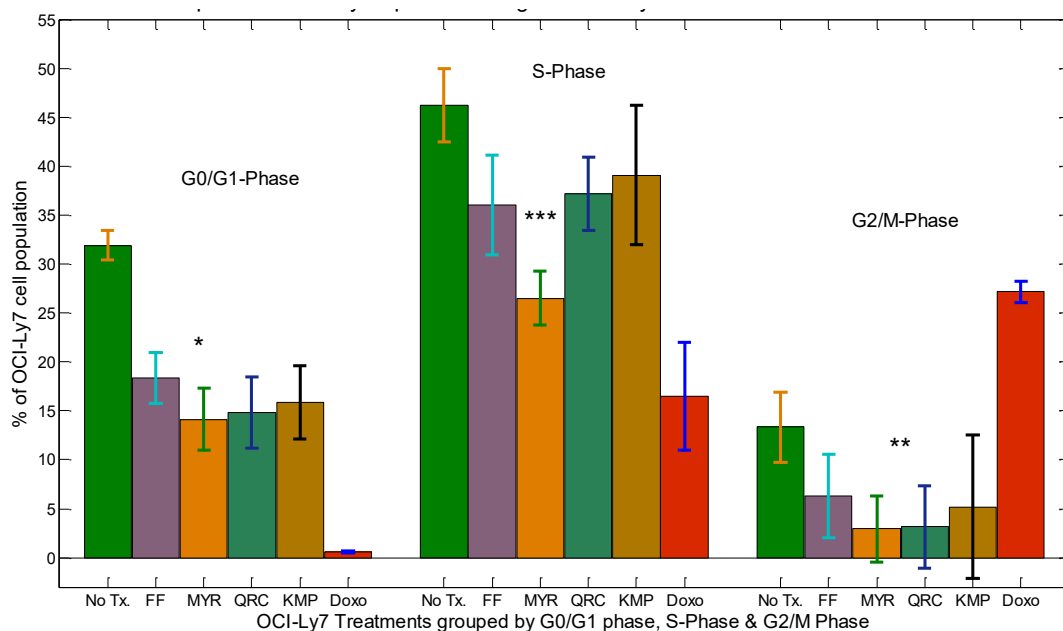


Figure 4-22. Comparison of cell cycle phases changes in OCI-Ly7 cell line treated with Flavonoid fraction (FF), myricetin (MYR), quercetin (QRC), kaempferol (KMP) & Doxorubicin (Doxo). Bars represent the percentage of the cell population present in its respective cell cycle phase. Error bars represent the standard deviation.

Among all the treatments myricetin showed to be the most effective, it presented cell arrestment activity in all cell cycle phases. Myricetin was tested at the IC_{50} determined in the cytotoxicity assay which was 97.76 μM

The highest activity was identified at S and G0/G1 phases where myricetin was able to reduce S population to a 28.4% out of 51.4% (p-value = 0.006), and G0/G1 population was reduced to 11.7% out of 30.4% (p-value = 0.01). However, the G0/G1 arrest of myricetin was not as effective as the control with doxorubicin which reduced G0/G1 population to 0.6% out of 31.8% (p-value = 0.0005).

Other studies reported that quercetin was able to arrest human leukemic T-cells in the late G1 phase of the cell cycle at a 70 μM [27]. In comparison with our results, quercetin

arrested G0/G1 phase at 30 μ M. Therefore quercetin is more effective arresting G0/G1 phase in lymphoma B-cells than in leukemic T-cells.

In comparison with studies in different cell lines, quercetin arrests G1 phase in oral cancer cells at 50 μ M [26], The G1 population was reduced to 20% out of 55%.

It has been reported that doxorubicin mainly arrest G2/M phase [30], [31], however the population in G2/M phase may seem increased rather than decreased, previous research has reported that when a population is increased in comparison with the no treatment control, it is that the treatment may be involved with the phase checkpoint arrest [32]. The same study reported that doxorubicin may also arrest S and G1 phase due to its capacity to intercalate DNA and inhibit topoisomerase II [32].

Comparing with different cell lines myricetin, quercetin and kaempferol induced cell cycle arrest G2/M in human esophageal squamous cell carcinoma (KYSE-510 cells) [22].

Table 4-12 details the statistical difference between treated and untreated cells, for instance, OCI-Ly7 population in G0/G1 phase treated with flavonoid fraction is less than untreated OCI-Ly7 population in G0/G1 phase being statistically different with a p-value = 0.006 according to a two tailed t-paired test.

All treatments showed significant G0/G1 phase arrest ($p < 0.05$). The flavonoid fraction along with myricetin were the only treatments that reduced S phase with a significant difference ($p < 0.05$). As regards G2/M phase the flavonoid fraction was the only treatment that showed significant arrest (p-value = 0.048). However it is suggested to perform the cell cycle assay at different incubation times.

The cell cycle analysis of the treatments; FF, myricetin, quercetin and kaempferol on both SU-DHL-4 and OCI-Ly7 cell line are included in Appendix E Figures E-1 to E-7. In Appendix E is included the raw data of each assay in Table E-1.

Table 4-9 Cell cycle analysis. Statistical difference between treated and untreated OCI-Ly7 cells.

Treatment\OCI-Ly7 Phases	p- values		
	G0/G1	S	G2/M
Flavonoid fraction	0.006	0.045	0.048
Myricetin	0.011	0.006	0.052
Quercetin	0.017	0.053	0.082
Kaempferol	0.016	0.213	0.103
Doxorubicin	0.001	0.019	0.007

4.9 CHARACTERIZATION OF ANIMAL MODEL

We reported that 7 mice out of 9 from the OCI-Ly7 group developed tumors as a result of the OCI-Ly7 cell line inoculation this is a 77% of success in comparison to the 60 % reported in [36]. There was only one mouse that developed tumor as a result of the inoculation with the SU-DHL-4 cell line in the period of experimentation. It is suggested to extent the study of SU-DHL-4 cell line for one month more due to SU-DHL-4 cell line has a slower growth rate in comparison with OCI-Ly7 cell line.

Figure 4-23 shows the tumor masses extracted from OCI-Ly7 inoculated mice.

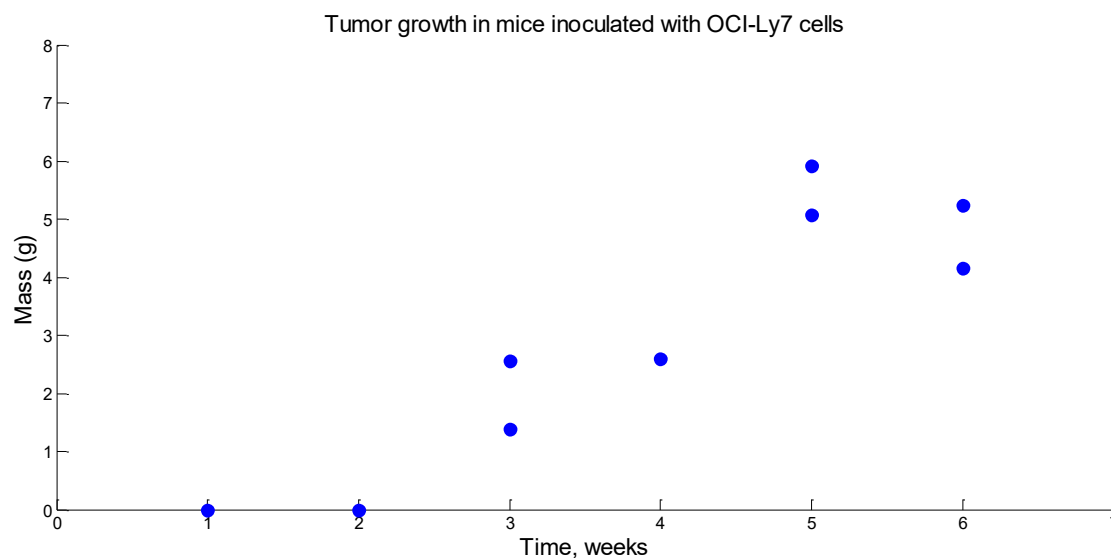


Figure 4-23 . Tumor growth of mice inoculated with OCI-Ly7 cells. Each dot in the graphic represents the complete tumor mass for one mouse. At weeks 3, 5 and 6 two mice were sacrificed.

After three weeks since inoculation, for OCI-Ly7 inoculated mice, tumor was detectable at bear sight. In the autopsies it was found that from all the mice that developed tumors, all of them presented subcutaneous tumor and two of them developed also intraperitoneal tumors.

Figure 4-24A depicts a mouse with intraperitoneal tumor 6 weeks after inoculation. Figure 4-24B depicts a mouse with subcutaneous tumor 6 weeks after inoculation and Figure 4-24C shows a control mouse without inoculation.

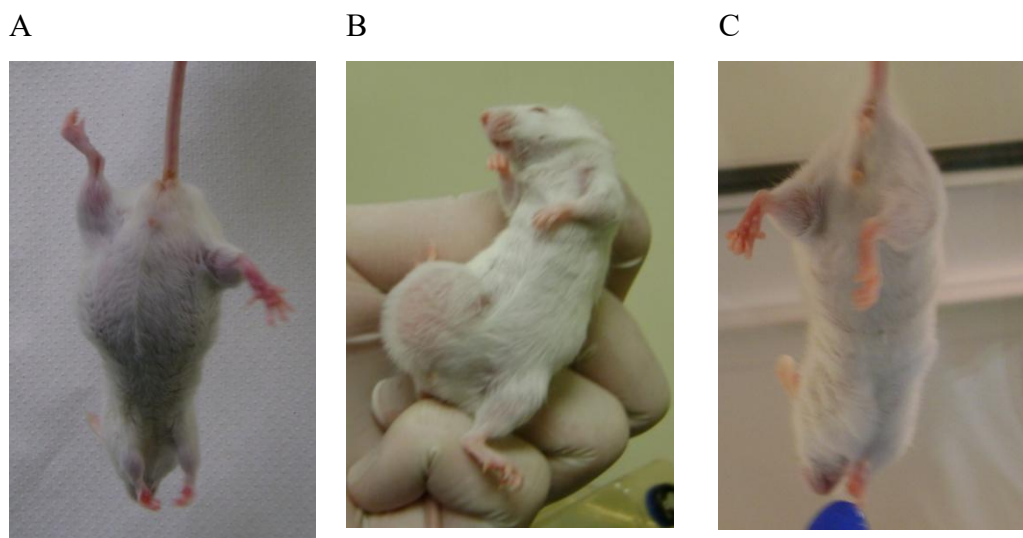


Figure 4-24. Presence of tumors in mice inoculated with OCI-Ly7 cell line in comparison with a control mouse without inoculation. A. Intraperitoneal tumor. B. subcutaneous tumor. C. Control mouse.

The Figure 4-25 depicts a the average weight of the mice control group (without inoculation) in comparison with the group of inoculated mice with the OCI-Ly7 cell line. without inoculation. The 0 day is the date of inoculation. It is demonstrated that there was no statistical change in the weight of mice due to normal growth. It is shown that, 17 days after inoculation, the mice started to earn weight as a response of the tumoral growth.

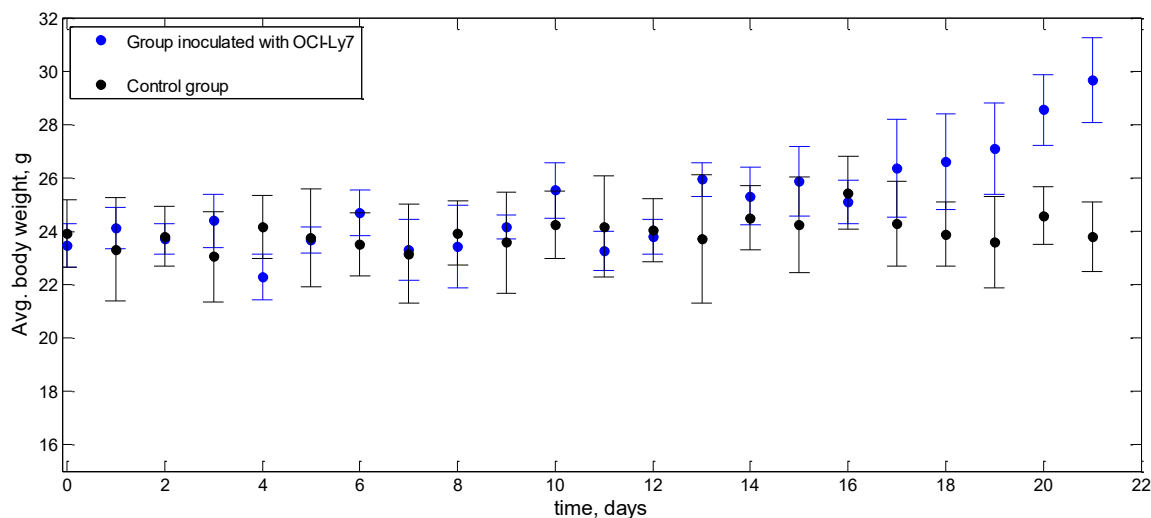


Figure 4-25. Average weight of control mice (without inoculation) in comparison with the inoculated mice, n=8 . Errorbars represent the standard deviation.

Regarding to the evaluation of organs, two mice presented splenomegaly and hepatomegaly and two mice presented an increase in size in the right kidney. In Figures G-1 to G-4 of Appendix F it is detailed the mass measured for each organ. These were isolated cases and in there were three mice that presented tumor that did not presented growth in liver, spleen or kidneys in comparison with the group of controls.

According to the results presented in the characterization of the animal model it was decided to use the OCI-Ly7 cell line for the animal model with treatment and to keep performing the inoculation intraperitoneal due to the rate of success obtained.

4.10 DETECTION OF FLAVONOIDS IN PELLETS

This analysis was performed to administer BBE and FF by embedding them into the pellets. Figure 4-26 depicts the chromatograms for the pellets embedded with flavonoids. The black dotted lines is the chromatogram of a mixture of myricetin, quercetin and kaempferol (standard 5 ppm), which was used to compare retention times. And it is presented that retention times of pellets chromatograms peaks match with standards peaks. Also the maximum absorption wavelengths are confirmed. According to the areas obtained the maximum concentrations of myricetin, quercetin and kaempferol were 3.2 μ M, 6.18 μ M and 4.47 μ M, respectively. These concentrations were the result of embedding the pellet with FF at 20 mg/mL. Here it was decided to increase 10-times the concentration of the FF and also the concentration for the BBE.

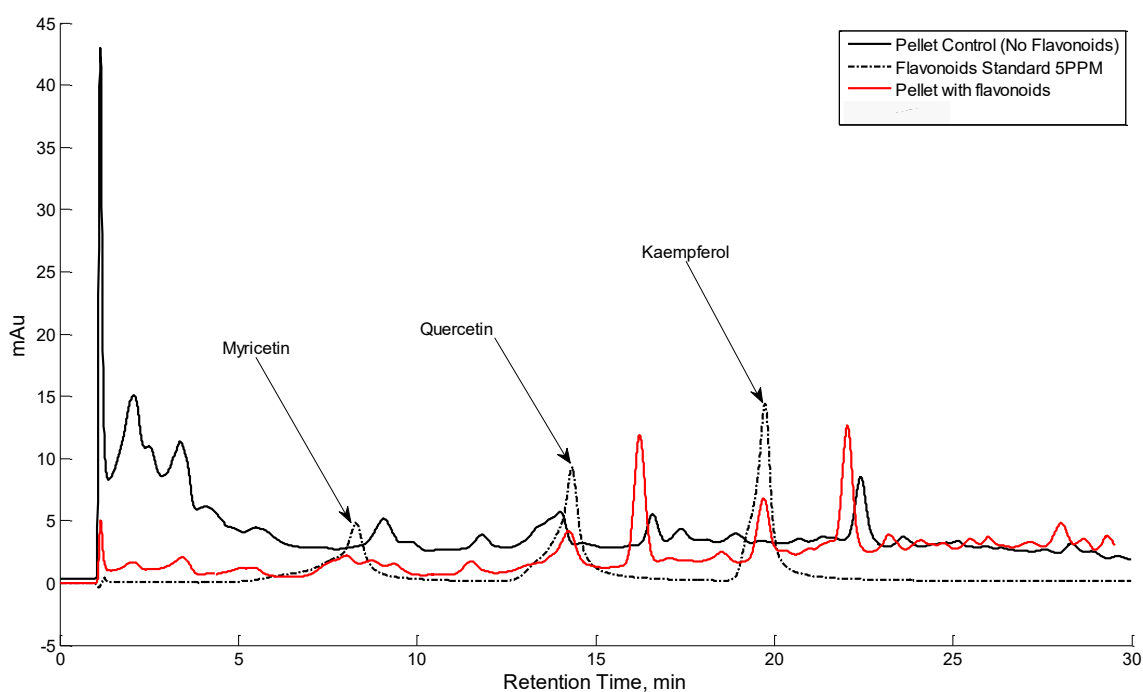


Figure 4-26 Chromatograms obtained at 365 nm to show the presence of flavonoles in pellets.

A group of three CD1 mice were fed with these embedded pellets and each mouse consumed one pellet per day which was the average amount of pellets consumed in the characterization of the animal model (for pellets with a mean weight of 4.5 g). According to

this there was no problem to administrate the BBE and the FF in the pellets. The final concentration of the BBE and the FF within the pellet was 20 mg/mL and 15 mg/mL respectively. Mice consumed approximately one pellet per day then the mean consumption of BBE and FF in one day was 600 µg and 450 µg respectively.

4.11 DETECTION OF FLAVONOIDS METABOLITES IN PLASMA

As it is illustrated in Figure 4-27, there are several peaks product of FF administration. The black chromatogram labeled as Basal (third one from front to back) shows no peak at all, the blue Basal 2 chromatogram has been enriched with quercetin as an internal control to monitor any changes in the plasma samples preparation, and as we can see there is a discrete displacement in the retention time of quercetin peak, which give us some evidence to infer that flavonoids or it metabolites may be displaced as a product of the plasma sample procedure. However, there are several peaks that match with the standard retention time, but the sample concentration was under the detection limit of absorption spectra in order to present second evidence of confirmation.

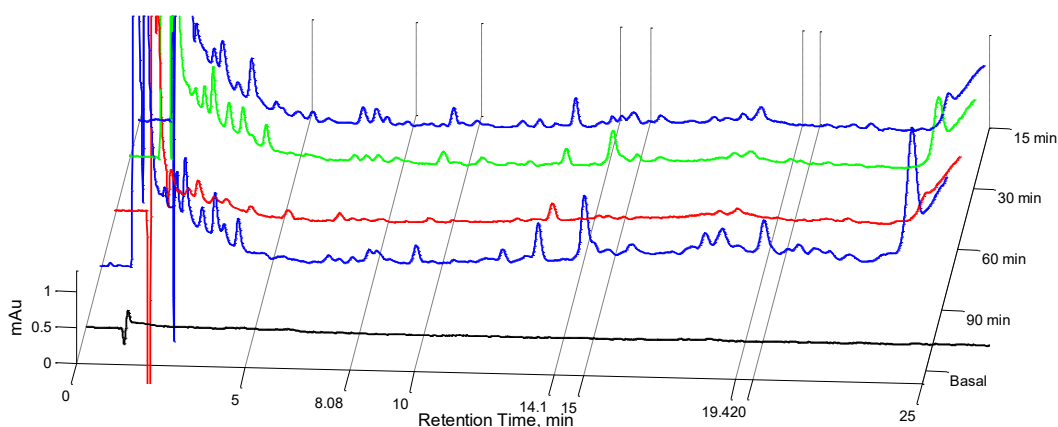


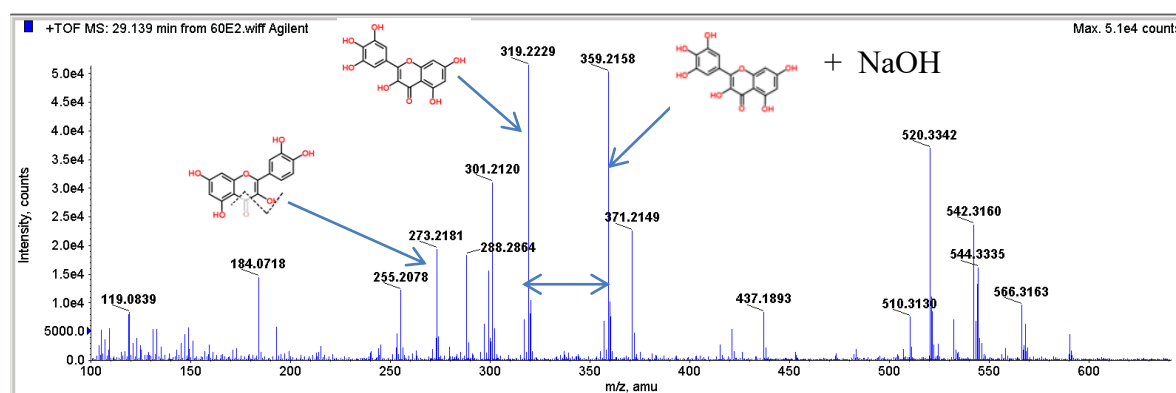
Figure 4-27. Flavonoids profile in plasma samples obtained at 15, 30, 60 and 90 min compared with a mouse simple without flavonoids administration

Unfortunately the amount of plasma that can be drawn from a 30 g mouse is too low and it cannot be detected in such a way to present a legible absorption spectra in a HPLC/DAD analysis to give confirmation of present compounds. Then we proceeded to analyze plasma samples by mass spectrometry.

4.11.1 MASS SPECTROMETRY FLAVONOIDS DETECTION

The Figure 4-28 details the mas spectrum for a mouse plasma sample at 60 minutes of administration of the FF. Figure 4-28 A shows the detection of myricetin aglycone as product of parent ion fragmentation with $m/z=319.22$ [$C_{15}H_{10}O_8$]. An abundant fragment ions was detected with $m/z=273.21$ [$C_{14}H_9O_7$] due to ring cleavage. It was suggested to come as a product of quercetin metabolite fragmentation as it is reported by [35], the mass of the compound that contains this ion was 520.3 and it was not identified. Figure 4-28B shows the detection of kaempferol aglycone as product of parent ion fragmentation with $m/z=287.12$ [$C_{15}H_8O_6$]. the mass of the compound that contains this ion was 435.1 and it was not identified.

A



B

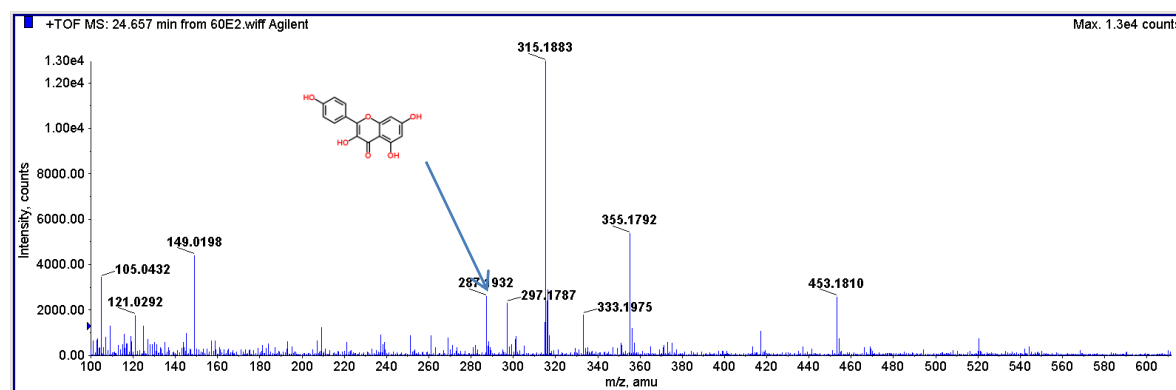


Figure 4-28. A. TOF-MS spectrum of 60 minutes mouse plasma sample. Flavonoids detected were myricetin, kaempferol and a fraction of quercetin.

The identification of the fragment product of ring cleavage has been done based on the results presented by [35].

The metabolites and fragments of flavonoids present in the plasma samples at 15, 30, 60 and 90 mins are summarized In table 4-10 where we can give confirmation the flavonoids have been metabolized and remain present in blood stream giving confirmation with basal mouse who has not flavonoid metabolite or fragment detected.

Table 4-10. Ion fragments detected in mice plasma samples.

Compound proposed	m/z = [M-H] ⁺	Structure	Basal	Blood sample (min)			
				15	30	60	90
Myricetin	319.04	[C ₁₅ H ₁₀ O ₈]	--	√	√	√	√
Quercetin	303.0451	[C ₁₅ H ₉ O ₇]	--	--	--	√	√
Kaempferol	287.0506	[C ₁₅ H ₈ O ₆]	--	√	√	√	√
QRC-fragment	273.21	[C ₁₄ H ₉ O ₇]	--	√	√	√	√

The glycosylated flavonoids were not identified as the parent ions neither the standards. It was suggested that flavonoids, possibly, were metabolized by hepatic glucorinidation or methylation, even intestinal flora may be hydrolyzing them, however the information presented was enough to infer that flavonoid metabolites are present in mice plasma. More research is required to specify exactly what metabolites were found.

4.12 ANIMAL MODEL WITH TREATMENT

Two dates were established as reference points. The day 0 was the day of lymphoma cells inoculation and the 20th day was the date in which the administration of treatments started. At 20th day 4 mice presented palpable tumors. In Figure 4-32A it is shown the location where one of the first tumors appeared (gray circle) in a mouse of the no treatment group. It was not big enough to be detected at bear sight however it was palpable. In Figure 4-32B it is presented the same mouse five days later. This mouse weighed 22.5 g at the inoculation day, 26.7 g at the beginning of treatment and 33.6 g by the date of death which was 10 days after beginning the treatment. The tumor weighed 7.04 g. Therefore it is suggested that the difference of weight at the beginning and at end of the treatment may be an indicator of the tumor growth.

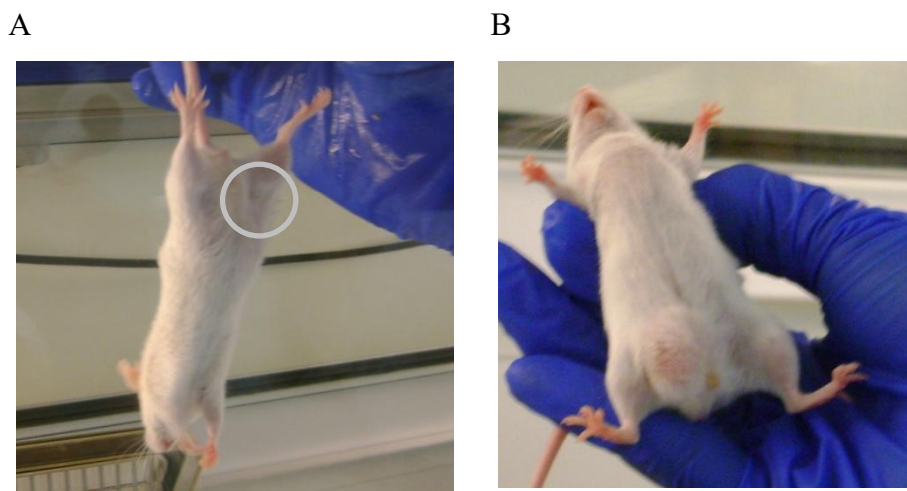


Figure 4-29. Mouse of placebo group inoculated with 10^7 OCI-Ly7 cells A. zone of palpable tumor at 20th day. B. Tumor evolution 5 days later.

Figure 4-33 depicts how the mouse of Figure 4-32 was earning weight since the inoculation day which is labeled as day zero. It is shown that there is a tendency to gain and lose weight every two days. And from 17th day to 21st day this pattern is not followed anymore. This same behavior of body weight increase was observed for the rest of the group as it is described in Figure 4-34.

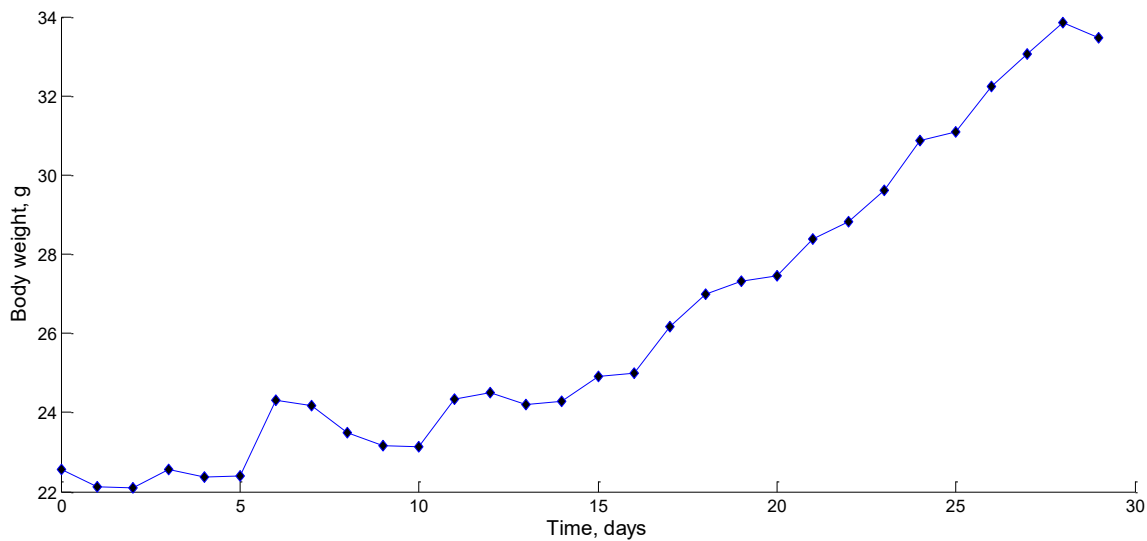


Figure 4-30. Body weight increase in a mouse which was one of the first to present palpable tumor. This was a mouse of the placebo group.

Figure 4-34 details that on 21st day 37 mice out of 45 presented an increase of 1.5 g in body weight. All the measures of weight were performed in the morning between 9 a.m. to 11 a.m. We used this information along with the tumors that were palpable to start treatments on 21st. In a research that used garlic as treatment in lymphoma animal model, they started the treatment 24 h after inoculation [34]. We could not proceed that way because we were not able to detect the tumor without killing the mouse in the process and it was necessary to wait until visible signs of tumor showed up because on the assumption that a mouse did not present a tumor at the end of the experiment, it was not possible to conclude if that happened as a result of the treatment or if it was a result of an unsuccessful graft.

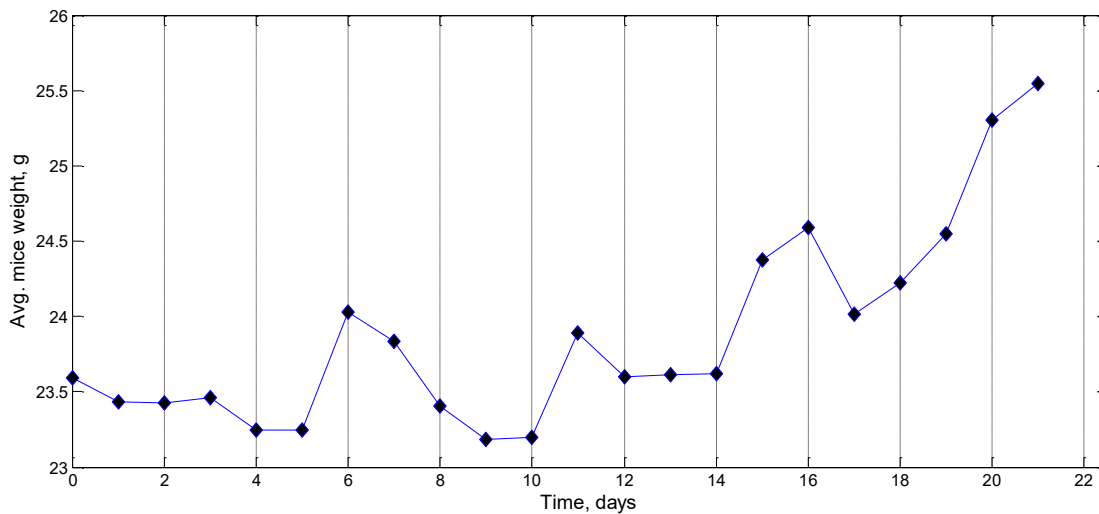


Figure 4-31. . Increase of body weight in OCI-Ly7 inoculated mice.

The Figure 4-35 illustrates the difference of body weight if mice since the beginning of treatments. This difference was measured 9 days after treatment. And it is shown that the means of groups BBE, QRC and CTX are significantly different in comparison with placebo group. In Table 4-11 it is detailed the one-way ANOVA analysis performed to determine that there is a difference between groups. The Kruskal-wallis test was perform to determine which of these groups were different from each other.

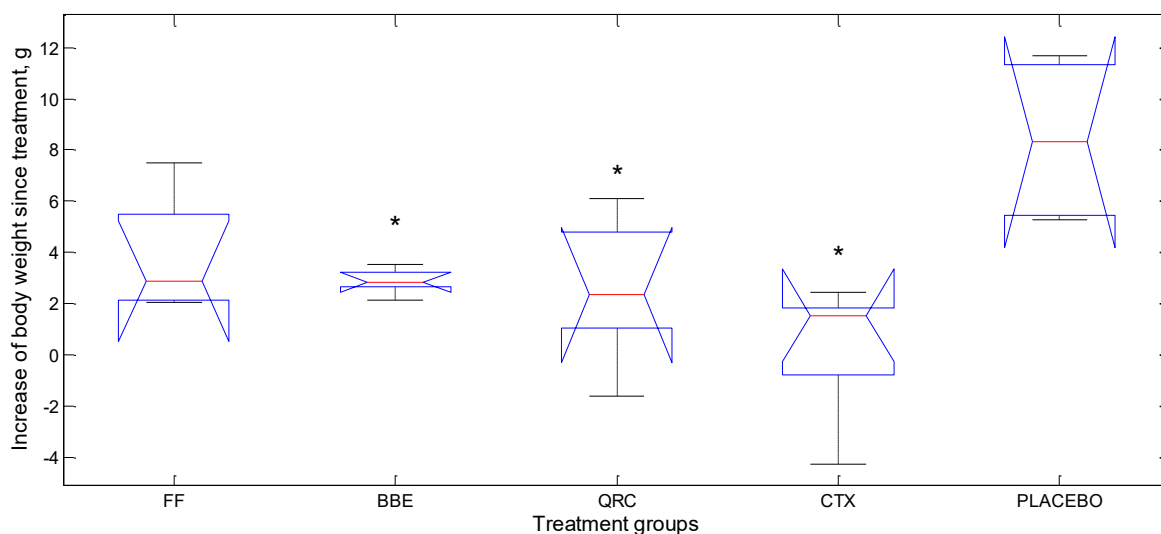


Figure 4-32. Box plot to compare the increase of body weight since treatment. Each box plot represents the difference in weight comparing the 9th day with the begging of treatment day. * $P < 0.0035$. FF stands for Flavonoid fraction group, BBE stands for

black bean extract group, QRC stands for quercetin group and CTX stands for cyclophosphamide group.

Table 4-11. One-way ANOVA of difference in body weight (20th day to 29th day) according to treatments.

Source	SS	df	MS	F	Prob>F
Treatments	151.96	4	31.99	5.82	0.0035
Error	117.408	18	6.5226		
Total	269.368	22			

The Figure 4-36 details, the average increase of weight for each group within 9 days after the beginning of treatment. It is detailed that the group of CTX as well as the group of BBE presented a maximum increase of weight of 2 g. The FF group presented a maximum increase of 4 g, and the placebo group presented a maximum increase of 2.5 g.

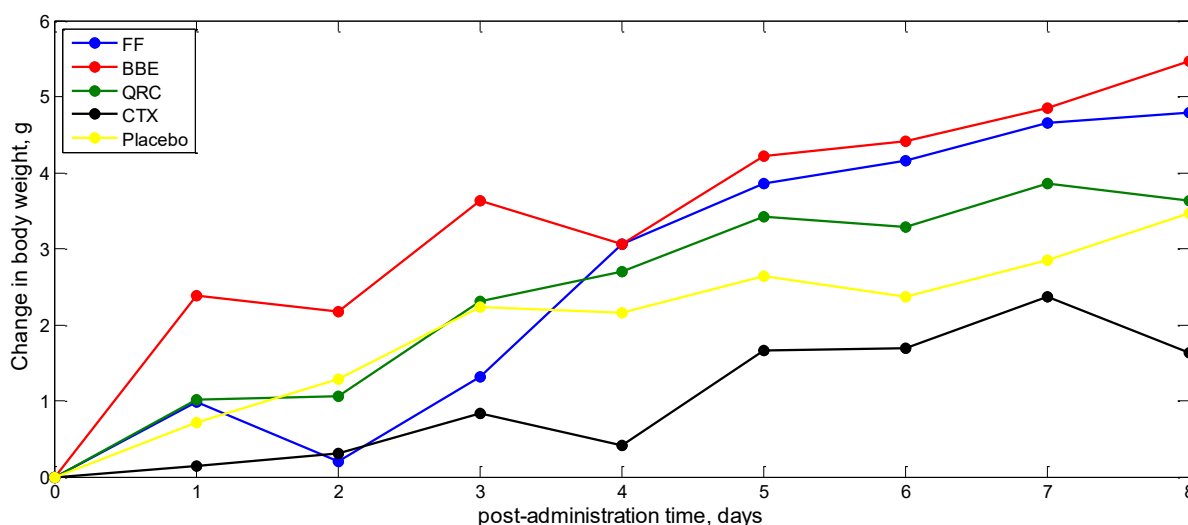


Figure 4-33. average of change in weight since administration of treatments. Blue line, Flavonoid fraction group (FF, n= 4), red line is black bean extract group (BBE, n= 5). Green line is quercetin group (QRC, n=4), Yellow line is Placebo group (n=3) and cyclophosphamide is the black line (CTX, n=5)

The box plot illustrated in Figure 4-37 details the tumor mass distribution resultant for each treatment. There was no significant difference between treatments. Perhaps the treatments started too late and the possible effect of treatments in the evolution of tumor was not able

to be detected. The kruskal-wallis test was perform to determine which of these groups were different from each other.

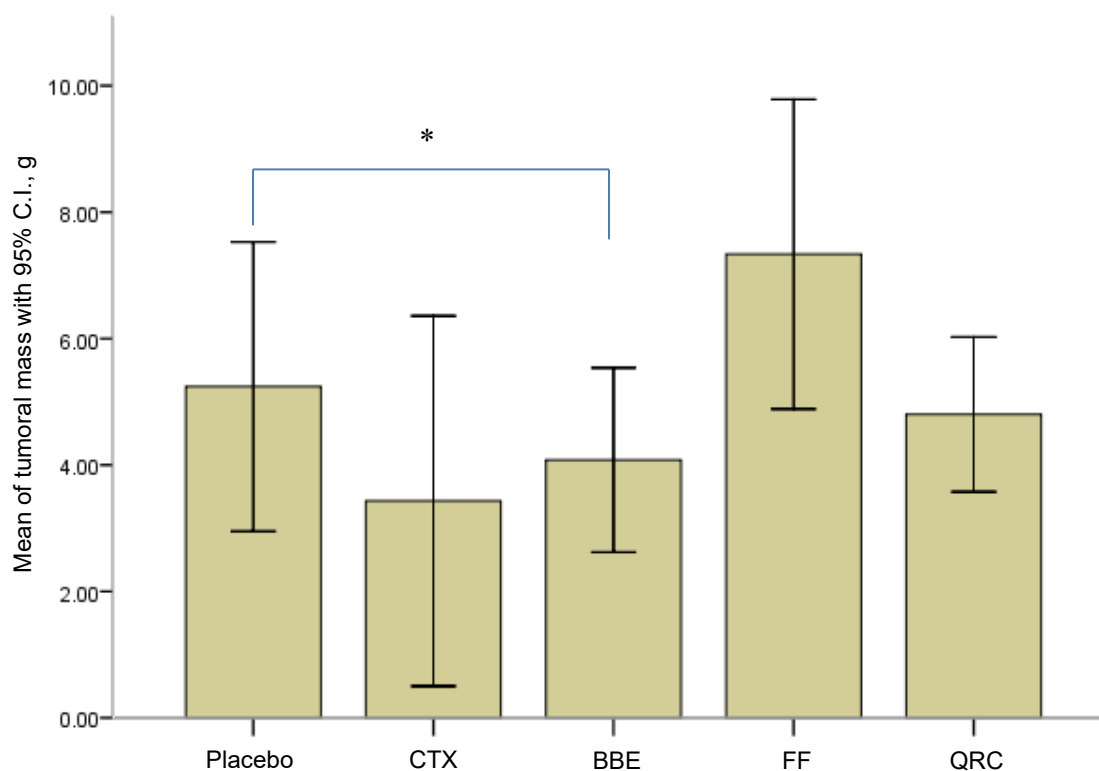


Figure 4-34. Mean of Tumor mass (g) for each treatment group. Errorbars represent the 95% confidence interval. Statistical difference between groups is determined with a P = 0.12, according to the kruskal-Wallis test.

Figure 4-38 details the survival curves of treatment groups in mice. It is illustrated that when there was 50% of the population there was an increase in survival for 5 days for BBE and CTX groups and an increase in survival of 6 days for FF group. It is also presented that the placebo group had a tendency to die earlier than the treatment groups. The last mouse of placebo group died at 34th day since inoculation. The last mice of both, FF treatment group and CTX treatment group, died at 44th day. In general the BBE presented a statistical difference ($P < 0.1$) of survival in comparison with the placebo group and it was not different from the CTX group (positive control) according to the log rank test. It is suggest then that the treatment with black bean extract may have implications as anti-neoplastic agent.

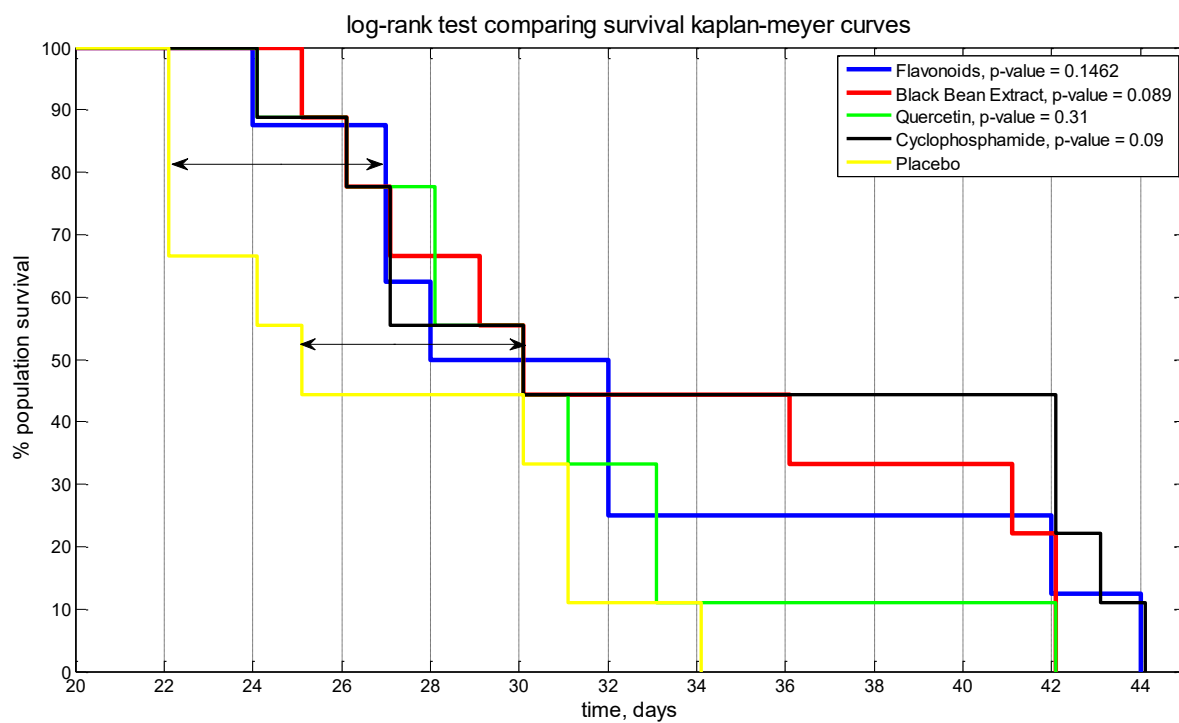


Figure 4-35. Kaplan Meyer survival curves evaluated with log rank test between groups.

5 CONCLUSIONS AND RECOMENDATIONS

The methanolic extraction from hulls of black bean and the flavonoid fraction obtained from black bean extract, have demonstrated to be cytotoxic to both OCI-Ly7 and SU-DHL-4 cell lines and not toxic to NIH3-T3 and VERO cell lines.

The flavonoid fraction showed to be more cytotoxic than the purified glycosylated flavonoids myricetin – 3 glycoside, quercetin – 3 glycoside and kaempferol – 3 glycoside.

The flavonoids myricetin, quercetin and kaempferol presented the highest cytotoxicity and the quercetin was the most cytotoxic among all the treatments tested.

The IC₅₀ determination was successful and it was confirmed by apoptosis assays were populations of apoptotic and viable cells distributed approximately at 50%.

Black bean extract, flavonoid fraction and aglycone flavonoids showed to cause cell death mediated by apoptosis, this has been confirmed by the over expression of Bax protein and interruption of G₁/G₀ phase of cell cycle.

Quercetin was the best flavonoid found to lead cells to apoptosis followed by kaempferol and then Myricetin.

Myricetin, Quercetin and kaempferol arrested cell cycle at G₀/G₁ phase. Myricetin and quercetin arrested also G₂/M phase but only quercetin was able to arrest all the phases in the cell cycle.

It was not possible to detect glycosylated flavonoids, aglycone flavonoids or metabolites flavonoids in mice plasma by HPLC with DAD/MWD. The mass spectra confirms the presence of fragment ions of flavonoid metabolites, however the main molecule has not been identified.

The black bean extract showed to increase the survival time in a specific period of the treatment however it was not enough to be compared to known treatments such as cyclophosphamide and it is suggested to increment dose in treatment and also to start the treatment by the time of inoculation as a preventive study.

It is also recommended to perform a LD50 assay in order to identify the optimal way to administer the black bean extract and to be certain about how much more the dose can be increased.

It is concluded then that black bean extract and flavonoids myricetin, quercetin and kaempferol have anti-neoplastic properties treating SU-DHL-4 and OCI-Ly7 cell lines. However more research is needed nonetheless to determine specific interaction of black bean extract.

6 REFERENCES

- [1] Griffiths, M.J., Murria, K.H., Russo, P.C. 1988. *Oncología Básica Fisiología, Evaluación y Tratamiento*. La Prensa Médica Mexicana, México. 3(13): 393-396.
- [2] Armitage, J.O., Weissenburger, D.D. 1998. New approach to classifying non-Hodgkin's lymphomas: clinical features of the major histologic subtypes. *Non-Hodgkin's Lymphoma Classification Project. Journal of Clinical Oncology*. 16(8): 2780-2795.
- [3] Ignacio, G., Martínez, M., Martínez, C. 2007. Registro de linfomas: diagnóstico de acuerdo a la Organización Mundial de la Salud, características clínicas y distribución geográfica durante el 2006. Abstract del congreso Nacional de Hematología, organizado por la AMEH, Acapulco 2007.
- [4] Arcamone F. 1985. Properties of antitumor anthracyclines and new developments in their application: Cain memorial award lecture. *Cancer Research*. 45(12 Pt 1): 5995-5999.
- [5] Jelic, S., Milanovic, N., Tomasevic, Z., Matković, S. and Gavrilović, D. 1999. Comparison of two non-anthracycline-containing regimens for elderly patients with diffuse large b cell lymphoma--possible pitfalls in results reporting and interpretation. *Neoplasma*. 46(6): 394-399.
- [6] Winkel-Shirley B. 2001. Flavonoid Biosynthesis. A Colorful Model for Genetics, Biochemistry, Cell Biology, and Biotechnology. *Plant Physiology*. 126(2): 485-493.
- [7] Son, Y.O., Lee, K.Y., Lee, J.C. 2005. Selective antiproliferative and apoptotic effects of flavonoids purified from *Rhus verniciflua* stokes on normal versus transformed hepatic cell lines. *Toxicology Letters*. 155(1): 115-125.
- [8] Davis, D.D., Diaz-Cruz, E.S., Landini, S., Kim, Y.W. and Brueggemeier, R.W. 2008. Evaluation of synthetic isoflavones on cell proliferation, estrogen receptor binding affinity,

and apoptosis in human breast cancer cells. The journal of steroid biochemistry and molecular biology. 108(1-2): 23-31.

[9] Elisia, I., Kitts, D.D. 2008. Anthocyanins inhibit peroxy radical-induced apoptosis in Caco-2 cells. Molecular and cellular biochemistry. 312(1-2): 139-145.

[10] Gutierrez-Urbe, J.A., Serna-Saldivar, S.R.O., Moreno-Cuevas, J.E., Hernandez-Brenes, C., Guajardo-Touche, E.M. Cancer cell growth inhibition by black bean (*Phaseolus vulgaris* L) extracts. U.S. Patent Application 2006024394/A1. February 2, 2006.

[11] Garcia-Patiño, M., Evaluación in vitro de un extracto de Frijol Negro (*Phaseolus Vulgaris*) y sus fracciones sobre la producción de óxido nítrico y TNF-alfa, Tesis presentada como requisito parcial para obtener el grado académico de maestría en ciencias con especialidad en biotecnología, Diciembre, 2010.

[12] Delves, P.J., and Roitt, I.M. 2000. Advances in immunology, The new England Journal of Medicine. 343(1):37-38.

[13] Wildman, R.E.C. 2007. Handbook of nutraceuticals and functional foods 2nd edition, Taylor & Francis group, Florida, USA. 2-9p.

[14] Lin, L.Z., Harnly J.M., Pastor-Corrales M.S., Luthria, D.L. 2007. The polyphenolic profiles of common bean (*Phaseolus vulgaris* L.). Food Chemistry 107(2008):399–410.

[15] Dictionary of Natural Products, The Chapman & Hall/CRC Chemical Database. consulted by: May 5th 2011. Available at: <http://dnp.chemnetbase.com/dictionary-search.do?method=view&id=1967108&si=>

[16] Esptein, A.L., Levy, R., Kim, H., Henle, W. Henle, G. and Kaplan, H.S. 1978. Biology of the human malignant lymphomas IV. Functional Characterization of Ten Diffuse Histiocytic Lymphoma Cell Lines. *Cancer*. 42:2379-2391.

- [17] Austin, C.A., Patel, S., Ono, K., Nakane, H. and Fisher, L.M. 1992. Site-specific DNA cleavage by mammalian DNA topoisomerase II induced by novel flavone and catechin derivatives. *The biochemical journal*. 282(Pt 3): 883-889.
- [18] Koopman, G., Reutelingsperger, C.P., Kuijten, G.A., Keehnen, R.M., Pals, S.T., and van Oers, M.H. 1994. Annexin V for flow cytometric detection of phosphatidylserine expression on B cells undergoing apoptosis. *Blood*, 84(5): 1415-1420.
- [19] MACS, Miltenyi Biotec, Staining of apoptotic and dead cells, Annexin V FIT-C kit, http://www.miltenyibiotec.com/download/datasheets_en/363/DS130_092_052.pdf consulted by: May 5th 2011.
- [20] Liu, F.T., Agrawal, S.G., Movasaghi, Z., Wyatt, P.B., Rehman, I.U., Gribben, J.G., Newland, A.C., and Jia, L. 2008. Dietary flavonoids inhibit the anticancer effects of the proteasome inhibitor bortezomib. *Blood*, 112(9): 3835-3846.
- [21] Brisdelli, F., Coccia, C., Cinque, B., Cifone, M.G., and Bozzi, A. 2006. Induction of apoptosis by quercetin: different response of human chronic myeloid (K562) and acute lymphoblastic (HSB-2) leukemia cells. *Molecular and cellular biochemistry*. 296(1-2): 137–149.
- [22] Zhang, Q., Zhao, X.H. and Wang, Z.J. 2009. Cytotoxicity of flavones and flavonols to a human esophageal squamous cell carcinoma cell line (KYSE-510) by induction of G2/M arrest and apoptosis. *Toxicology In vitro*. 23(5):797-807.
- [23] Safa, M., Kazemi, A., Zand, H., Azarkeivan, A., Zaker, F and Hayat, P. 2009. Inhibitory role of cAMP on doxorubicin-induced apoptosis in pre-B ALL cells through dephosphorylation of p53 serine residues. *Apoptosis*. 15(2):196–203

[24] BD Flow cytometry Applications, DNA Cell cycle analysis on BD FACSCanto™ II technical information web page
http://www.bd.com/videos/bdb/dna_canto2_course/home.html.

Consulted by:

[25] News Bulletin for Axis-shield density gradient media, 2007, Consulted by: November 17th Available at: <http://www.axis-shield-density-gradient-media.com/Biological%20Separations%20Lymphoprep.pdf>

[26] Haghiac, M., and Walle, T. 2005. Quercetin Induces Necrosis and Apoptosis in SCC-9 Oral Cancer Cells, *Nutrition and cancer*. 53(2): 220–231.

[27] Yoshida, M., Yamamoto, M., and Nikaido, T. 1992. Quercetin Arrests Human Leukemic T-Cells in Late G1 Phase of the Cell Cycle, *Cancer Research*. 52(23):6676-6681.

[28] Lamson, D.W., and Brignall, M.S. 2000. Antioxidants and Cancer III: Quercetin. *Alternative Medicine Review*. 5(3):196-20.

[29] Yuqing Zhang, Aaron Y. Chen, Min Li, Changyi Chen, and Qizhi Yao. 2008. Ginkgo biloba Extract Kaempferol Inhibits Cell Proliferation and Induces Apoptosis in Pancreatic Cancer Cells. *Journal of Surgical Research*. 148(1):17-23.

[30] Al-Katib, A., Arnold, A.A., Aboukameel, A., Sosin, A., Smith, P., Mohamed, A.N., Beck, F.W., Mohammad, R.M. 2010. I-kappa-kinase-2 (IKK-2) inhibition potentiates vincristine cytotoxicity in non-Hodgkin's lymphoma, *Molecular Cancer*. (1)9:228.

[31] Tabe, Y., Sebasigari, D., Jin, L., Rudelius M., Davies-Hill, T., Miyake, K., Miida, T., Pittaluga, S., and Raffeld, M. 2009. MDM2 Antagonist Nutlin-3 Displays antiproliferative and Proapoptotic Activity in Mantle Cell Lymphoma. *Clinical Cancer Research*. 15(3):933-42.

- [32] Hawtin R.E., Stockett D.E., Wong O.K., Lundin C., Helleday T., Fox J.A. 2010. Homologous recombination repair is essential for repair of vosaroxin-induced DNA double-strand breaks. *Oncotarget*. 1(7):606-19.
- [33] Jung, J.Y., Kim, H.J., Kim, S.K., Kim, B.S., Lee, S.H., Park, Y.S., Park, B.K., Kim, S.J., Kim, J., Choi, C., Kim, J.S., Cho, S.D., Jung J.W., Roh, K.H., and Kang, K.H. 2010. Apoptotic Effect of Quercetin on HT-29 Colon Cancer Cells, via the AMPK Signaling Pathway, 2010, *J. Agricultural and Food Chemistry*. 58(15): 8643–8650.
- [34] Padilla-Camberos, P., Zaitseva, G., Padilla, C. and Puebla, A.M. 2010. Antitumoral Activity of Allicin in Murine Lymphoma L5178Y, *Asian Pacific Journal of Cancer Prevention*. 11(5):1241-1244.
- [35] Guo, J., Xue, C., Duan, J.A., Shang, E.x., Qian, D., Tang, Y., Ouyang, Q., and Sha, M. 2011. Fast Characterization of Constituents in HuangKui Capsules Using UPLC–QTOF-MS with Collision Energy and MassFragment Software, *Chromatographia, An International Journal for Rapid Communication in Chromatography, Electrophoresis and Associated Techniques*. 73(5-6):447-456.
- [36] Schimdt-Wolf, I.G.H., Negrin, R.S., Kiem, H.P., Blume, K.G. and Weissman, I.L. 1991. Use of a SCID mouse/human lymphoma model to evaluate cytokine-induced killer cells with potent antitumor cell activity. *The journal of experimental medicine*. 174(1): 139-149.
- [37] Landa-Solisa, C., Gonzalez-Espinosa, D., Guzman-Soriano, B., Snyder, M., Reyes Teran, G., Torres, K. and Gutierrez A.A., 2005, MicrocynTM: a novel super-oxidized water with neutral pH and disinfectant activity. *Journal of Hospital Infection*. 61(4): 291–299.
- [38] “Research Animal anesthesia, Analgesia and surgery” of Alison C. Smith and Michael Swindle, DVM, September 1994. 338-372p.

- [39] “Manejo de animales de laboratorio del centro nacional de productos biológicos del Instituto Nacional de Lima, 2009”. 23-40p.
- [40] Day, A.J., Mellon, F., Barron, D., Sarrazin, G., Morgan, M.R.A. and Williamson, G. 2001. Human Metabolism of Dietary Flavonoids: Identification of Plasma Metabolites of Quercetin, *Free Radicals Research*. 35(6):941-952.
- [41] Man, S., Bocci, G., Francia, G., Green, S.K., Jothy, S., Hanahan, D., Bohlen, P., Hicklin, D.J., Bergers, G. and Kerbel, R.S. 2002. Antitumor Effects in Mice of Low-dose (Metronomic) Cyclophosphamide Administered Continuously through the Drinking Water *Cancer Research* 62(10): 2731–2735.
- [42] Bland, J.M. and Altman, D.G. 2004. Statistic notes, Log rank test, *British Medical Journal*. 328:1073.
- [43] Hollander, M., and D. A. Wolfe. 1999. *Nonparametric Statistical Methods*. Hoboken, NJ: John Wiley & Sons, Inc.
- [44] Kang, T. and Liang, N 1997. Studies on the inhibitory effects of quercetin on the growth of HL-60 leukemia cells. *Biochemical Pharmacology*. 54(9):1013–1018.
- [45] Weingartner, O., Bohm, M. and Laufs, U. 2008. "Controversial role of plant sterol esters in the management of hypercholesterolaemia". *European Heart Journal*. 30(4): 404
- [46] Feingold, K., and Moser, A.H. 1986. The effect of substrates and competitive inhibitors on the phosphatase-dependent activation of hepatic hydroxymethylglutaryl CoA reductase. *Archives of Biochemistry and Biophysics*. 249(1):46-52.
- [47] Jawanda, M.K. 2009. Antitumor Activity of Antioxidants- An Overview, *International Journal of dental clinics*. 1(1): 3-7.
- [48] Brower, V. 2005. A nutraceutical a day may keep the doctor away. *European Molecular Biology Organization*. 6(8): 708–711.

A. APPENDIX A

HPLC Agilent 1200 series with Diode Array Detector from Agilent Technologies

Modules:

Degasser, Part Number: G1322A, Serial Number: JP62356654, Manufacturer: Tokio Japan.

Quaternary Pump, Part Number: G1211A, Serial Number: DE62959033, Manufacturer: Waldbrunn, Germany.

ALS, Part Number: G1329A, Serial Number: DE6475997, Manufacturer: Waldbrunn, Germany.

TCC, Part Number: G1316A, Serial Number: DE63073454, Manufacturer: Waldbrunn, Germany.

DAD, Part Number: G1615B, Serial Number: DE63057687, Manufacturer: Waldbrunn, Germany.

ANALYT FC, Part Number: G1364C, Serial Number: DE63055501, Manufacturer: Waldbrunn, Germany.

HPLC Agilent 1200 series with Diode Array Detector from Agilent Technologies with all spectra storage

Modules:

Degasser, Part Number: G1322A, Serial Number: JP93572324, Manufacturer: Tokio Japan.

Quaternary Pump, Part Number: G1311A, Serial Number: DE62972160, Manufacturer: Waldbrunn, Germany.

ALS, Part Number: G1329A, Serial Number: DE64775020, Manufacturer: Waldbrunn, Germany.

TCC, Part Number: G1316A, Serial Number: DE43649773, Manufacturer: Waldbrunn, Germany.

DAD, Part Number: G1315D, Serial Number: DE64259117, Manufacturer: Waldbrunn, Germany.

Semi preparative HPLC from Hewlett Packard, USA.

Modules:

Degasser, Part Number: G1322A, Serial Number: JP63204258, Manufacturer: Tokio Japan.

Quaternary Pump, Part Number: G1311A, Serial Number: US70601530, Manufacturer: USA.

ALS, Part Number: G1329A, Serial Number: US72101798, Manufacturer: USA.

ColComp, Part Number: G1316A, Serial Number:US64401718 , Manufacturer: USA.

Detector, Part Number: G1315D, Serial Number: JP64202580, Manufacturer: Tokio, Japan.

BD FACS Canto TM II, Manufacturer: BD Biosciences San Jose, CA, USA.

Serial Number: V96100240

Synergy HT, Manufacturer: Biotek ® Instruments Winooski, Vermont, USA.

Serial Number: 204800

Software Gen 5 TM ELISA, Manufacturer: Biotek ® Instruments Winooski, Vermont, USA.

Ver. 1.01.14, Serial Number: YBZD KRRX WGYW RD

B. APPENDIX B

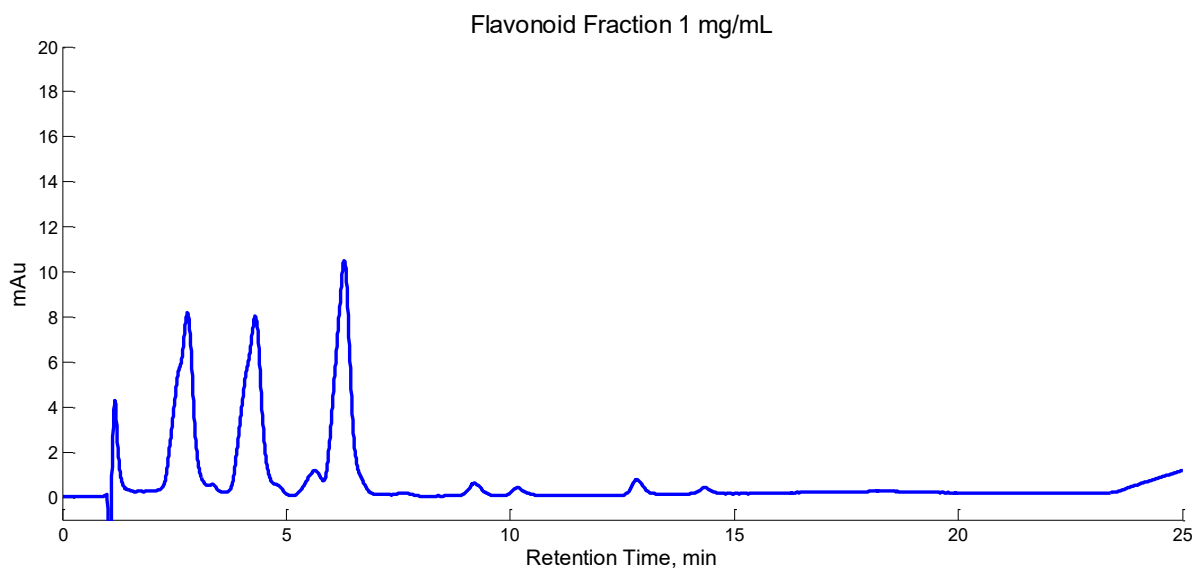


Figure B-1. Chromatogram of Flavonoid Fraction at 1 mg/mL

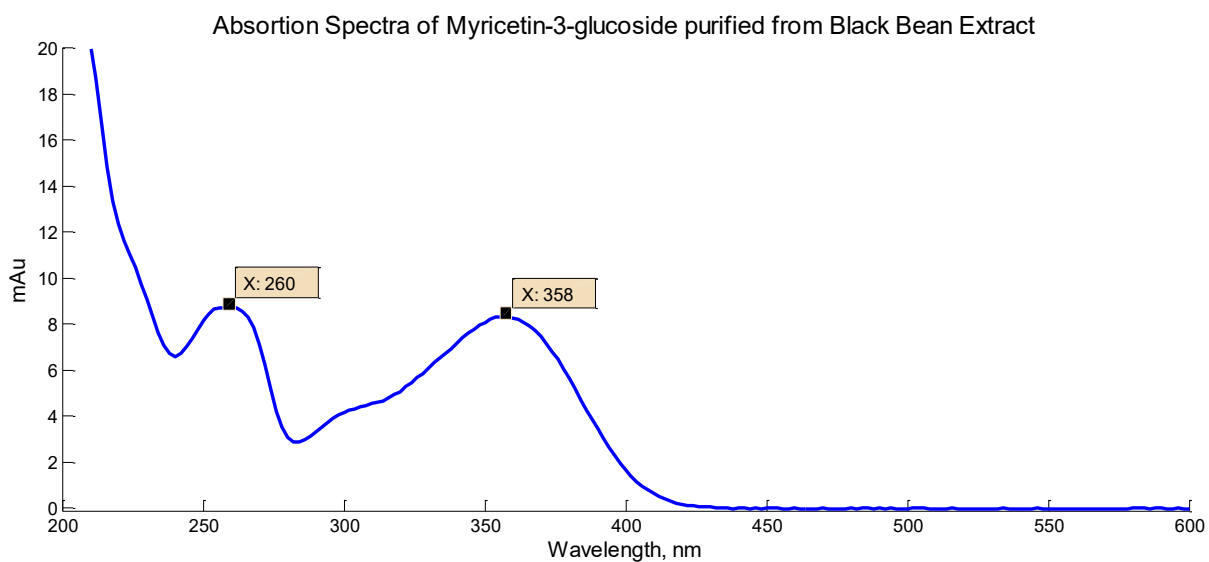


Figure B-2. Absorption spectra of Myricetin-3-glucoside purified from Black Bean Extract. $\lambda_1 = 260$ nm and $\lambda_2 = 358$ nm

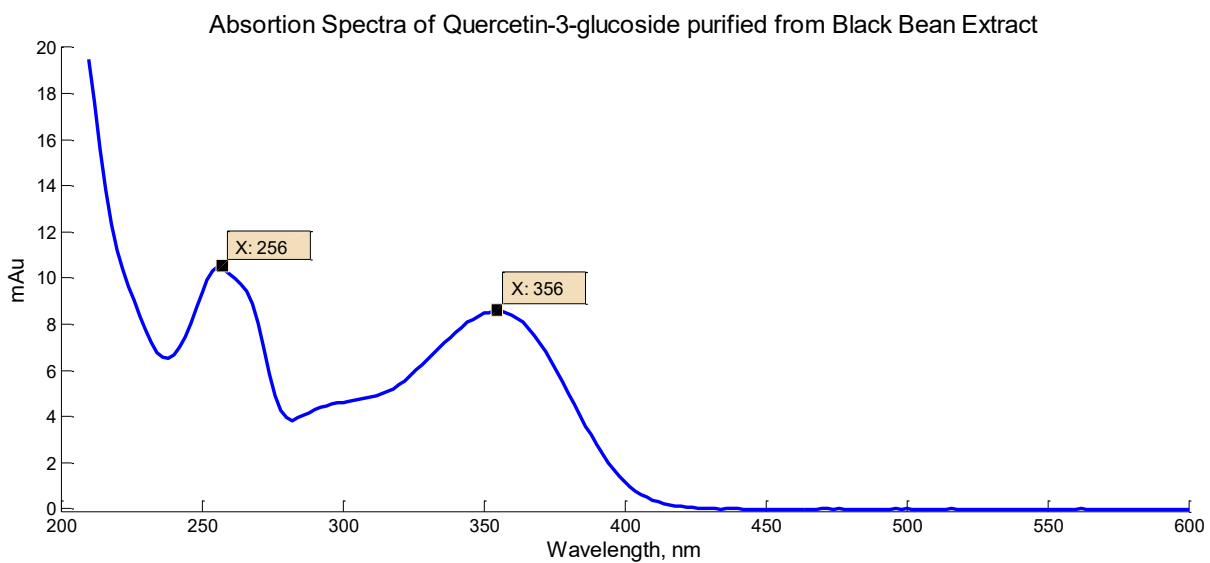


Figure B-3. Absorption spectra of Quercetin-3-glucoside purified from Black Bean Extract

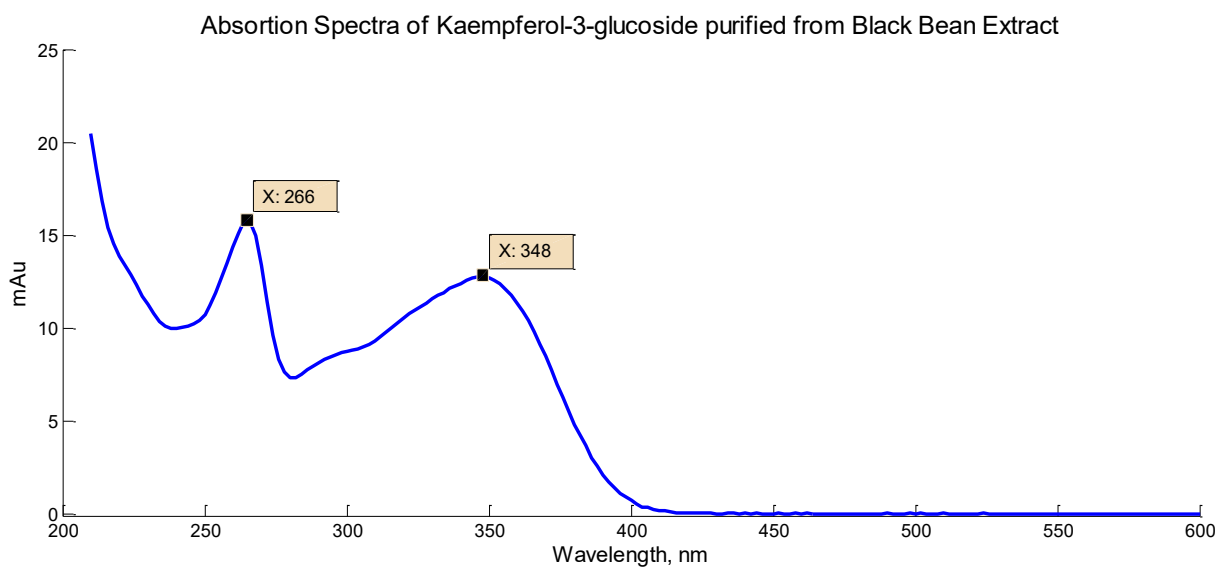


Figure B-4. Absorption spectra of Kaempferol-3-glucoside purified from Black Bean Extract

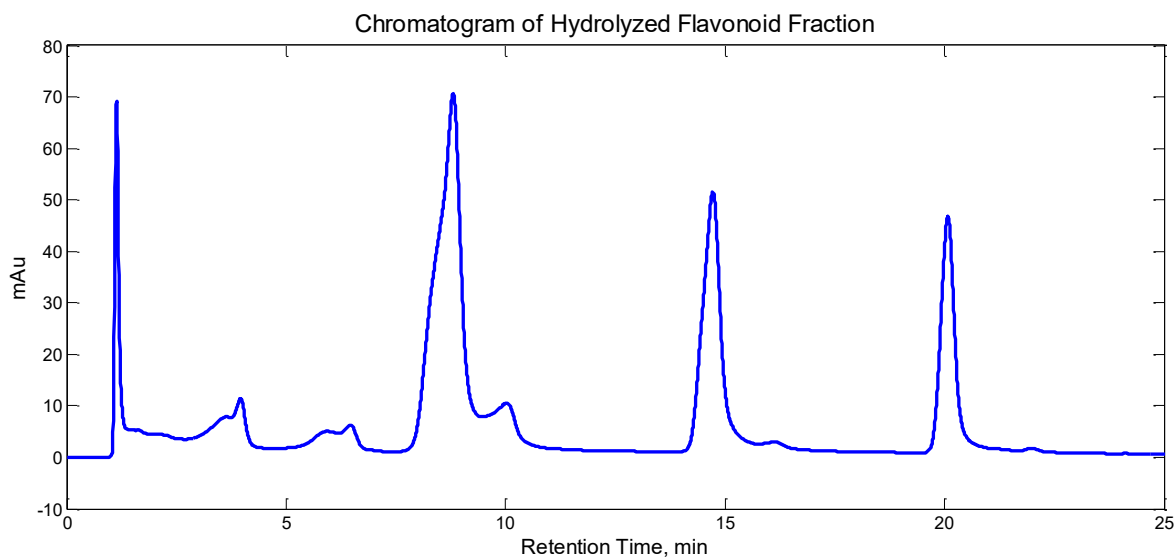


Figure B-5. Chromatogram of Hydrolyzed Flavonoid Fraction at 12.408 mg/mL

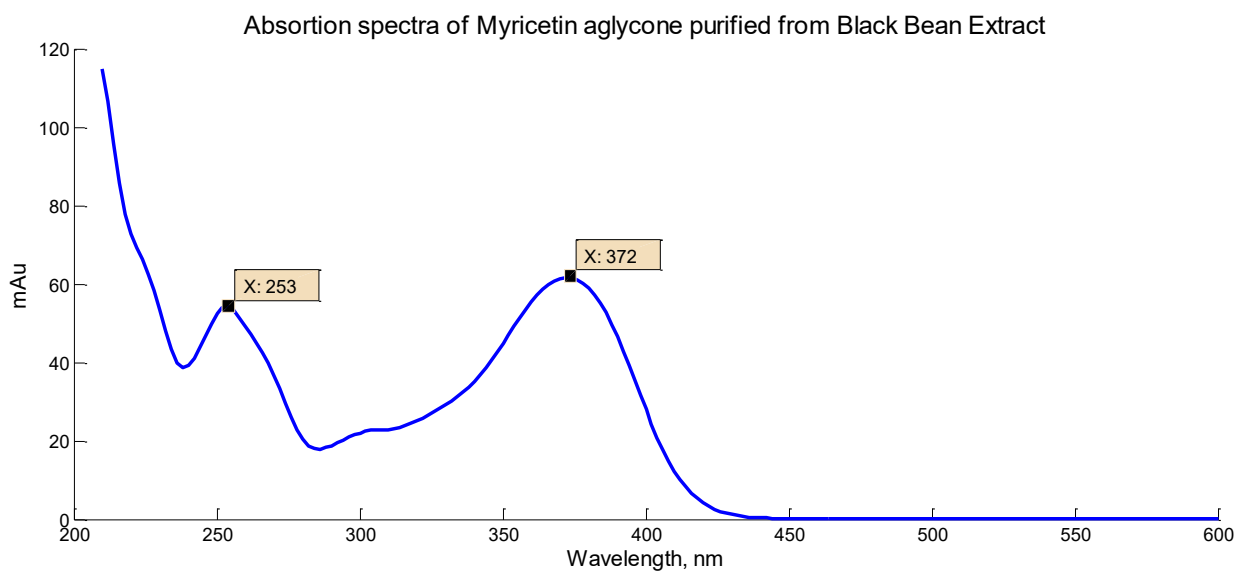


Figure B-6. Absorption spectra of Myricetin purified from Black Bean Extract

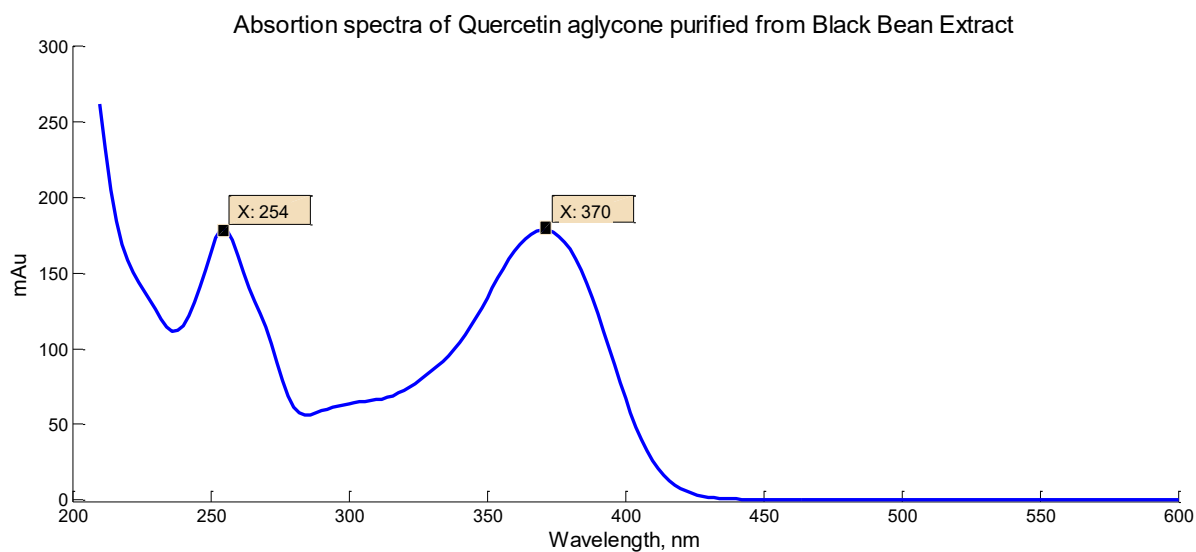


Figure B-7. Absorption spectra of Quercetin purified from Black Bean Extract

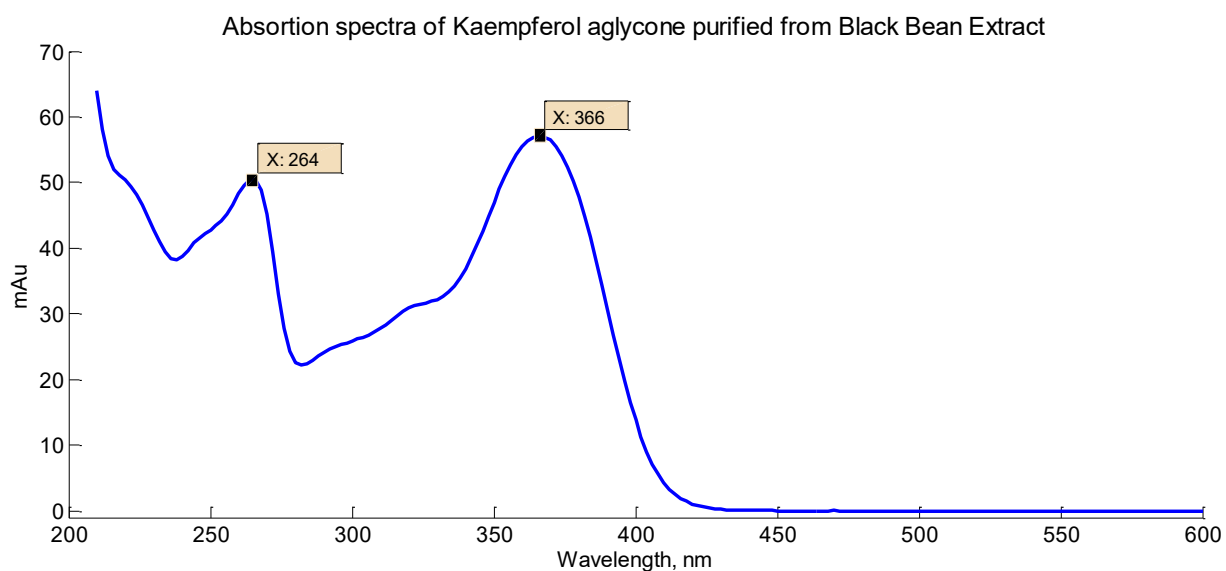


Figure B-8. Absorption spectra of Kaempferol purified from Black Bean Extract

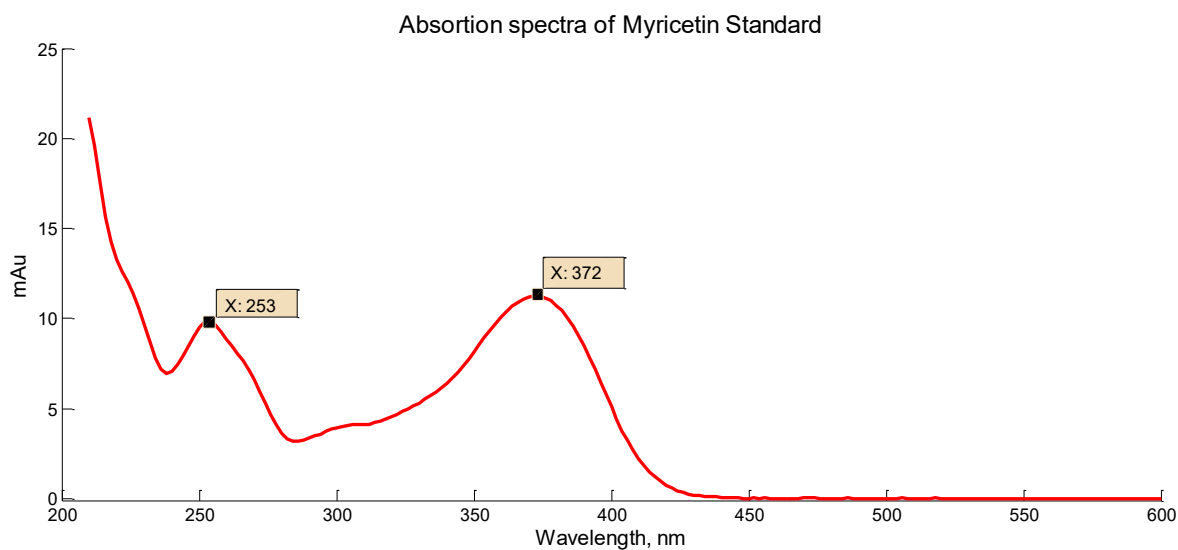


Figure B-9. Absorption spectra of Myricetin Standard

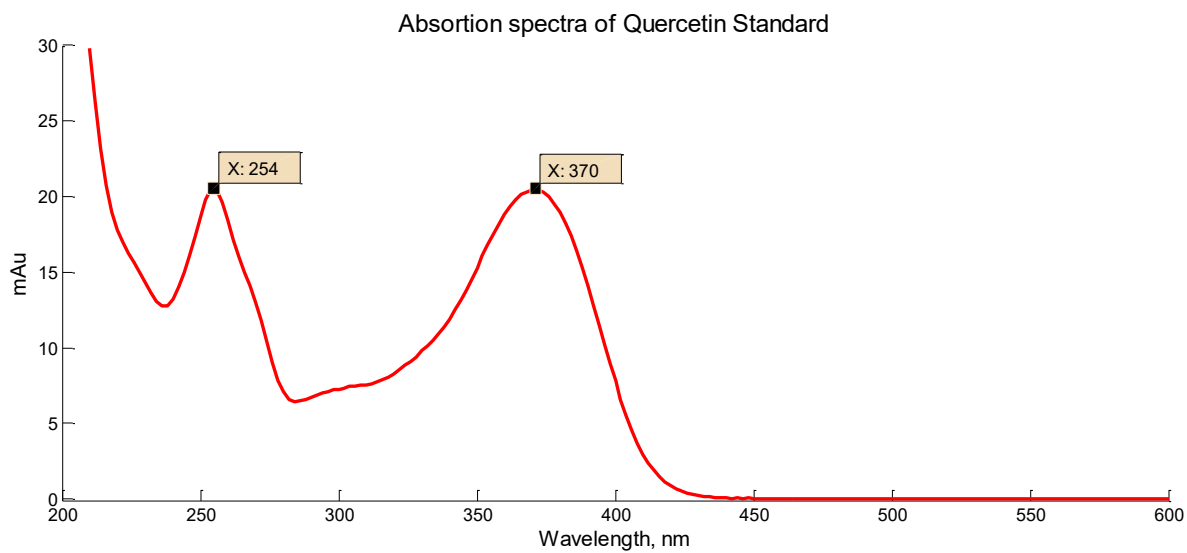


Figure B-10. Absorption spectra of Quercetin Standard

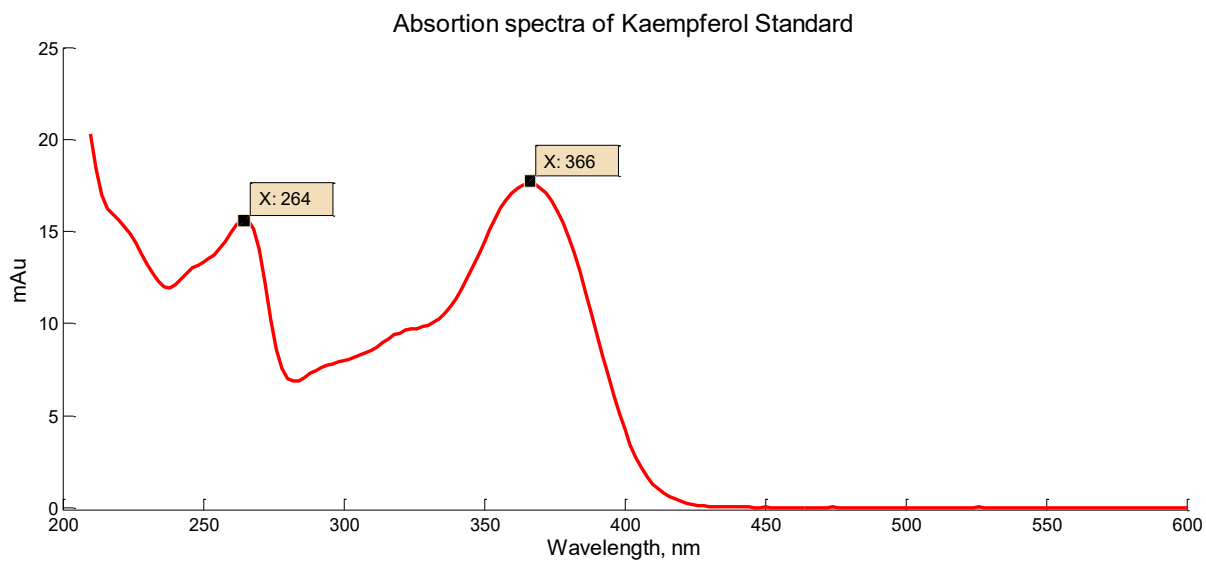


Figure B-11. Absorption spectra of Kaempferol Standard

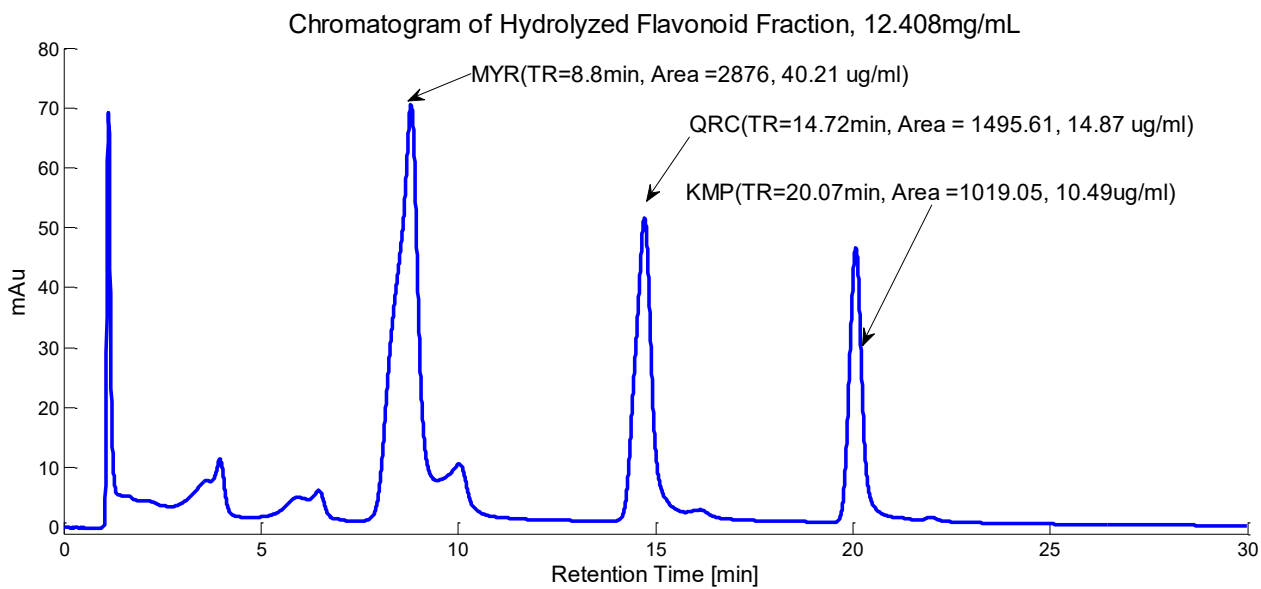


Figure B-12. Chromatogram and quantification of hydrolyzed flavonoid fraction at 12.408 mg/mL

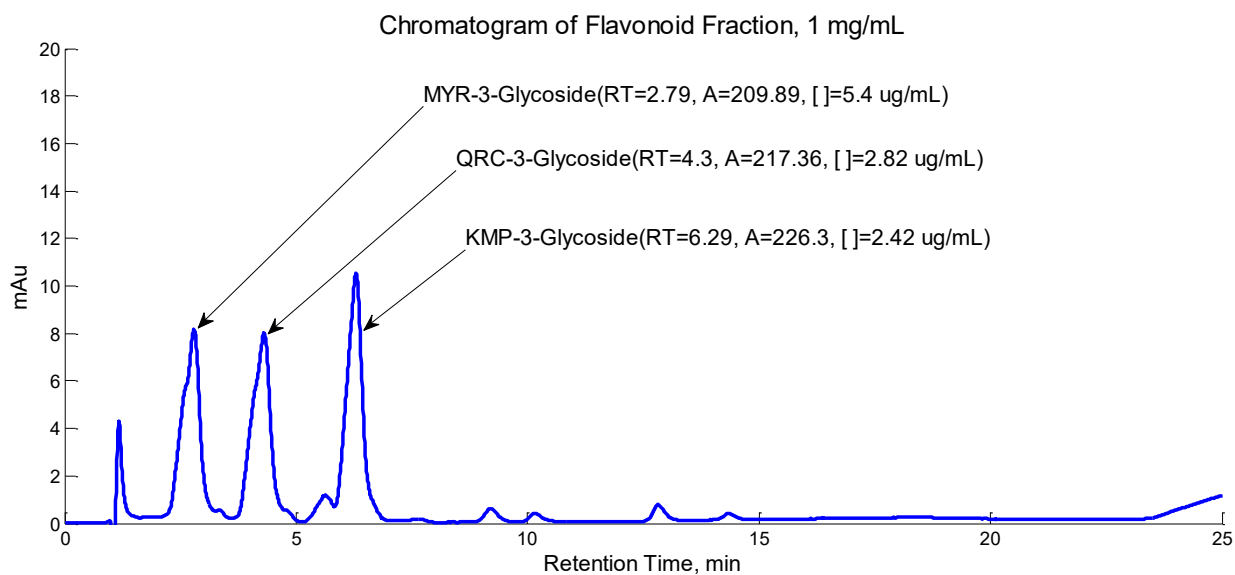


Figure B-13. Chromatogram and quantification of flavonoid fraction at 1 mg/mL

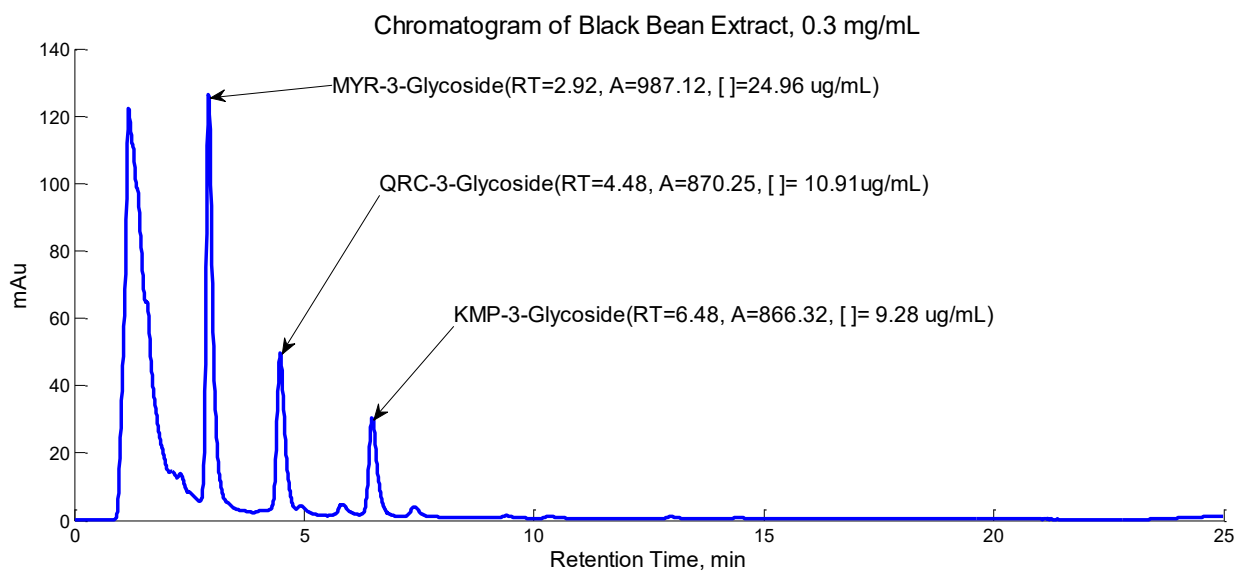


Figure B-14. Chromatogram and quantification of Black Bean Extract at 0.3 mg/mL

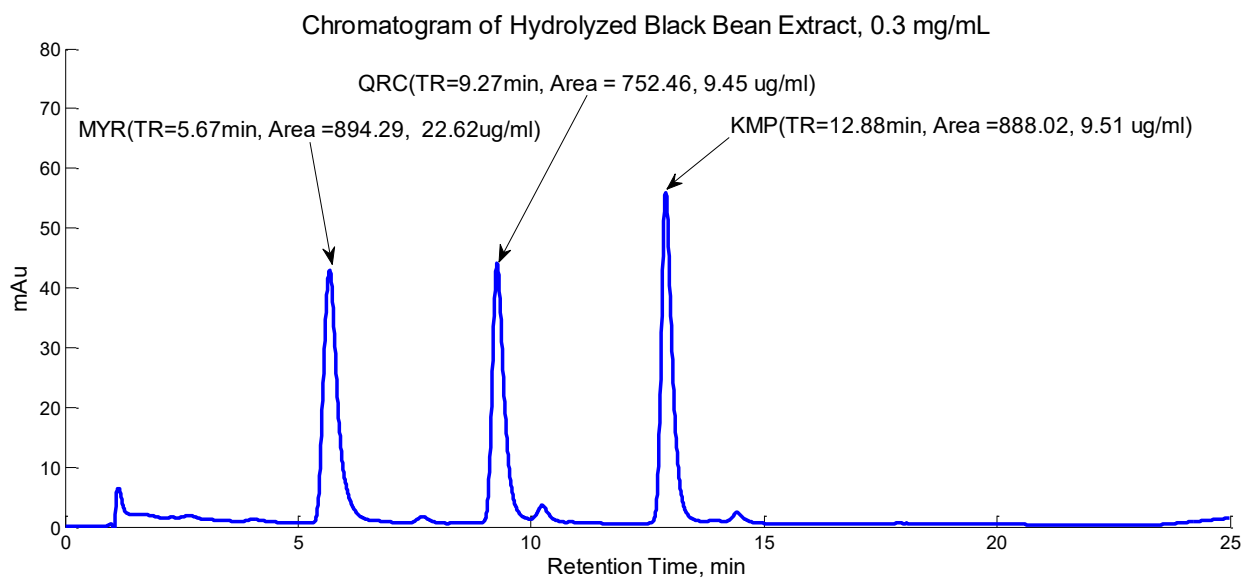


Figure B-15. Chromatogram and quantification of Hydrolyzed Black Bean Extract at 0.3 mg/mL

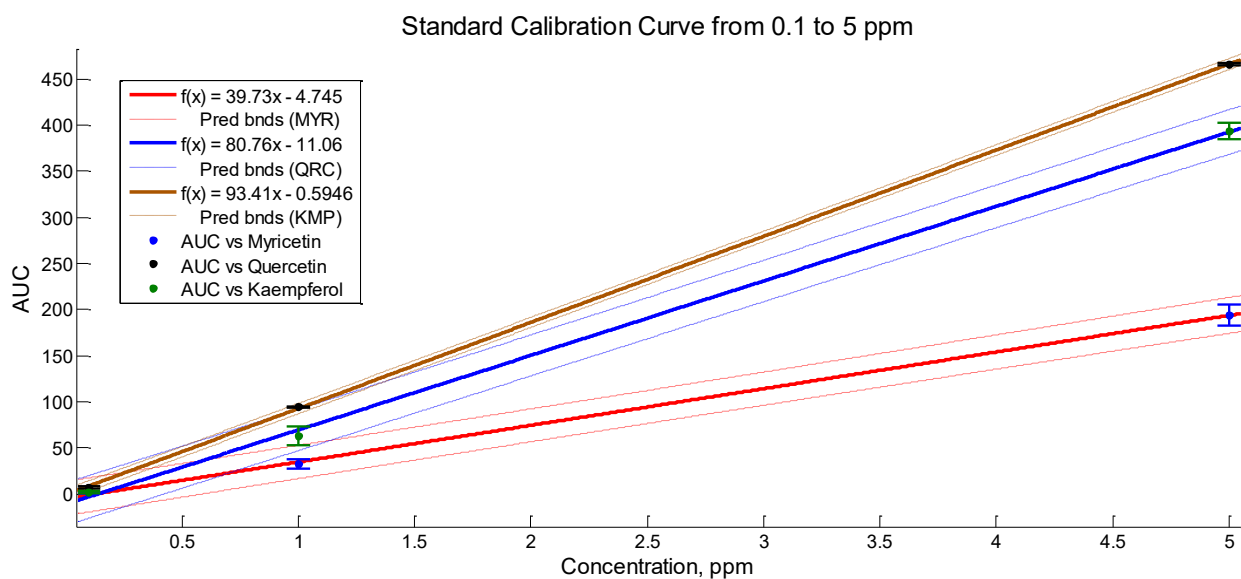


Figure B-16. Standard calibration curves of Myricetin, Quercetin and Kaempferol (0.1 to 5ppm)

Table B-1. Linear regression and goodness of fit for standards calibration curves from 0.1 to 5 ppm

Linear model:	$\bar{f}(\vec{x}) = p_1 \vec{x} + p_2$	MYRICETIN	QUERCETIN	KAEMPFEROL
Coefficients (with 95% confidence bounds):	p1:	39.73	80.76	93.41
		(37.09, 42.38)	(77.46, 84.06)	(92.59, 94.23)
	p2:	-4.745	-11.06	-0.5946
		(-12.54, 3.05)	(-20.77, -1.348)	(-3.004, 1.815)
Goodness of fit:	SSE:	358.1	555.9	34.21
	R-square:	0.9945	0.9979	0.9999
	Adjusted R-square:	0.9937	0.9976	0.9999
	RMSE:	7.153	8.912	2.211

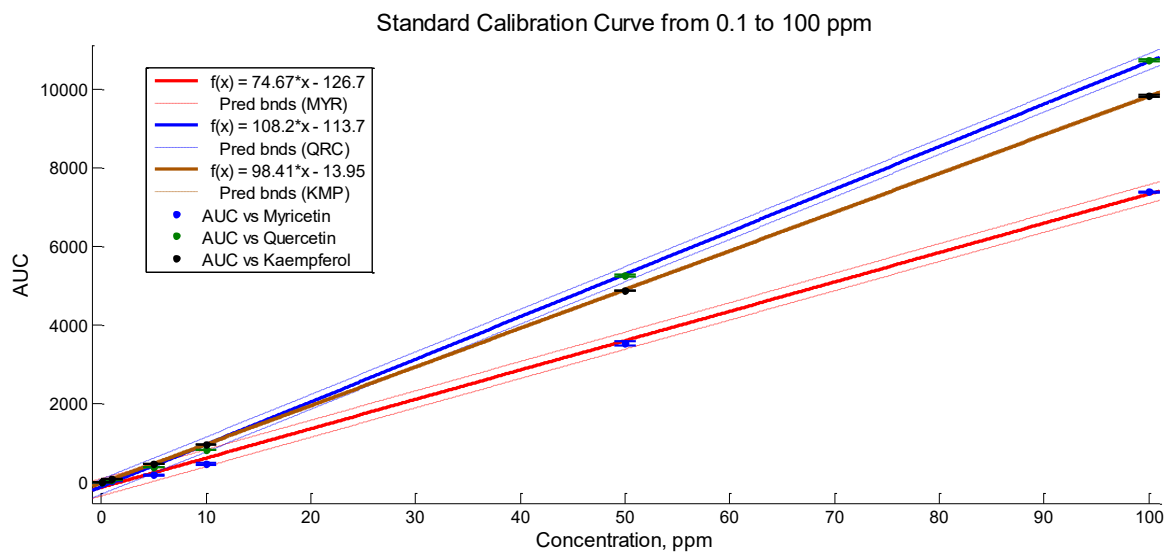


Figure B-17. Standards calibration curves of of Myricetin, Quercetin and Kaempferol (0.1 to 100ppm)

Table B-2. Linear regression and goodness of fit for standards calibration curves from 0.1 to 100 ppm

Linear model:	$\widehat{f(\vec{x})} = p_1 \vec{x} + p_2$	MYRICETIN	QUERCETIN	KAEMPFEROL
Coefficients (with 95% confidence bounds):	p1:	74.67	108.2	98.41
		(73.32, 76.03)	(107, 109.4)	(98.17, 98.66)
	p2:	-126.7	-113.7	-13.95
		(-188.9, -64.5)	(-167.9, -59.55)	(-25.28, -2.625)
Goodness of fit:	SSE:	1.57E+05	1.20E+05	5228
	R-square:	0.9988	0.9996	1
	Adjusted R-square:	0.9988	0.9995	1
	RMSE:	99.19	86.46	18.08

C. APPENDIX C

CELL GROWTH KINETIC ASSAY

The aim of this assay was to determine the period in which SU-DHL-4 and OCI-Ly7 cells remain in log phase due to it is indicated in the cell titer blue assay manufacturer's instructions as a condition for the reagent to work. 20 mL of cells in suspension (both SU-DHL-4 and OCI-Ly7 lines) were set to grow with three different cell densities. Several cell counts were performed by means of neubauer hemocytometer and Trypan blue exclusion assay. According to the first derivative of the hill equation determined in figures C-1 and C-3, it was determined that for an initial cell density of 200000 cells/mL after one day of changing cell growth medium both cell lines, SU-DHL-4 and OCI-Ly7, enter into log phase. Both cell lines remained in log phase for 3 days without cell growth medium change.

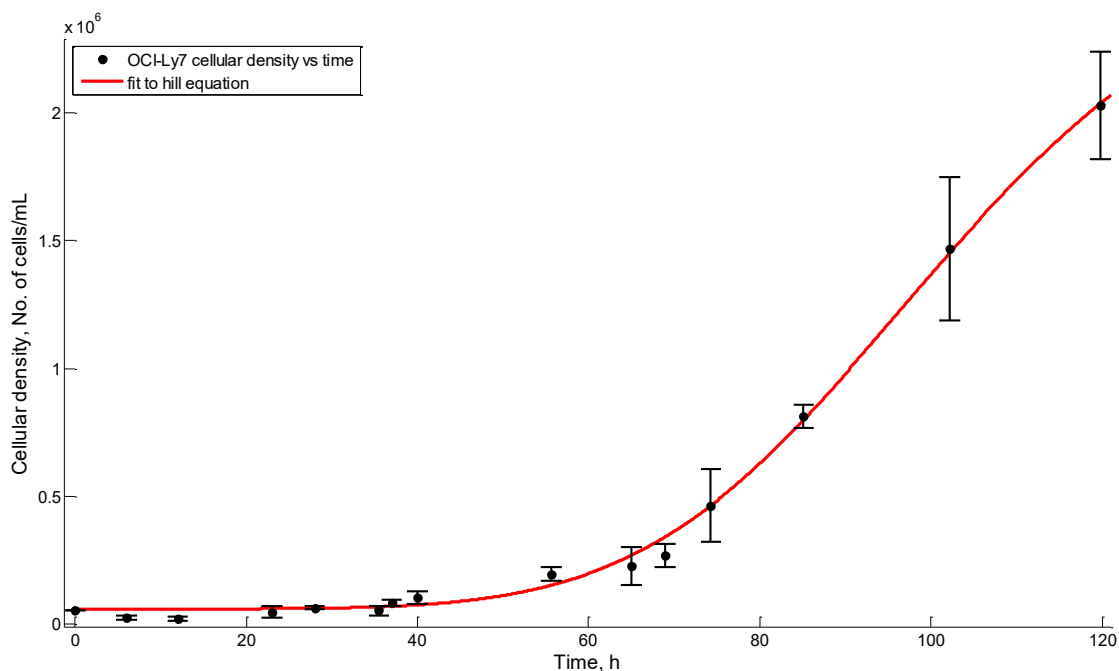


Figure C-1. Cellular density growth of OCI-Ly7 cell line in 5 days. General Model: $f(x) = a + (b-a)/(1+(c/x)^d)$, Coefficients (with 95% confidence bounds): $a = 6 \times 10^4$, $b = 2.88 \times 10^6$, $c = 102.7(90.63, 114.7)$, $d = 5.52 (4.3, 6.7)$, Goodness of fit: SSE: 4.31×10^{11} , R-square: 0.9719, Adjusted R-square: 0.9707, RMSE: 9.788×10^4

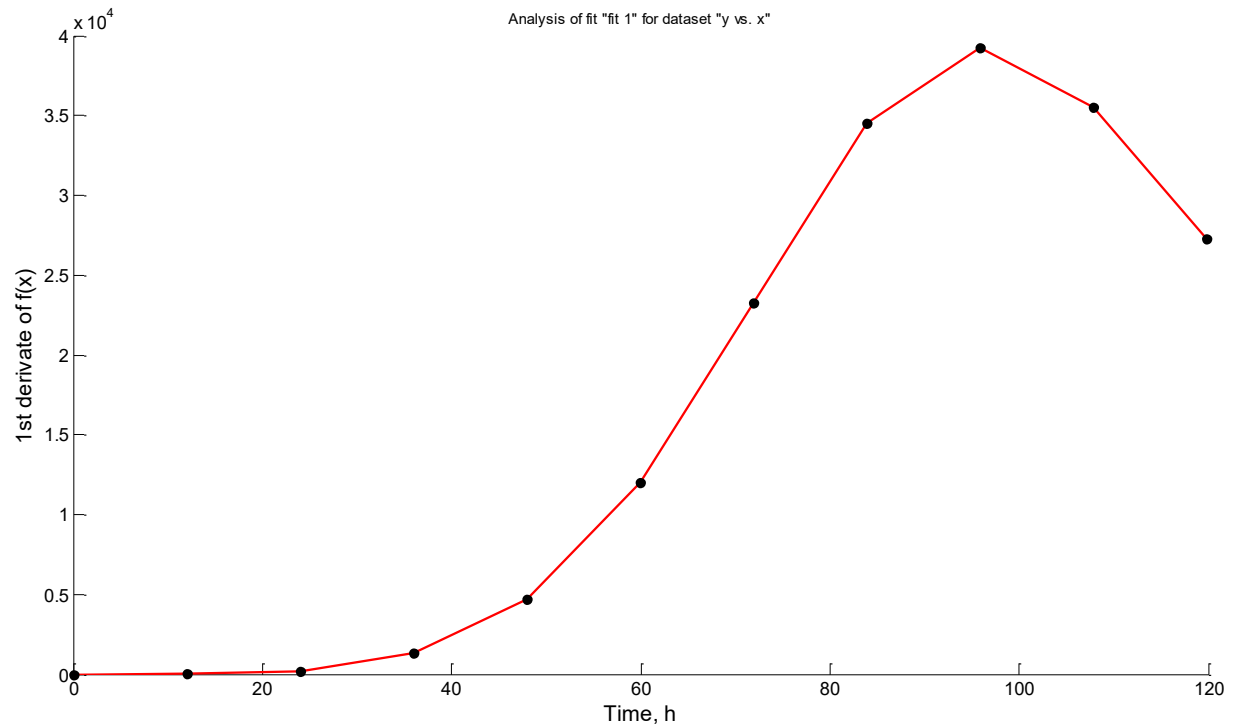


Figure C-2. First derivate of hill equation fitted to the OCI-Ly7 cell growth behavior.

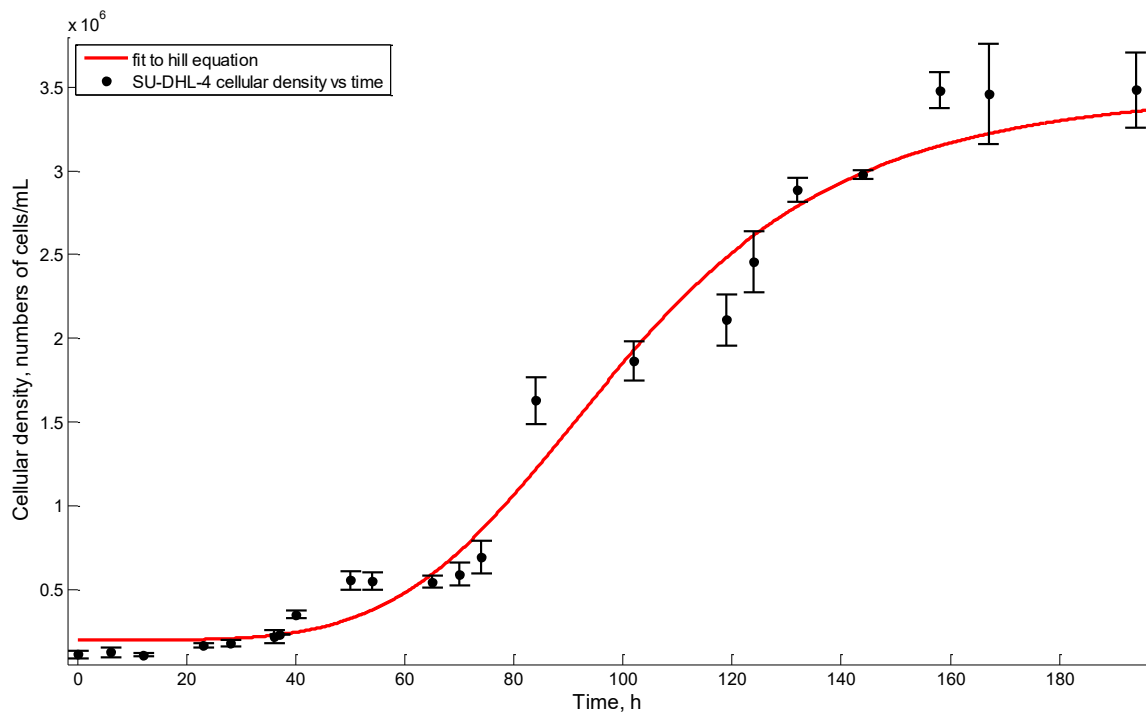


Figure C-3. Cellular density growth of SU-DHL-4 cell line in 7 days. General Model: $f(x) = a + (b-a)/(1+(c/x)^d)$, Coefficients (with 95% confidence bounds): $a = 2 \times 10^5$, $b =$

3.5e+6, c = 99.9(97.17, 102.6), d = 4.64 (4.16,5.12), Goodness of fit:, SSE: 2.59x10¹², R-square: 0.975, Adjusted R-square: 0.9749, RMSE: 2.015x10⁵

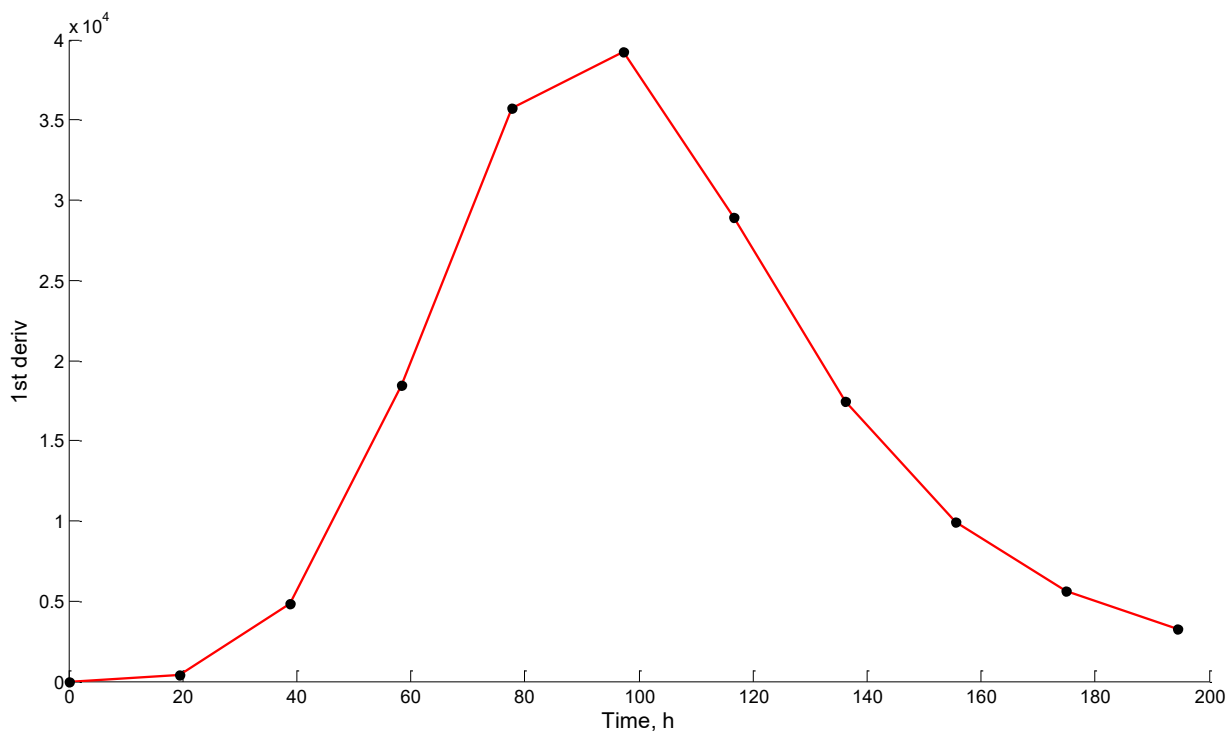


Figure C-4. First derivate of hill equation fitted to the OCI-Ly7 cell growth behavior.

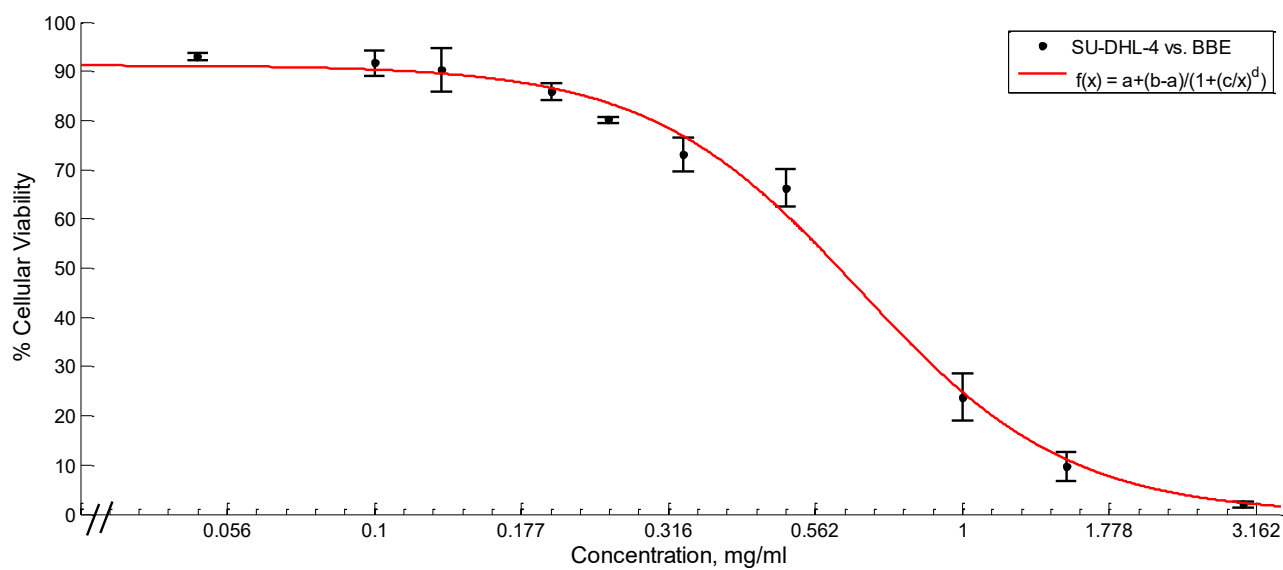


Figure C-5. Cellular Viability of SU-DHL-4 treated with Black Bean Extract. General Model: $f(x) = a + (b-a)/(1+(c/x)^d)$, Coefficients (with 95% confidence bounds): a = 2.557e-009 (fixed at bound), b = 96.36 (92.92, 99.81), c = 0.3363 (0.3009, 0.3716), d =

1.843 (-2.153, -1.532), Goodness of fit: SSE: 420.2, R-square: 0.9874, Adjusted R-square: 0.9862, RMSE: 4.473

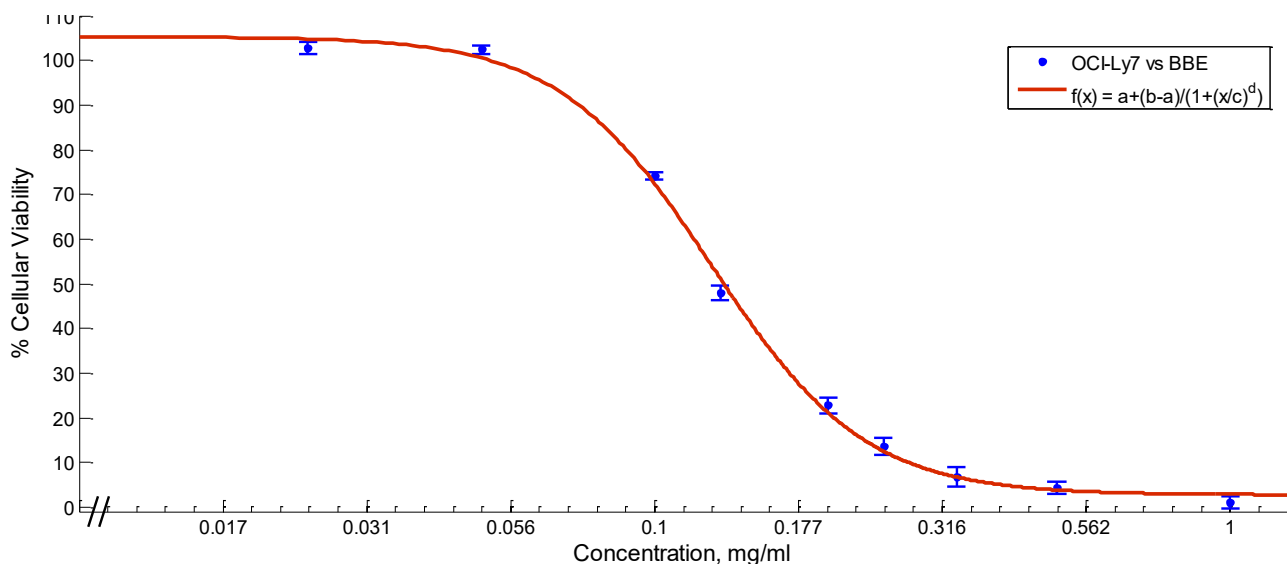


Figure C-6. Cellular Viability of OCI-Ly7 treated with Black Bean Extract. General Model: $f(x) = a + (b-a)/(1+(c/x)^d)$,Coefficients (with 95% confidence bounds): $a = 2.734$ (0.763, 4.705) $b = 105.3$ (102.8, 107.7) $c = 0.1257$ (0.1217, 0.1297) $d = -3.272$ (-3.607, -2.937) Goodness of fit: SSE: 128 R-square: 0.9969 Adjusted R-square: 0.9965 RMSE: 2.359

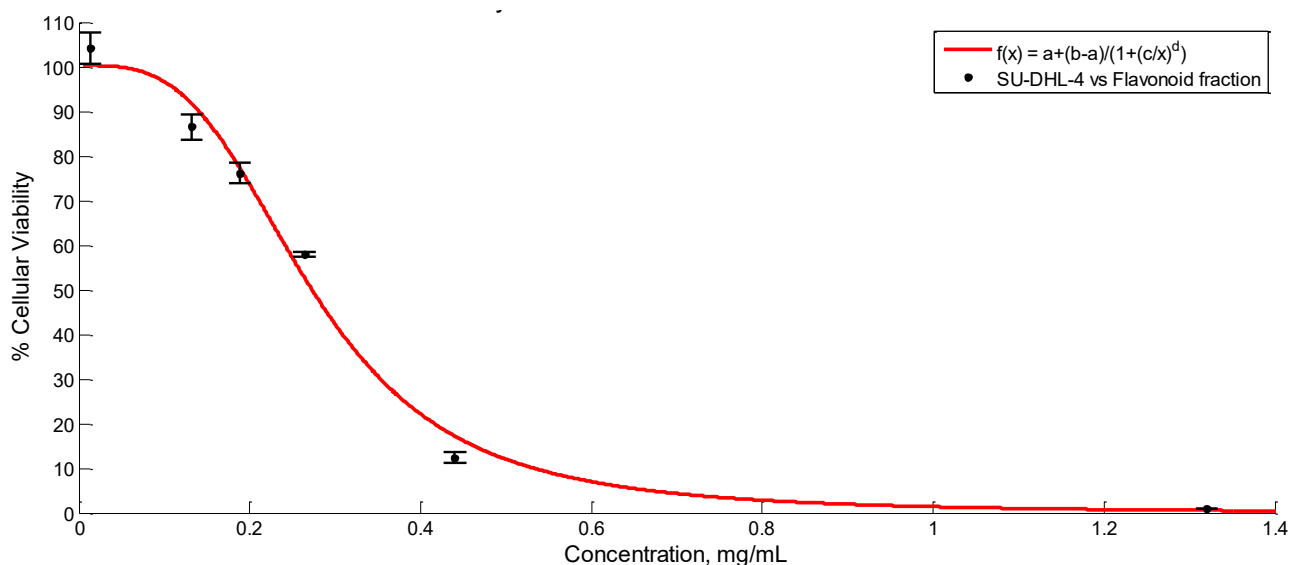


Figure C-7. Cellular viability of SU-DHL-4 treated with Flavonoid Fraction. General Model: $f(x) = a + (b-a)/(1+(c/x)^d)$ Coefficients (with 95% confidence bounds): $a = 3.731e-010$ (fixed at bound), $b = 97.3$ (92.66, 101.9), $c = 0.3014$ (0.2835, 0.3192), $hcoef = -4.469$ (-5.424, -3.513). Goodness of fit: SSE: 363.6, R-square: 0.9868, Adjusted R-square: 0.985, RMSE: 4.923.

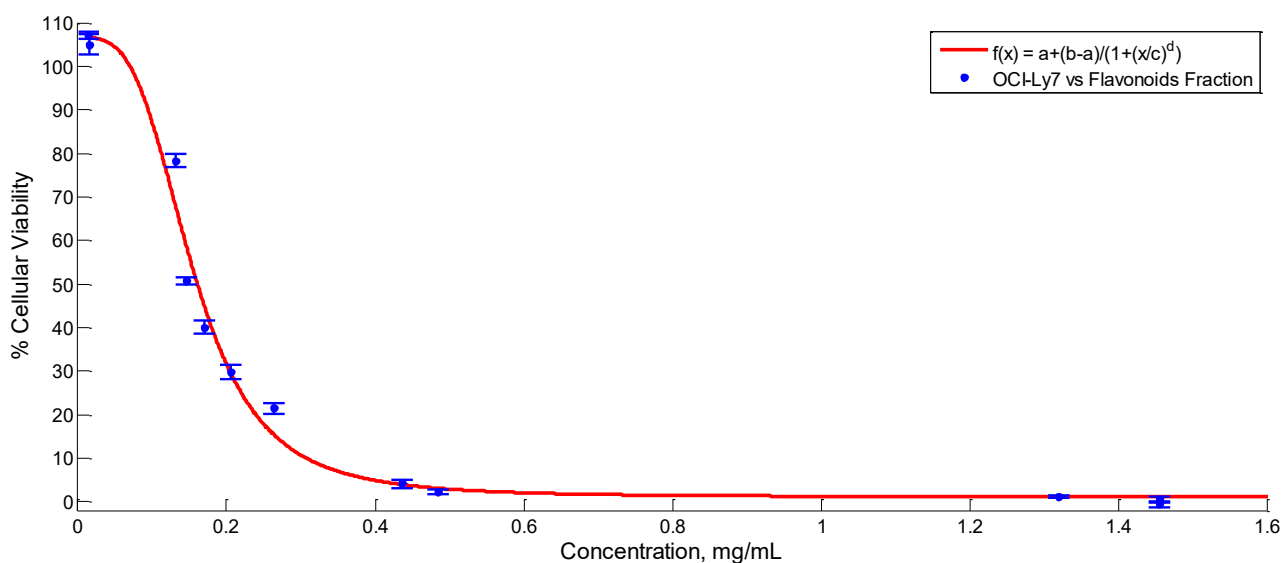


Figure C-8. Cellular viability of OCI-Ly7 treated with Flavonoid Fraction. General Model: $f(x) = a + (b-a)/(1+(x/c)^d$, Coefficients (with 95% confidence bounds): $a = 1.089$ (-1.85, 4.028), $b = 106.6$ (102.5, 110.8), $c = 0.1539$ (0.1468, 0.161), $d = -3.442$ (-4.091, -2.792), Goodness of fit: SSE: 803, R-square: 0.9852, Adjusted R-square: 0.9838, RMSE: 5.009.

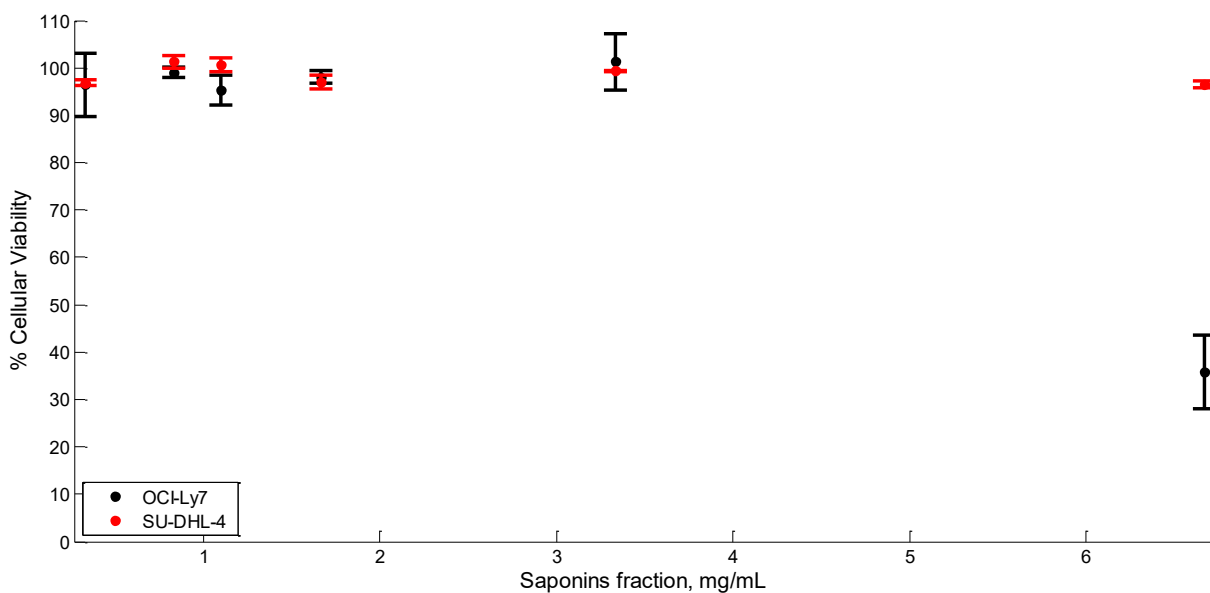


Figure C-9. Cellular viability of OCI-Ly7 and SU-DHL-4 cells treated with the saponin fraction.

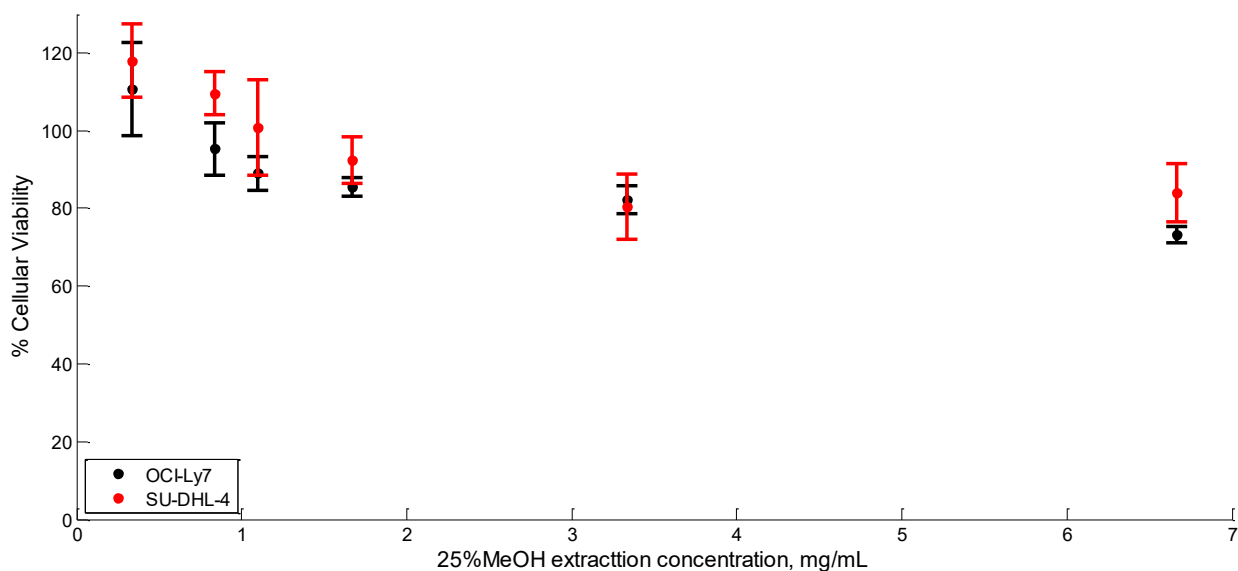


Figure C-10 Cellular viability of OCI-Ly7 and SU-DHL-4 cells treated with the phenolic acids fraction

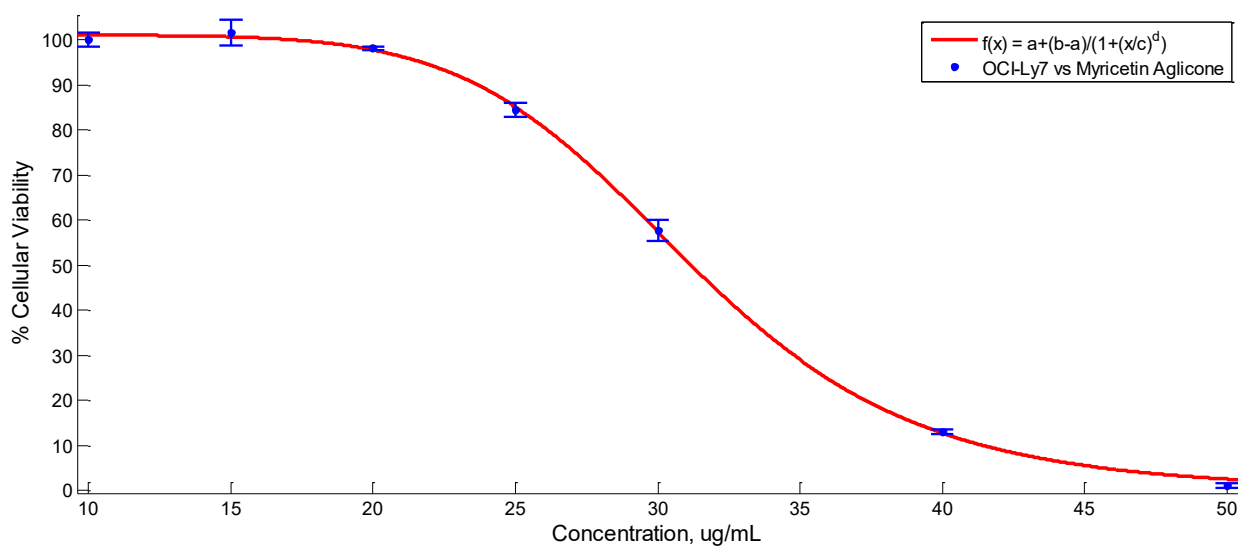


Figure C-11. Cellular viability of OCI-Ly7 treated with myricetin standard. General model: $f(x) = a + (b-a)/(1+(x/c)^d)$, Coefficients (with 95% confidence bounds): $a = 1.089$ (-1.85, 4.028), $b = 106.6$ (102.5, 110.8), $c = 0.1539$ (0.1468, 0.161), $d = -3.442$ (-4.091, -2.792), Goodness of fit: SSE: 803, R-square: 0.9852, Adjusted R-square: 0.9838, RMSE: 5.009.

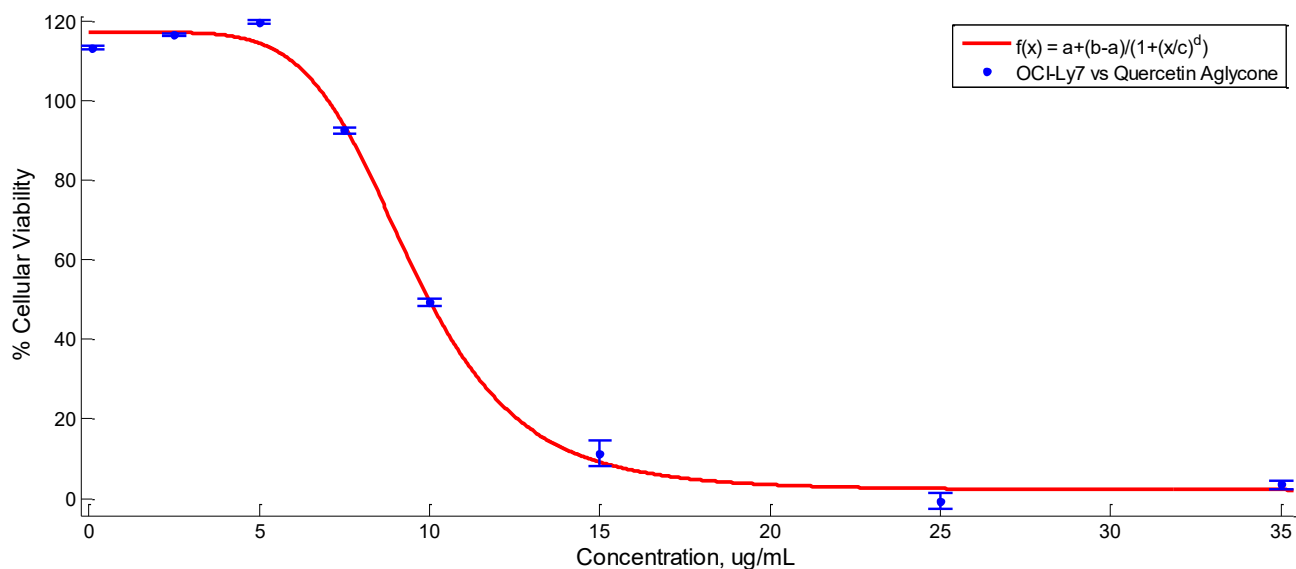


Figure C-12. Cellular viability of OCI-Ly7 treated with quercetin standard. General model: $f(x) = a+(b-a)/(1+(x/c)^d)$, Coefficients (with 95% confidence bounds): $a = 2.151 (-0.5047, 4.807)$, $b = 117.1 (114.6, 119.5)$, $c = 9.427 (9.201, 9.653)$, $d = -5.882 (-6.689, -5.075)$. Goodness of fit: SSE: 213.7, R-square: 0.9964, Adjusted R-square: 0.9959, RMSE: 3.269.

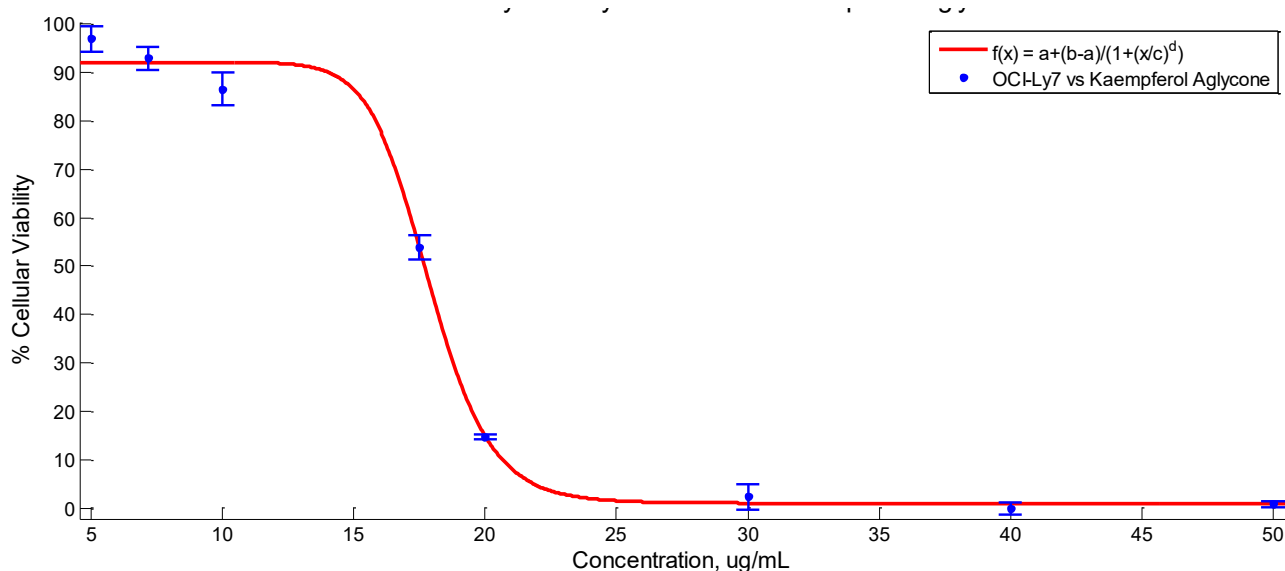


Figure C-13. Cellular viability of OCI-Ly7 treated with kaempferol standard. General model: $f(x) = a+(b-a)/(1+(x/c)^d)$, Coefficients (with 95% confidence bounds): $a = 1.039 (-0.3242, 2.402)$, $b = 125.2 (123.8, 126.5)$, $c = 17.11 (16.99, 17.24)$, $d = -13.36 (-15.02, -11.71)$. Goodness of fit: SSE: 75.97, R-square: 0.999, Adjusted R-square: 0.9988, RMSE: 1.949.

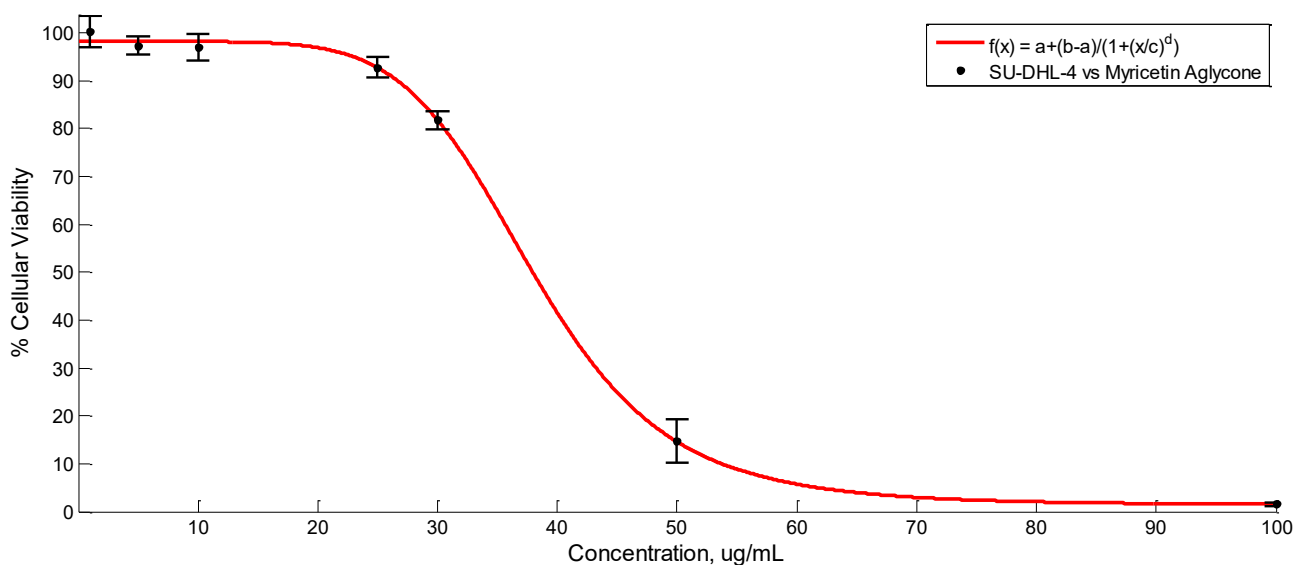


Figure C-14. Cellular viability of SU-DHL-4 treated with myricetin standard. General model: $f(x) = a + (b-a)/(1+(x/c)^d$, Coefficients (with 95% confidence bounds): $a = 1$, $b = 100$, $c = 0.03739$ (0.03566, 0.03911), $d = -6.297$ (-7.2, -5.395). Goodness of fit: SSE: 143.4, R-square: 0.9955, Adjusted R-square: 0.9952, RMSE: 2.994.

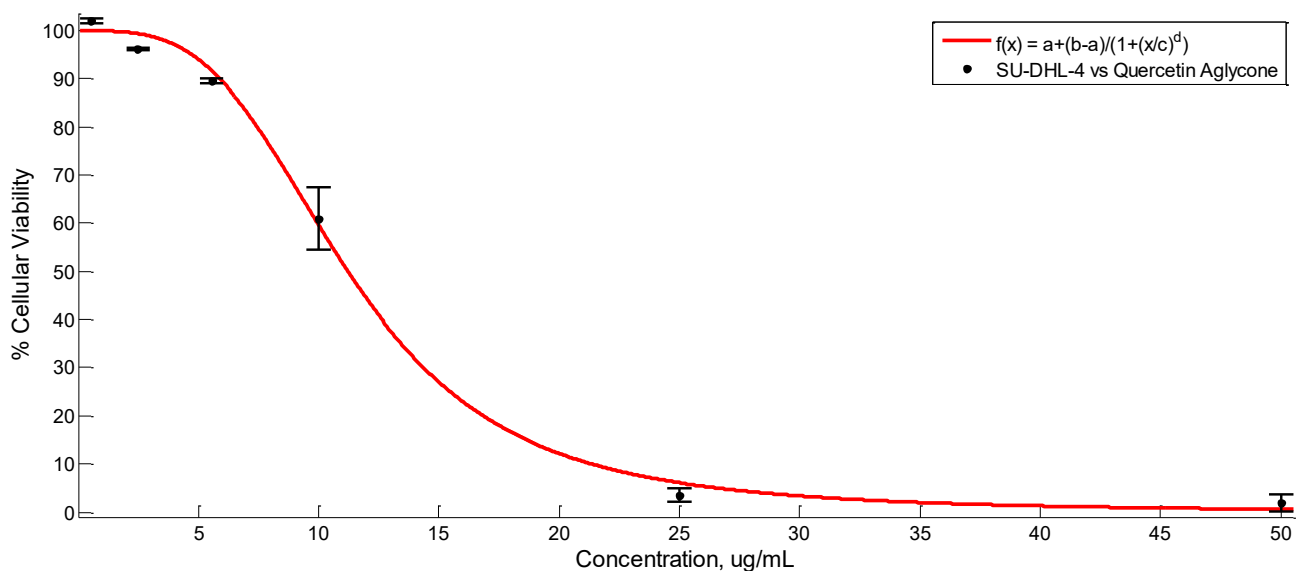


Figure C-15. Cellular viability of SU-DHL-4 treated with quercetin standard. General model: $f(x) = a + (b-a)/(1+(x/c)^d$, Coefficients (with 95% confidence bounds): $a = 2.086e-009$, $b = 97.85$ (96.4, 99.3), $c = 0.01108$ (0.009745, 0.01241), $d = -1.77$ (-1.997, -1.544). Goodness of fit: SSE: 81.33, R-square: 0.996, Adjusted R-square: 0.9954, RMSE: 2.329.

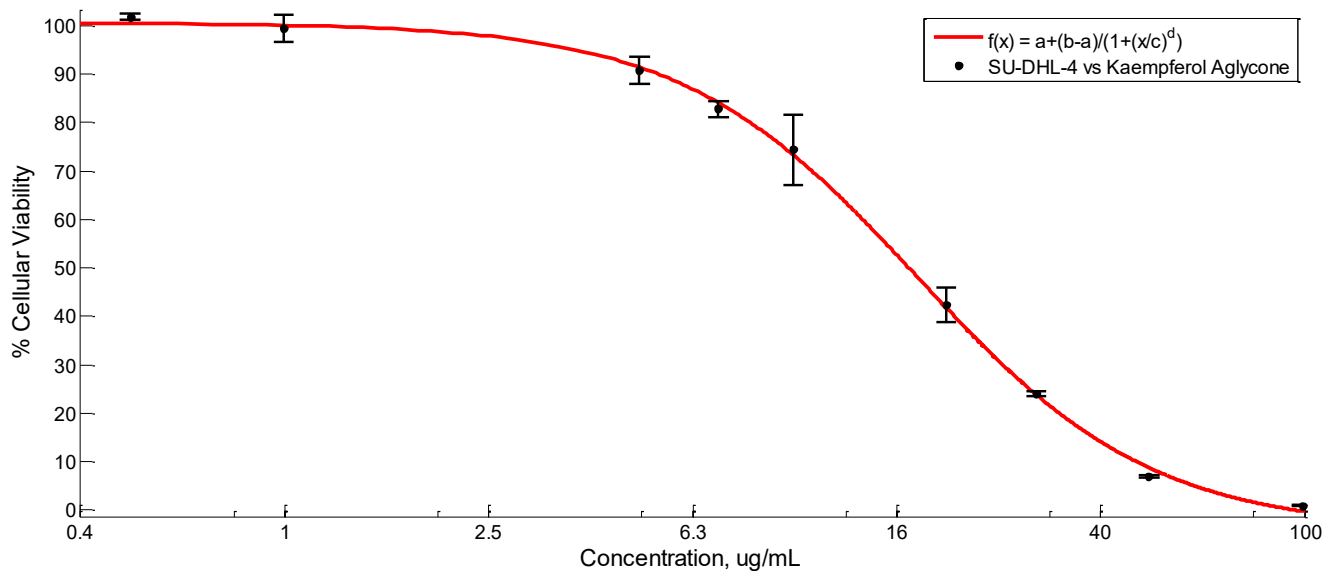


Figure C-16. Cellular viability of SU-DHL-4 treated with kaempferol standard. General model: $f(x) = a + (b-a)/(1+(x/c)^d)$, Coefficients (with 95% confidence bounds): $a = 5$, $b = 100$, $c = 0.01903$ (0.01705, 0.02101), $d = -2.105$ (-2.459, -1.751). Goodness of fit: SSE: 472, R-square: 0.976, Adjusted R-square: 0.9745, RMSE: 5.431. X-axis has been plotted as the logarithms to depict a smoother response of the waveform.

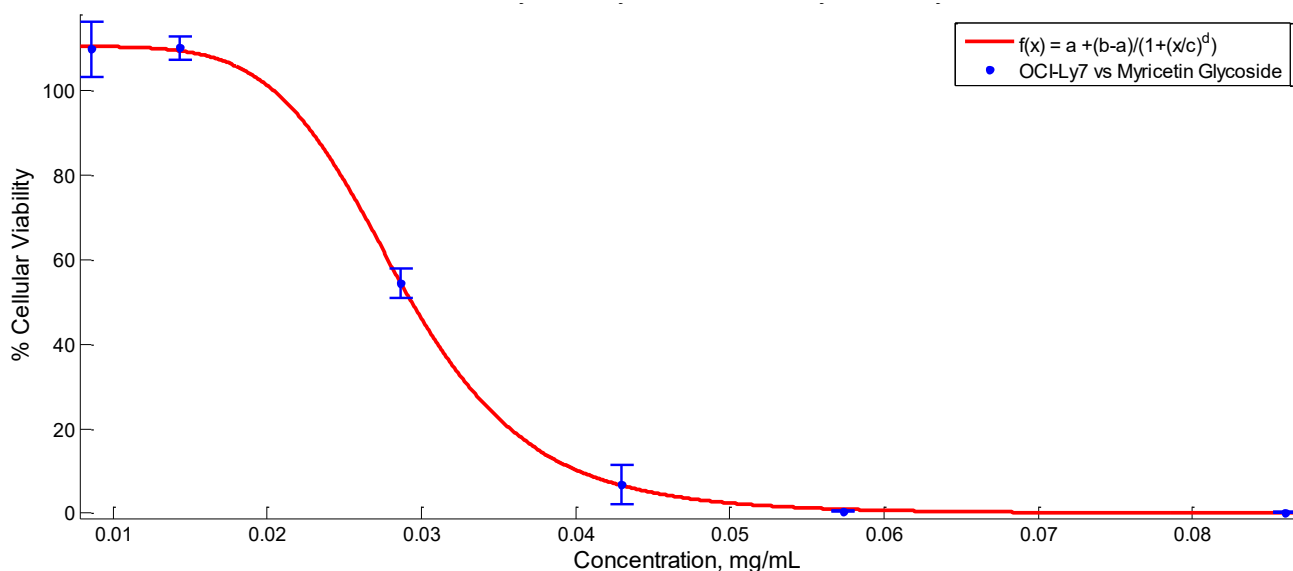


Figure C-17. Cellular viability of OCI-Ly7 treated with myricetin-3 glucoside. General model: $f(x) = a + (b-a)/(1+(x/c)^d)$, Coefficients (with 95% confidence bounds): $a = 1.949$ (-1208, 1212), $b = 109.3$ (104.9, 113.7), $c = 0.04503$ (-88.92, 89.01), $d = -16.51$ (-7.065e+005, 7.065e+005). Goodness of fit: SSE: 523.4, R-square: 0.9817, Adjusted R-square: 0.9778, RMSE: 6.114.

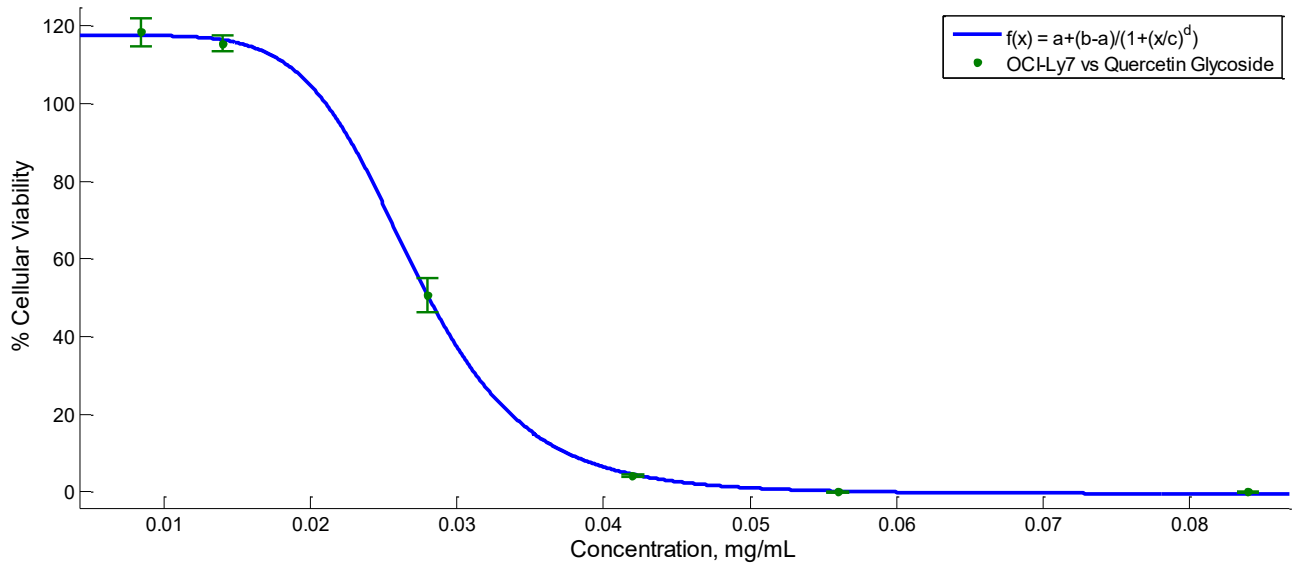


Figure C-18. Cellular viability of OCI-Ly7 treated with quercetin-3 glucoside.
General model: $f(x) = a + (b-a)/(1+(c/x)^d)$, **Coefficients (with 95% confidence bounds):**
a = 1.271 (-2.052e+005, 2.052e+005), **b** = 116.1 (111.3, 120.9), **c** = 0.13324 (-2.517e+006, 2.517e+006), **d** = -25.37 (-5.973e+010, 5.973e+010), **Goodness of fit:** SSE: 631.2, R-square: 0.9809, Adjusted R-square: 0.9768, RMSE: 6.715.

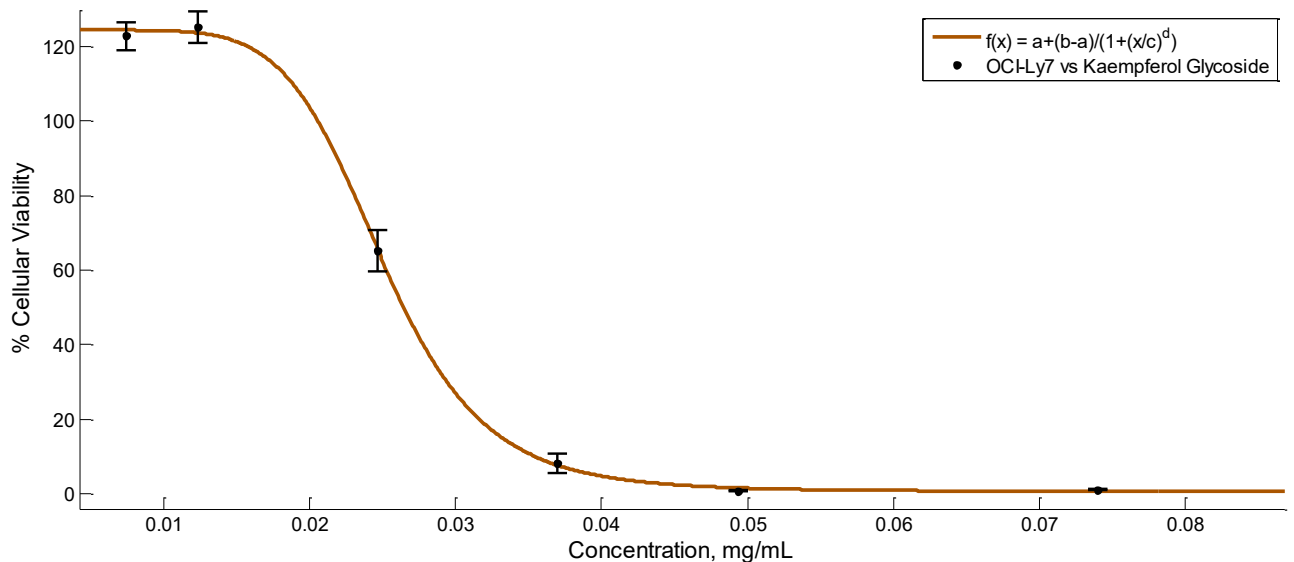


Figure C-19. Cellular viability of OCI-Ly7 treated with kaempferol-3 glucoside
General model: $f(x) = a + (b-a)/(1+(c/x)^d)$, **Coefficients (with 95% confidence bounds):**
a = 2.746 (-5.357e+005, 5.357e+005), **b** = 123.9 (118.1, 129.8), **c** = 0.18019 (-4.087e+006, 4.087e+006), **d** = -24.72 (-6.525e+010, 6.525e+010). **Goodness of fit:** SSE: 936.4, R-square: 0.9743, Adjusted R-square: 0.9687, RMSE: 8.178.

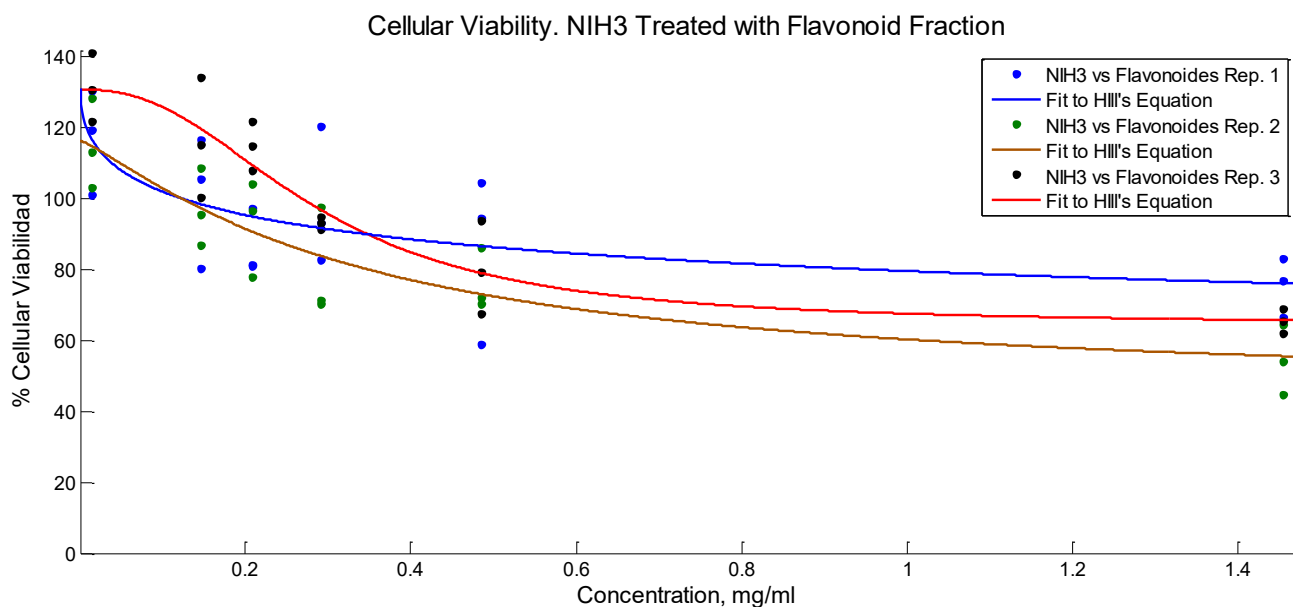


Figure C-20. Cellular Viability of NIH3 cells treated with flavonoid fraction

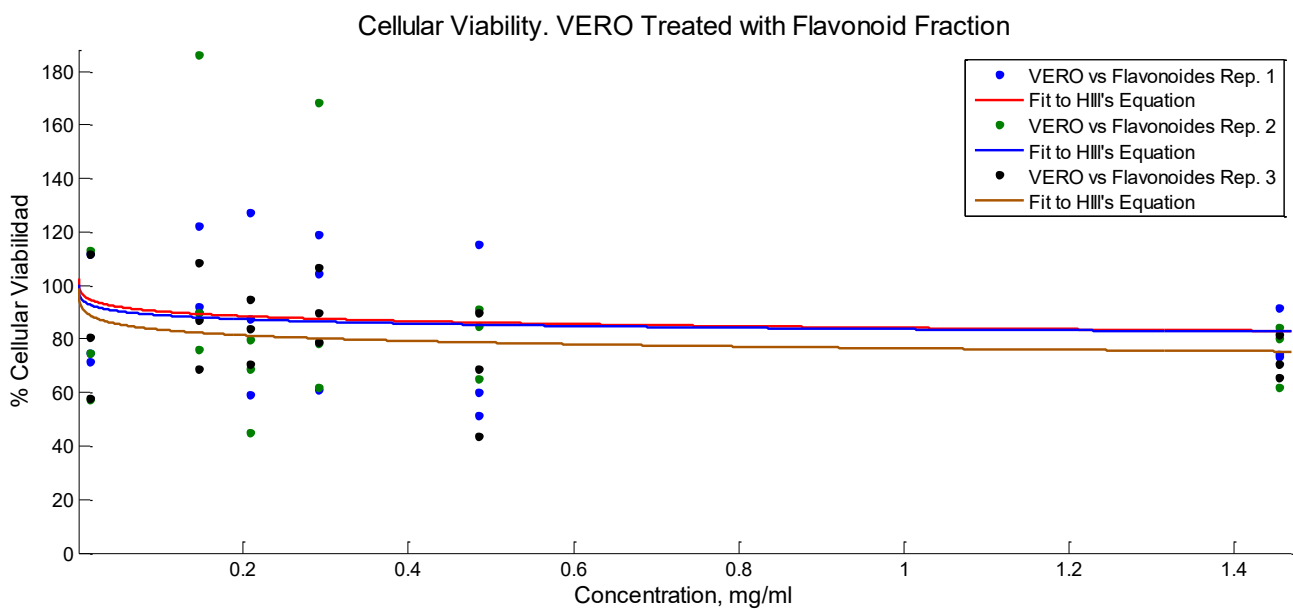


Figure C-21. Cellular Viability of VERO cells treated with flavonoid fraction

D. APPENDIX D

Annexin-V, PI and unstained cells control were analyzed with cells treated with doxorubicin after 24 h of incubation. These controls are required to validate the apoptosis assay.

The figure D-1 depicts the histogram of a population of unstained OCI-Ly7 cells treated with doxorubicin. Doxorubicin is a well-known drug that induces a Bax mediated mitochondria dependent apoptosis [23]. This control was run to identify the signal threshold. This threshold was set at 10^4 in the x-axis. Any signal exceeding the threshold was identified as a positive.

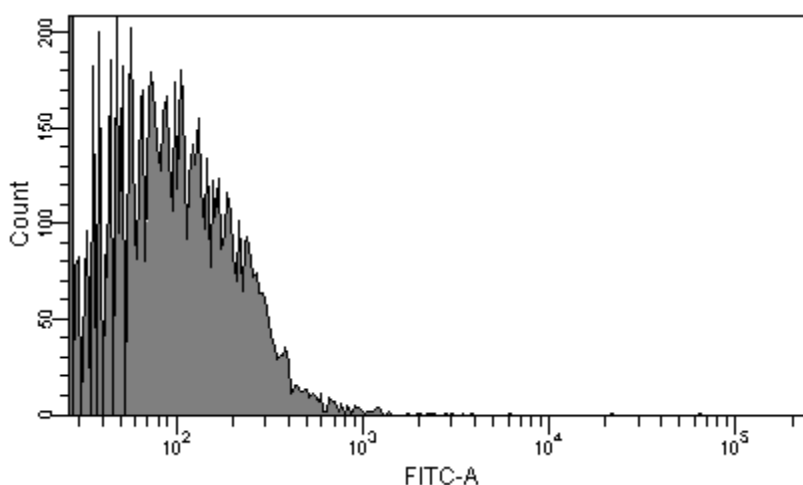
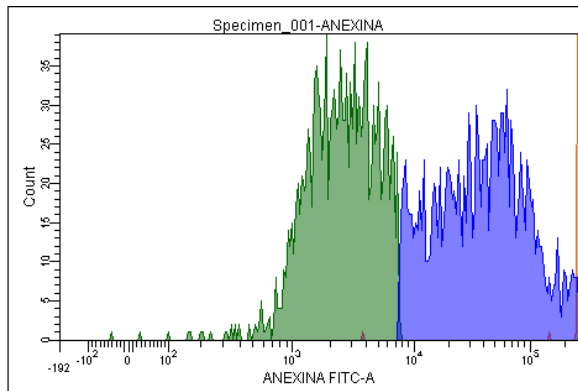


Figure D-1. Histogram of unstained cells control for apoptosis detection by flow cytometry.

On Figure D-2A it is detailed the Annexin-V control histogram. This blue histogram exceeded the threshold, detecting a population of OCI-Ly7 cells under apoptosis. The dot plot on Figure D-2B depicts the identification of the apoptotic population over the lower right quadrant. These quadrants were segmented setting up the x and y axis at the threshold level (10^4) determined in the unstained control assay.

A



B

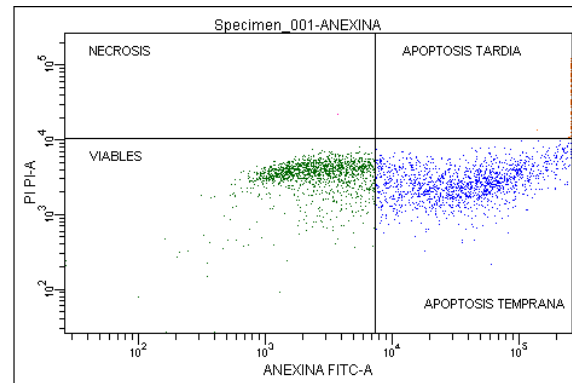
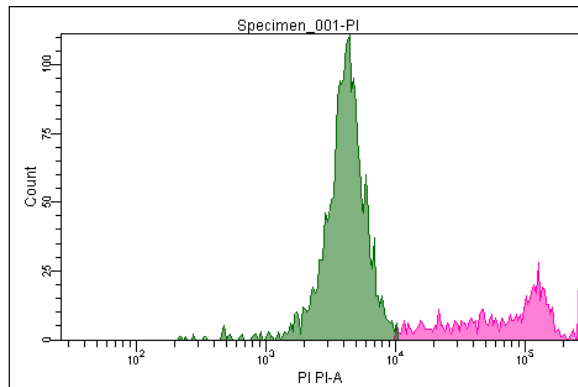


Figure D-2. Flow cytometry analysis of Annexin-V control for apoptosis detection.

On Figure D-3A it is details the histogram of two cell populations stained with PI. The green histogram represents viable cells and the pink histogram represents cells detected as PI positive. B. Dot plot of cells stained with Iodide propidium are detected as positive with an intensity signal higher that 10^4 (vertical-axis).

A



B

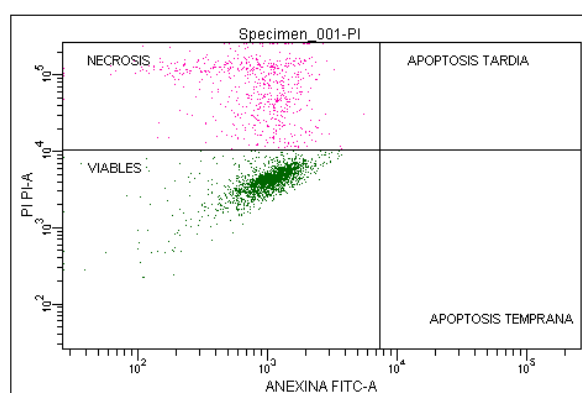
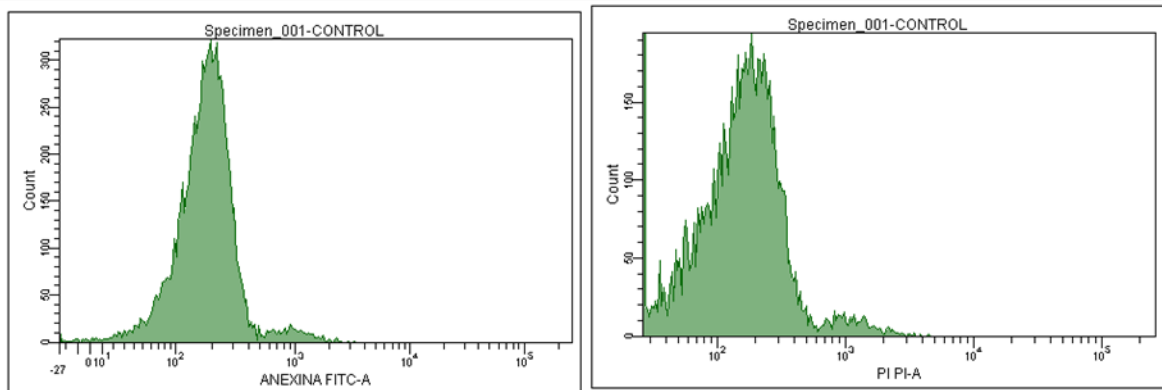


Figure D-3. . Flow cytometry analysis of Propidium Iodide (PI) control for apoptosis detection.

Figure D-4A depicts the histograms of OCI-Ly7 cells with no treatment. In both histograms the signal of the Annexin-V and PI histograms do not exceeded the threshold. Therefore this population of OCI-Ly7 cells is neither in apoptosis nor in necrosis. In Figure D-4B, the viable cells population is identified over the lower left quadrant labeled as viable.

A



B

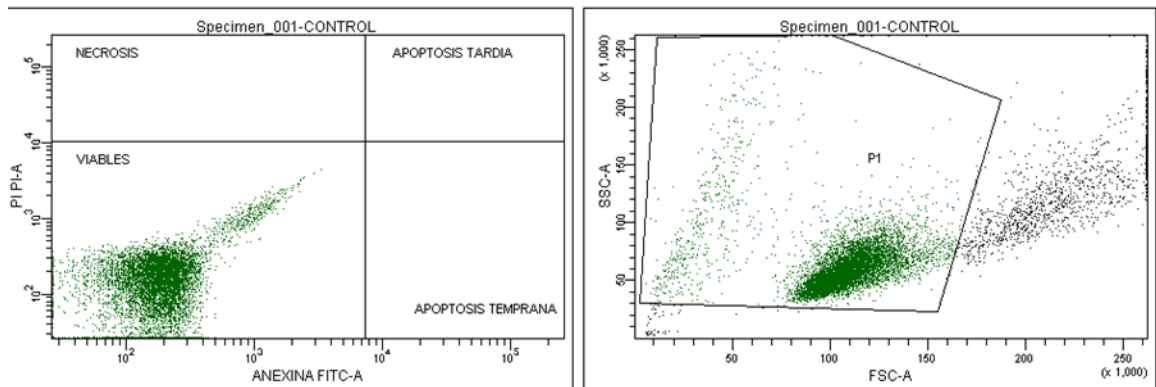


Figure D-4. Flow cytometry analysis of viable cells control for the identification of untreated cells.

Since the upper right quadrant is positive for Annexin-V and PI it was labeled as late apoptosis. The cells identified in this region are apoptotic too but the detection of DNA indicates that cell membrane integrity has been lost therefore they are in the late stage of apoptosis.

Table D-1 Apoptosis Assay. OCI-Ly7 cell populations under apoptosis and necrosis

Treatment	viable	apoptosis	necrosis
Control no treatment – i	90.2	8.8	1
Control no treatment – ii	91.2	8.2	0.7
Control no treatment – iii	88.9	9.9	1.2
Myricetin-I	52.5	44.7	2.8
Myricetin-II	54.9	41.6	3.6
Myricetin-III	73	25.4	1.5
Quercetin-I	55.3	43	1.7
Quercetin-II	49.9	49.6	0.5
Quercetin-III	72.6	25.4	2.1
Kaempferol-I	57.2	41.1	1.7
Kaempferol-II	65	32.9	2.1
Kaempferol-III	73.9	25	1.1
Flavonoid fraction – I	51.8	44.6	3.6
Flavonoid fraction – II	61.5	36.9	1.6
Flavonoid fraction – III	49.8	49.4	0.8
Black bean extract – I	56.8	41.3	1.9
Black bean extract – II	47.7	51.4	0.9
Black bean extract – III	61	37.8	1.2

Table D-2 Apoptosis Assay. SU-DHL-4 cell populations under apoptosis and necrosis

Treatment	viable	apoptosis	necrosis
Control no treatment – i	85.6	12.9	1.5
Control no treatment – ii	86.6	11.8	1.7
Control no treatment – iii	86.7	12	1.3
Myricetin-I	62.3	34.6	3.1
Myricetin-II	49.3	49	1.7
Myricetin-III	57	40.1	2.9
Quercetin-I	45.2	52.6	2.2
Quercetin-II	47.2	51.1	1.6
Quercetin-III	38.5	60.2	1.3
Kaempferol-I	71.8	26.1	2.1
Kaempferol-II	46.5	50.2	3.2
Kaempferol-III	51.2	46.9	1.9
Flavonoid fraction – I	48.7	48.1	3.2
Flavonoid fraction – II	52.7	45.2	2.1
Flavonoid fraction – III	49.1	47.1	3.8
Black bean extract – I	56.8	41.3	1.9
Black bean extract – II	47.7	51.4	0.9
Black bean extract – III	61	37.8	1.2

E. APPENDIX E

QUALITY CONTROLS FOR BAX ASSAY

The figure E-1 depicts the histogram of a population of unstained OCI-Ly7 cells treated with doxorubicin. A research study reported that doxorubicin increased Bax protein levels after 12 h of treatment in B-cell leukemia cells (NALM-6), [23]. This control was analyzed to identify the signal threshold and to identify how to distinguish a population that over expressed the Bax protein. This threshold was set at 10^3 in the x-axis. Any signal exceeding the threshold identifies a population with over expression of Bax.

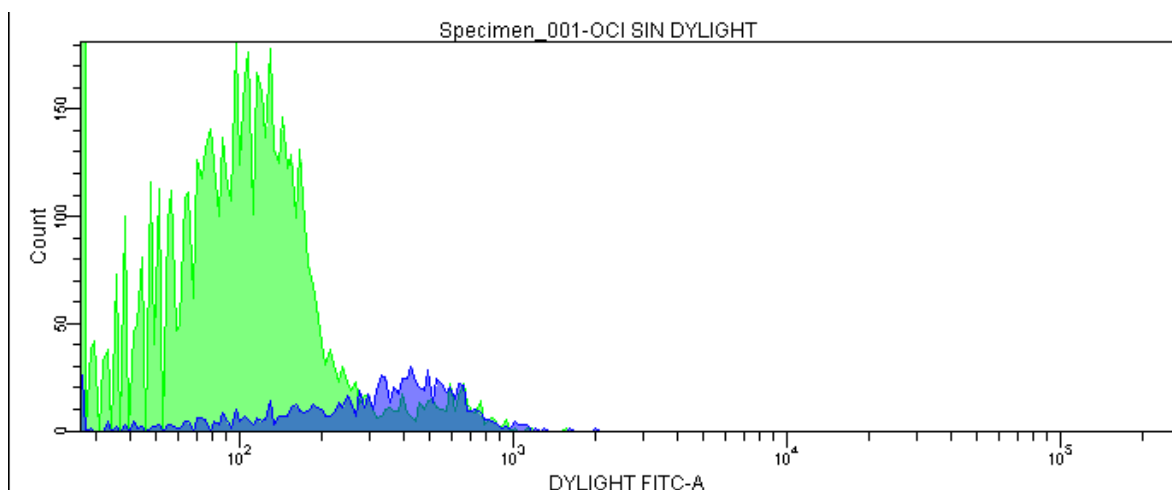


Figure E-1. Flow cytometry analysis of unstained cells control for protein Bax detection.

Figure E-2 depicts the histograms of OCI-Ly7 anti-Bax Dylight stained cells with no treatment. In comparison with Figure 3-10, the mean signal of the histogram is reported as 96 and the mean signal of the anti-Bax Dylight in the histogram of figure 3-11 is 128,312 indicating that there is a difference between stained and unstained populations. This difference was interpreted as Bax-positive population however these cells are not exceeding the 10^3 threshold. Therefore any population exceeded this 10^3 threshold was identified as cells with over expression of Bax.

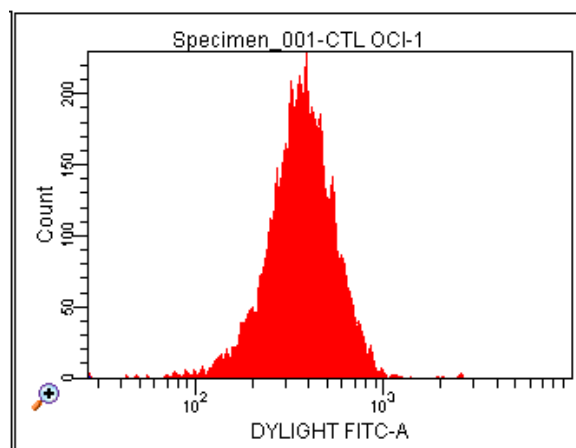


Figure E-2. Flow cytometry analysis of untreated cells control for protein Bax detection.

Figures E-3A and E-3B details the contour plots utilized in order to detail how populations of cells with Bax over expression set apart from populations with no over expression. The inner ellipse of these contour plot on A represented the mean ± 1 standard deviation of the histogram of Figure E-3B. The contour plot on B represented the OCI-Ly7 after 24 h treatment with flavonoids, where it is depicted that three different populations are setting apart from each other interpreted as different mean signal of Bax protein expression.

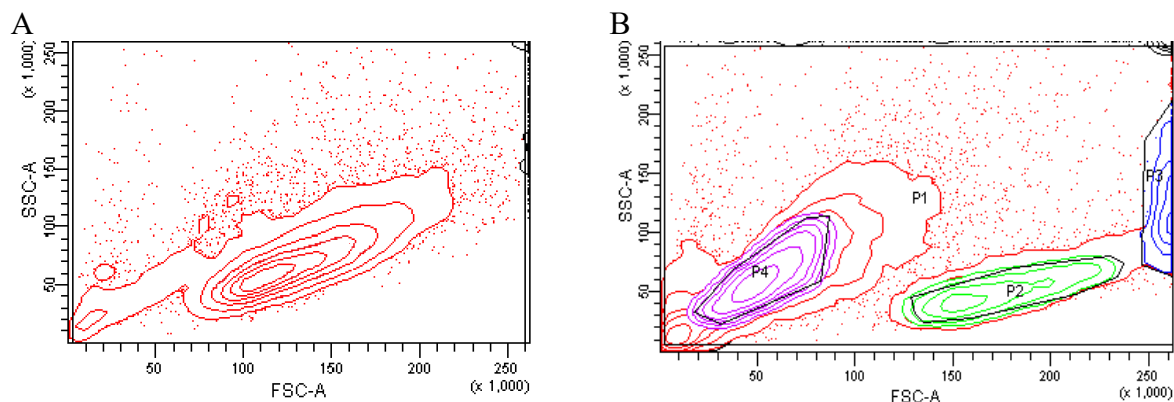


Figure E-3. Flow cytometry contour plot analysis of cells treated with doxorubicin in comparison with untreated cells.

ADDITIONAL RESULTS OF CELL CYCLE ANALYSIS OF OCI-LY7 CELLS

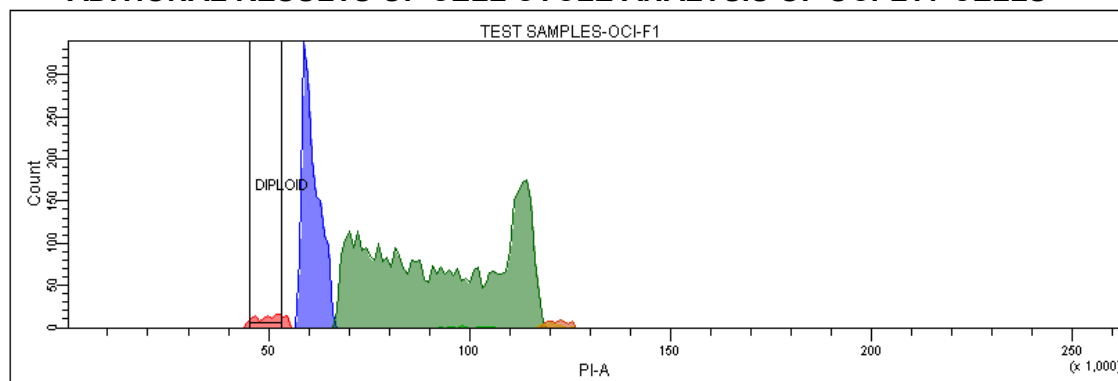


Figure E-4. Cell Cycle Analysis to OCI-Ly7 cells treated with Flavonoid Fraction

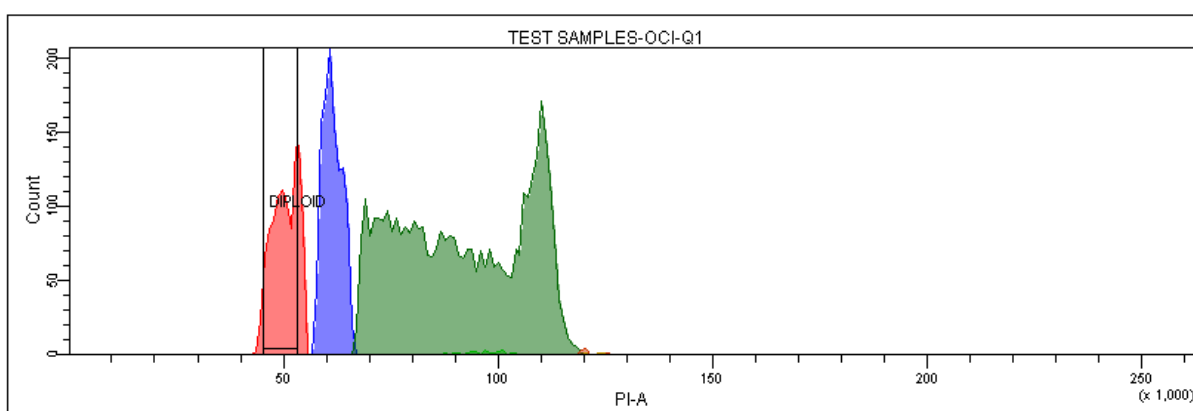


Figure E-5. Cell Cycle Analysis to OCI-Ly7 cells treated with Quercetin

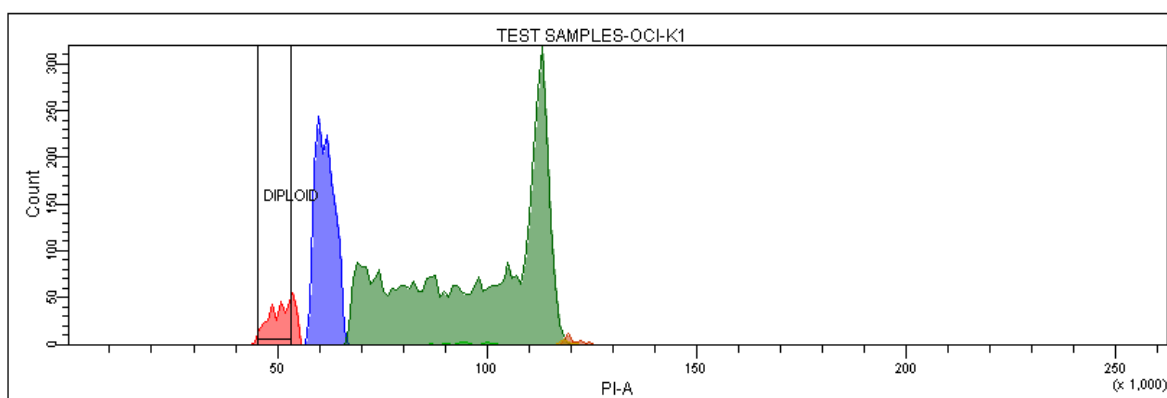


Figure E-6. Cell Cycle Analysis to OCI-Ly7 cells treated with Kaempferol

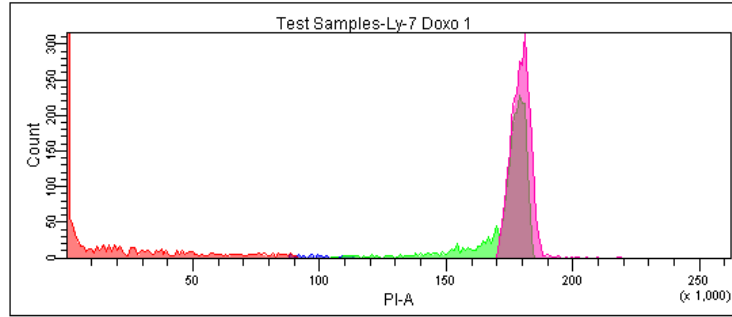


Figure E-7. Cell Cycle Analysis to OCI-Ly7 cells treated with Doxorubicin

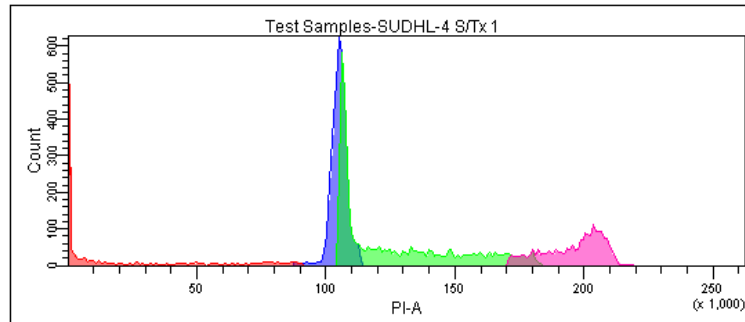


Figure E-8. Cell Cycle Analysis to untreated SU-DHL-4 cells

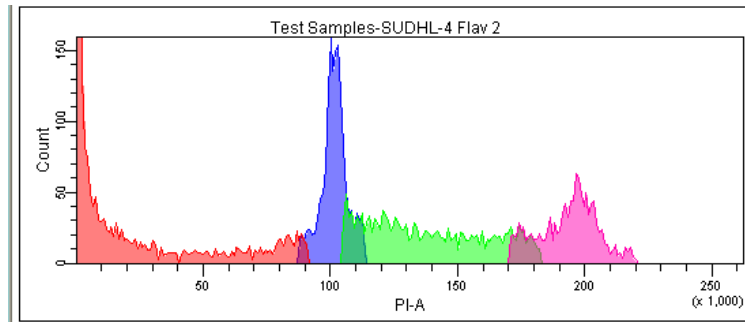


Figure E-9. Cell Cycle Analysis to SU-DHL-4 cells treated with Flavonoid Fraction

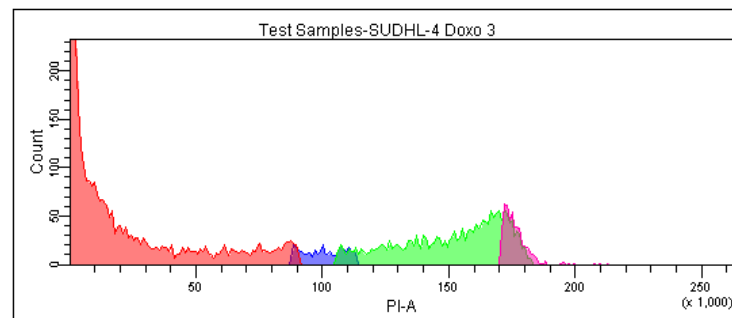


Figure E-10. Cell Cycle Analysis to SU-DHL-4 cells treated with Doxorubicin

Table E-1 Cell cycle analysis data of OCI-Ly7 treated with Flavonoid fraction, Myricetin, Quercetin & Kaempferol.

CELL CYCLE ASSAY # 1																									
	OCI-Ly7 No Tx.					FLAVONOIDS					MYRICETIN					QUERCETIN					KAEMPFEROL				
	1	2	3	mean	SD	1	2	3	mean	SD	1	2	3	mean	SD	1	2	3	mean	SD	1	2	3	mean	SD
G1/G0	30.4	29.6	32.8	30.95	1.65	14.5	14.3	19.3	16.03	2.831	11.7	10	10.8	10.9667	0.67	11	11.2	11.8	11.33	0.4	13	10	14	12.43	1.93993
S	51.4	44.3	46.8	47.52	3.579	41.14	41.2	43.9	42.08	1.576	28.4	29	27.6	28.4667	0.9	39	39.1	40.8	39.57	1.1	41	44	46	43.6	2.62298
G2	9.5	11.1	13.5	11.36	2.014	0.5	0.6	3.1	1.4	1.473	0.4	0.2	0.3	0.3	0.1	0.1	0.2	0.3	0.2	0.1	0.3	0.1	0.2	0.2	0.1
Doublets	0.3	1.07	0.5	0.622	0.397	0.2	0.2	0.4	0.267	0.115	0.1	0.1	0.2	0.13333	0.06	0	0	0.1	0.033	0.1	0.1	0.1	0.1	0.1	1.7E-17
CELL CYCLE ASSAY # 1																									
	OCI-Ly7 No Tx.					FLAVONOIDS					MYRICETIN					QUERCETIN					KAEMPFEROL				
	1	2	3	mean	SD	1	2	3	mean	SD	1	2	3	mean	SD	1	2	3	mean	SD	1	2	3	mean	SD
G1/G0	32.8	32	30.4	31.73	1.22	18.1	17.1	21.3	18.83	2.194	14.3	13	13.6	13.5	0.85	13	13.4	14.4	13.7	0.6	17	13	16	15.2	2.16564
S	46.8	40.9	51.4	46.37	5.263	39.5	39.7	38	39.07	0.929	27.4	29	27.9	28.1333	0.87	39	39.1	40.8	39.67	1	40	45	46	43.43	2.85365
G2	13.5	13.2	9.5	12.07	2.228	2.2	1.8	8.4	4.133	3.7	1.3	0.7	1.4	1.13333	0.38	0.4	0.6	0.6	0.533	0.1	1.2	0.3	1	0.833	0.47258
Doublets	0.5	1.5	0.3	0.767	0.643	0.5	0.4	0.7	0.533	0.153	0.2	0.1	0.2	0.16667	0.06	0	0.1	0.2	0.1	0.1	0.4	0.1	0.3	0.267	0.15275
CELL CYCLE ASSAY # 3																									
	OCI-Ly7 No Tx.					FLAVONOIDS					MYRICETIN					QUERCETIN					KAEMPFEROL				
	1	2	3	mean	SD	1	2	3	mean	SD	1	2	3	mean	SD	1	2	3	mean	SD	1	2	3	mean	SD
G1/G0	32.8	32	30.4	31.73	1.22	22.4	21.4	19	20.93	1.747	17	19	17.5	17.9333	1.21	19	18.8	20	19.4	0.6	19	19	22	20.03	1.90875
S	46.8	40.9	51.4	46.37	5.263	31.8	31.4	34	32.4	1.4	22.6	23	22.8	22.9333	0.42	32	31.6	32.8	32.27	0.6	28	34	29	30.23	3.21455
G2	13.5	13.2	9.5	12.07	2.228	10.4	10.8	7.6	9.6	1.744	7	7.3	7.9	7.4	0.46	7.7	8.9	9.4	8.667	0.9	15	10	19	14.57	4.2004
Doublets	0.5	1.5	0.3	0.767	0.643	2	1.1	0.7	1.267	0.666	0.5	0.9	0.7	0.7	0.2	1.1	0.8	0.8	0.9	0.2	4.2	2.1	3.2	3.167	1.0504

QUALITY CONTROLS FOR CELL CYCLE ANALYSIS

Step by step procedure was taken from [44]. These quality controls were performed using the DNA QC particles kit (Part. Number: 349523, Becton Dickinson Biosciences, San Jose, CA, USA) this kit contains four vials (A, B, C & D). Vial A contains chicken erythrocyte nuclei, or CEN. We use CEN to verify instrument linearity and resolution. Vial B contains calf thymocyte nuclei, or CTN. CTN's are used to assess doublet discrimination. Vial C contains 2 micron fluorescent beads used to check instrument alignment, stability, and coefficient of variation, especially if the CEN and CTN fail to perform as expected. Vial D contains the nucleic acid dye, propidium iodide, or PI. PI is an equilibrium dye which intercalates into the DNA of the CEN and CTN. CENs are non-cycling and are treated to contain singlets, doublets, and larger aggregates. CTN's are cycling, so we will see nuclei in G0/G1, S, and G2/M phases. These also contain aggregates. PI is excited by the 488 nm blue laser and its fluorescence will be detected by the PI detector already configured in the flow cytometer. The threshold was set to PI.

CEN AND CTN SAMPLES PREPARATION

1000 μ L of PI were added into two 12 x 75 mm BD Falcon tubes already labeled as CTN & CEN respectively. CEN tube was shaken by vortex and 40 μ L were added to the CEN tube. Next CTN tube was shaken by vortex and 40 μ L were added to the CTN tube. CEN & CTN samples were incubated at room temperature, away from light, for 10 minutes.

DETERMINATION OF RESOLUTION AND LINEARITY

CEN sample was run on the flow cytometer to determine resolution and linearity. To determine resolution, we had to identify the CV of the singlet's statistics. To determine linearity, we had to identify the Singlet's to Doublet's mean ratio. The conditions of resolution and linearity are detailed on table E-2:

Table E-2 Conditions of resolution and Linearity for Cell cycle analysis

$$SINGLET'S CV \leq 3$$

Condition of resolution

$1.95 \leq \text{SINGLETs TO DOUBLETs MEAN RATIO} \leq 2.05$ Condition of linearity

CEN CONTROL

CEN was analyzed to determine resolution and linearity. Singlets CV is 2.4, therefore, instrument has a good resolution. The linearity is confirmed by the quotient of PI-A mean of doublets divided by PI-A mean of singlets.

$$\frac{\text{PI - A mean (Doublets)}}{\text{PI - A mean (Singlets)}} = \frac{98636}{49602} = 1.988$$

CTN CONTROL

CTN are cycling so we will see nuclei in G₀/G₁, S and G₂/M phases and also contain aggregates. As it is illustrated in figure E-11. The flow cytometer depicts a dot plot in which we can discriminate doublets G₀/G₁ doublets from G₂/M singlets which is the main object of CTN control. Green population represents the G₀/G₁ phase. Blue population represents the synthesis phase and the red population represents the G₂/M phase. The purple population is represented as G₀/G₁ doublets which are detected as two G₀/G₁ singlets attached.

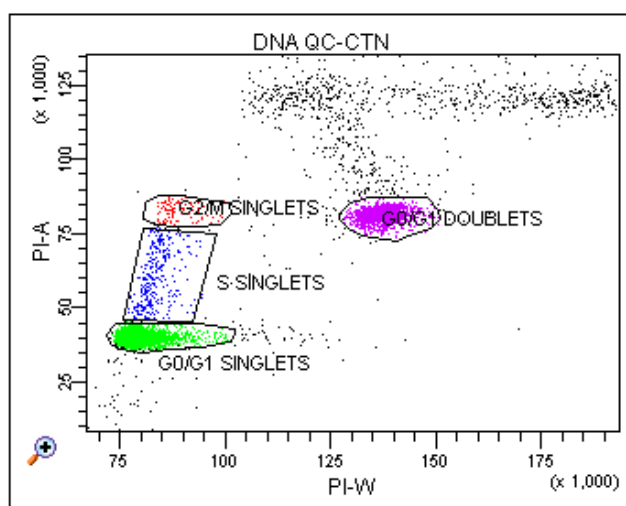


Figure E-11. Flow cytometry dot plot analysis of CTN (calf thymocyte nuclei) stained with PI (propidium iodide) dot plot.

DNA PLOIDY ANALYSIS

It is required a test sample of at least 5.0×10^5 cancer cells for the staining procedure for DNA ploidy analysis. An additional sample tube of the specimen mixed with Peripheral Blood Mononuclear cells or PBMC's was prepared and used as a control.

PBMC's are non-cycling cells that remain in the G_0/G_1 phase and can be used as a diploid standard. Any signal higher or lower than this is the guide to identify aneuploidy with the DNA index.

The DNA index is calculated as the rate of the mean PI signal of the specimen who in this case is OCI-Ly7 over the PI signal of the diploid standard.

$$DNA\ Index = \frac{Mean\ of\ specimen}{Mean\ of\ STD} \quad (Eq. 5)$$

Lymphoprep protocol taken from [25] was used to isolate mononuclear cells as follows. 3 mL of blood was drawn from a no cancer male 28 year old subject and placed into a tube with EDTA. Blood was diluted in NaCl 0.9% solution in a 1:1 proportion. In a 15 mL Corning tube 3 mL of lymphoprep were added and the 6 mL solution of blood was carefully poured into the 15 mL tube in order to form two phases and not mixing them. The tube with the two phases was centrifuged at 600 g for 20 min at room temperature. And finally the Mononuclear cells (white, translucent phase, Figure E-12, Image taken from [25]) was pipetted out and it was ready to be run on the flow cytometer.

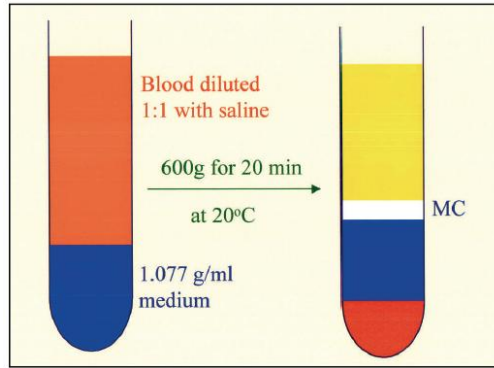


Figure E-12. Graphic procedure for peripheral blood mononuclear cells isolation.

The PBMC's were mixed with OCI-Ly7 cells in 1:1 proportion (v/v) and then analyzed by flow cytometry. 20000 events were recorded.

Mean PI of the specimen(OCI-Ly7) was identified as 62383 and the mean PI for PBMC was 49779, then DNA index is calculated using Eq. 5:

$$DNA\ Index = \frac{Mean\ of\ specimen}{Mean\ of\ STD} = \frac{62382}{49779} = 1.253$$

Therefore hyperploidy of OCI-Ly7 is established with a DNA Index of 1.253

F. APPENDIX F

FLAVONOID STANDARDS DETECTION

In Figure F-1A it is detailed the total ions chromatogram of myricetin, quercetin and kaempferol standards and Figure F-1B depicts the chromatogram of the extracted ions of myricetin, quercetin and kaempferol standards at the following respective ranges of mass; (319.0, 319.2), (303.0, 303.2), (287.0, 287.2). The mass spectra of the flavonoids extracted from these chromatograms are shown in Figure 3-17.

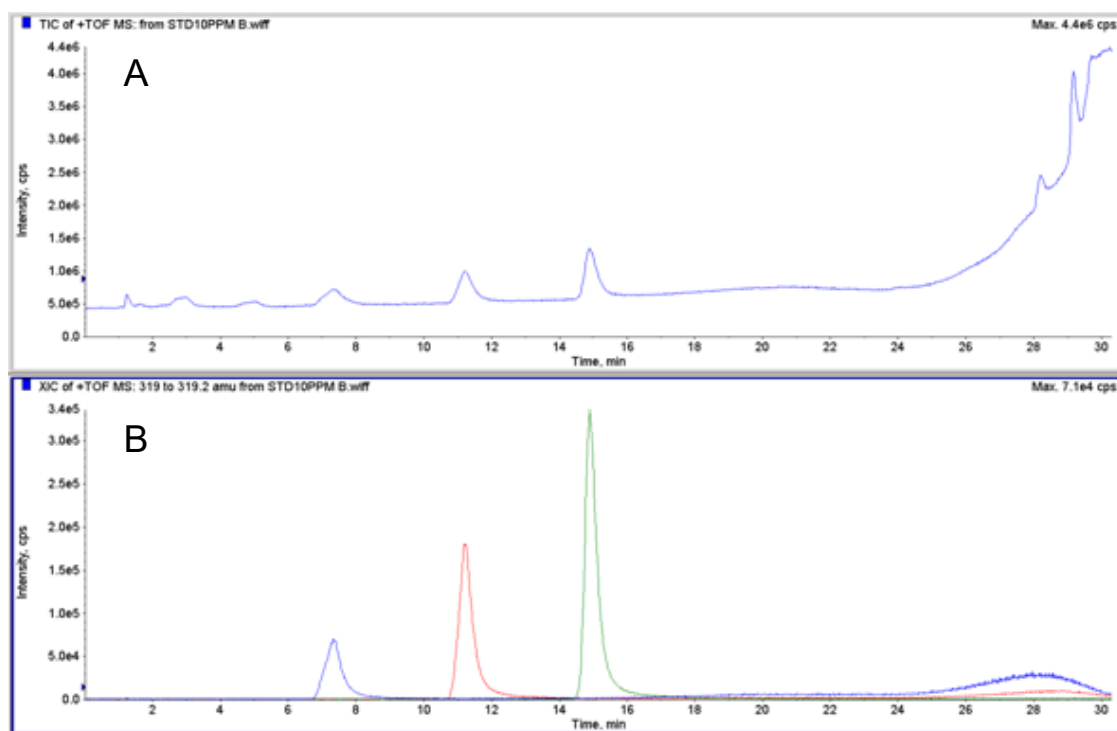


Figure F-1 . A. Chromatogram of total ions and extracted ions of flavonoids standards for mass spectra analysis.

In Figures F-2A, F-2B and F-2C it is detailed the mass spectra for myricetin, quercetin and kaempferol respectively indicating the abundant fragment ions along with its corresponding structure. In Figure F-2A The parent ion of myricetin is detected with a m/z ratio of 319.0378 [C₁₅H₁₀O₈]. In Figure F-2B the parent ion of quercetin is identified with a m/z ratio of 303.0451 [C₁₅H₉O₇]. In Figure F-2C the parent ion of kaempferol is identified with a m/z ratio 287.0506 [C₁₅H₈O₆]. These abundant fragments were taken as the reference to identify the presence of myricetin, quercetin and kaempferol in the samples tested.

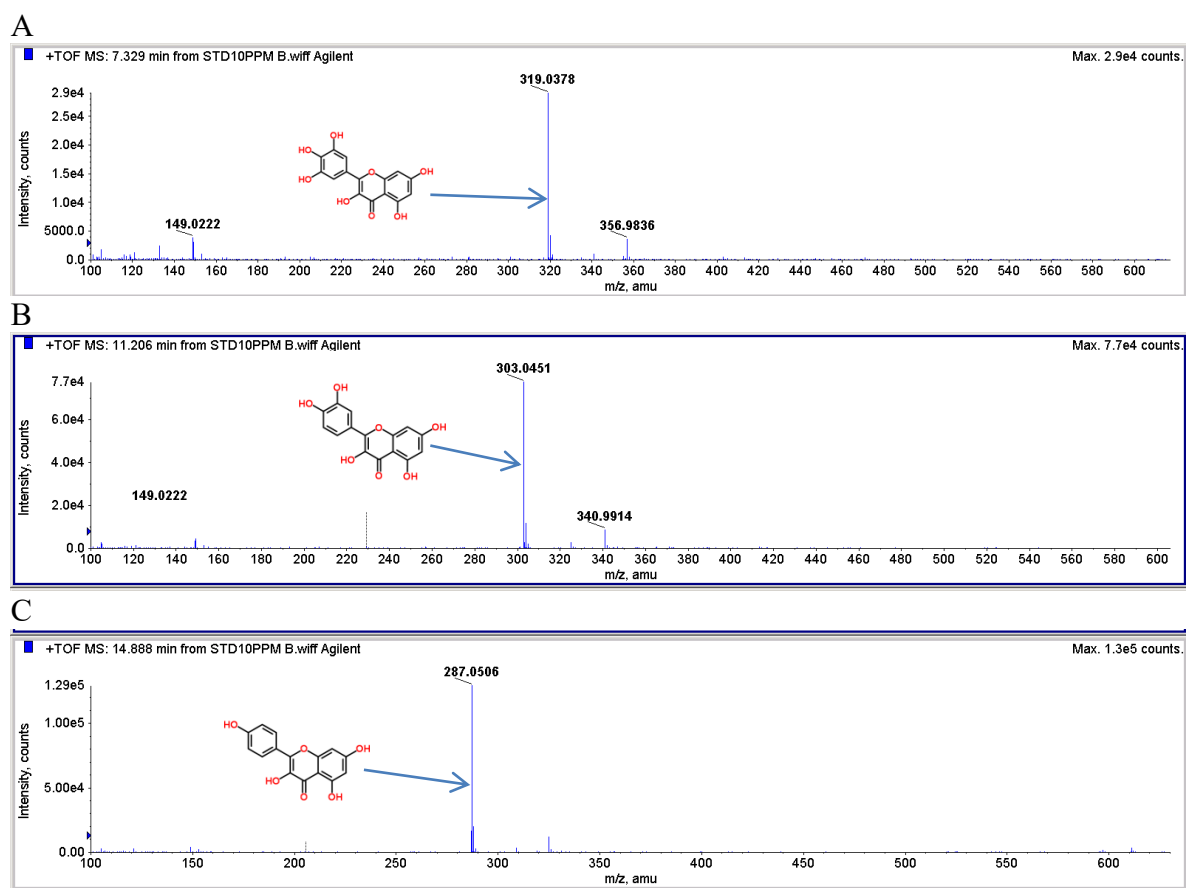
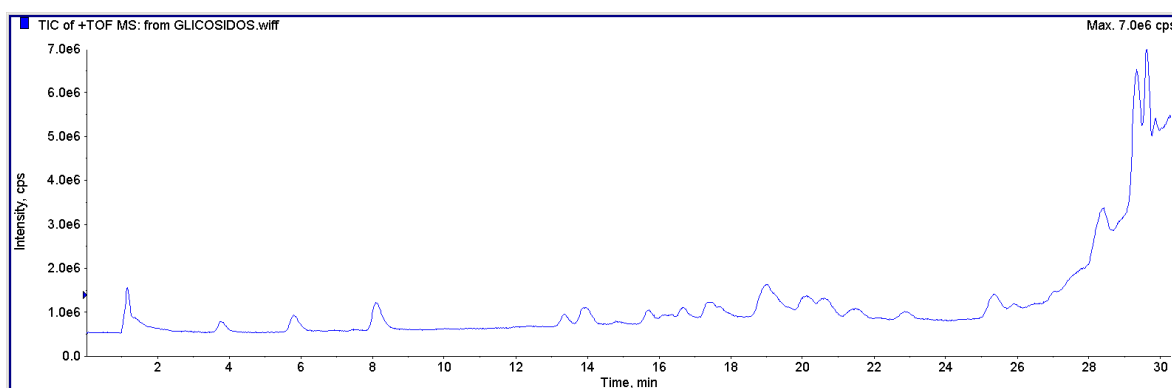


Figure F-2. Mass spectra analysis of myricetin, quercetin and kaempferol standards.

GLYCOSYLATED FLAVONOIDS DETECTION

In Figure F-3A it is detailed the total ions chromatogram of glycosylated flavonoids from FF. The Figure F-3B depicts the chromatogram of the extracted ions of glycosylated myricetin, quercetin and kaempferol. These ions were extracted at the following respective ranges of mass (319.0, 319.2), (303.0, 303.2), (287.0, 287.2). The mass spectra of the glycosylated flavonoids extracted from these chromatograms are shown in Figure 3-19.

A



B

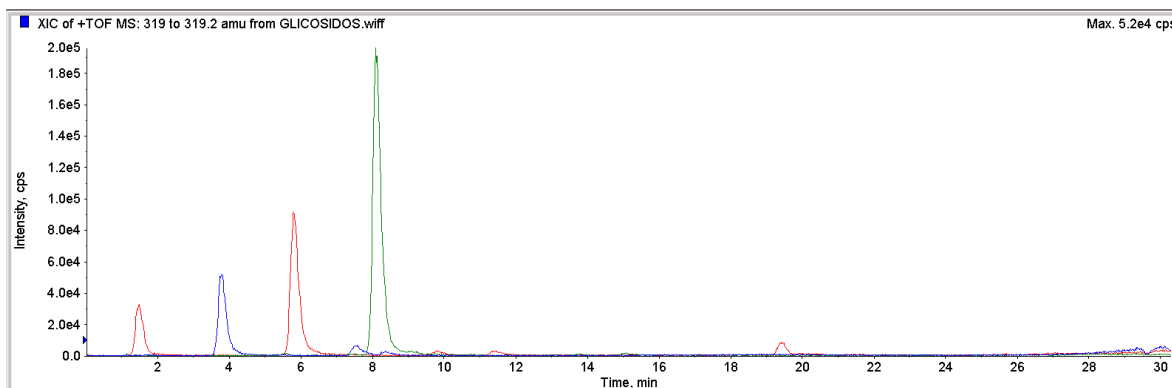


Figure F-3 . Chromatogram of total ions and extracted ions of flavonoid fraction for mass spectra analysis.

In Figures F-4A, F-4B and F-4C it is detailed the mass spectra for glycosylated flavonoids respectively indicating the abundant fragment ions along with its corresponding structure. It is also presented that the presence of the flavonoids can be identified in two forms, as glycoside flavonoid (parent ion) or as aglycone which is the result of ion fragmentation caused by the voltage of ionization.

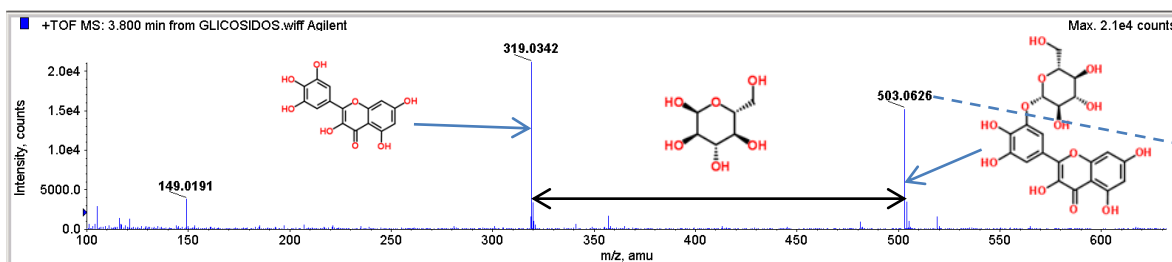
Figure F-4A details the parent ion identified for myricetin-3-glucoside with a m/z ratio of 503.06 [$C_{21}H_{22}O_{14}$] generated at 3.8 min. The base peak is identified as myricetin aglycone with m/z ratio of 319.04 [$C_{15}H_{10}O_8$]. This is the result of the lost of the glycoside due to fragmentation of the parent ion.

Figure F-4B details the parent ion identified for quercetin-3-glucoside with a m/z ratio of 487.07 [$C_{21}H_{21}O_{13}$] generated at 5.827 min. The base peak is identified as quercetin aglycone with a m/z ratio of 303.0425 [$C_{15}H_{10}O_8$]. This is the result of the loss of the glycoside due to fragmentation of the parent ion.

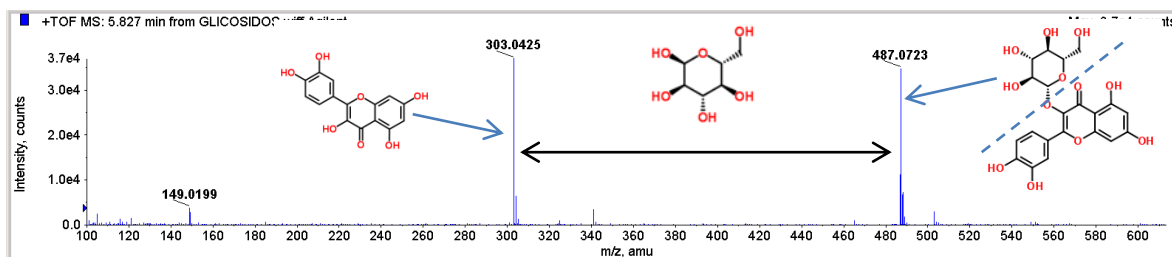
Figure F-4C details the parent ion identified for kaempferol-3-glucoside with a m/z ratio of 471.07 [$C_{21}H_{20}O_{12}$] generated at 8.086 min. The base peak is identified as kaempferol aglycone with a m/z ratio of 287.04 [$C_{15}H_{10}O_8$]. This is the result of the loss of the glycoside due to fragmentation of the parent ion.

These abundant fragments were taken as the reference to identify the presence of glycosylated myricetin, quercetin and kaempferol in the samples tested.

A



B



C

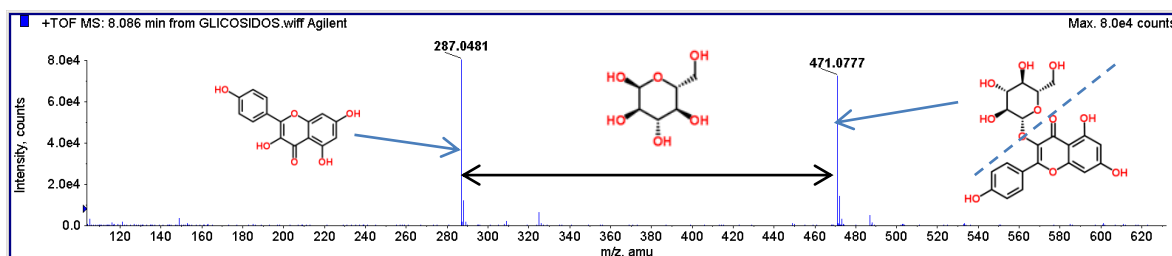


Figure F-4 . Mass spectra analysis of glycosylated myricetin, quercetin and kaempferol.

G. APPENDIX G

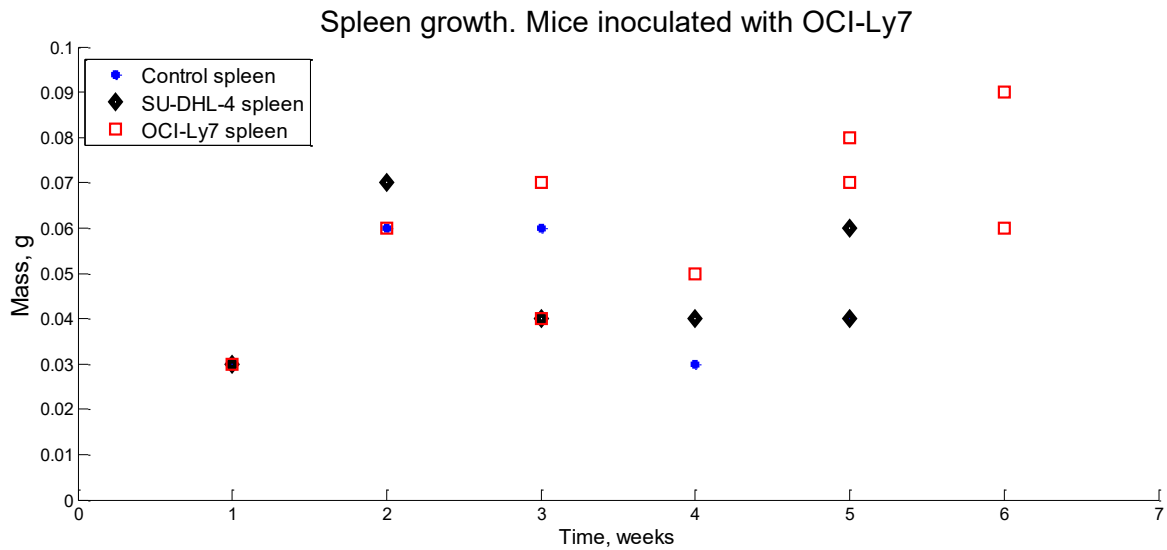


Figure G-1. Comparison of spleen mass of mice inoculated with OCI-Ly7 (squares), mice inoculated with SU-DHL-4 (rhombus) and mice not inoculated (dots).

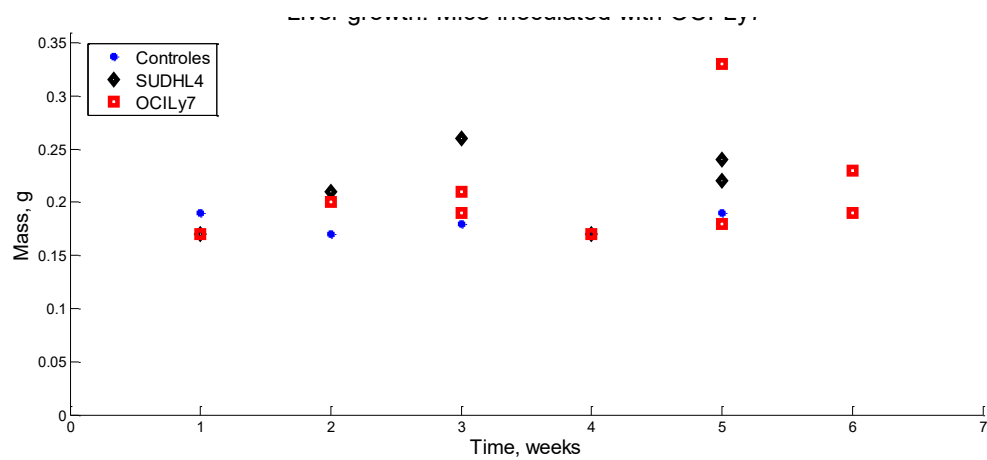


Figure G-2. Comparison of liver mass of mice inoculated with OCI-Ly7 (squares), mice inoculated with SU-DHL-4 (rhombus) and mice not inoculated (dots).

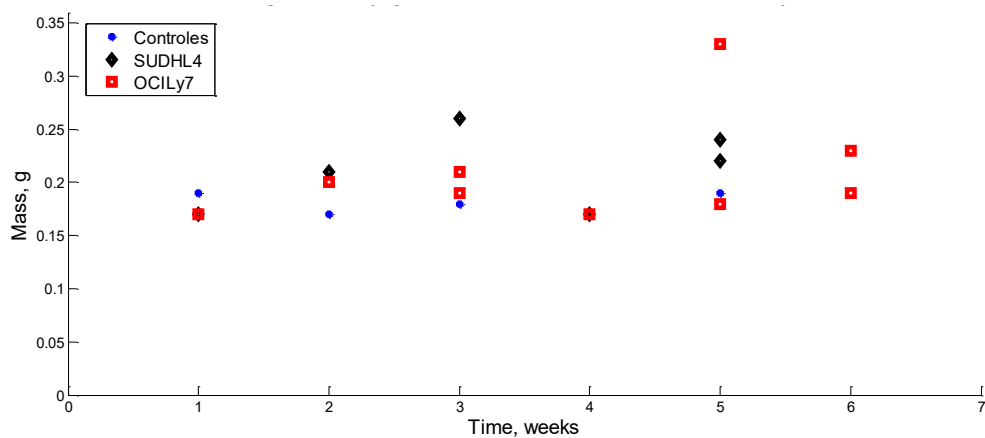


Figure G-3. . Comparison of right kidney mass of mice inoculated with OCI-Ly7 (squares), mice inoculated with SU-DHL-4 (rhombus) and mice not inoculated (dots).

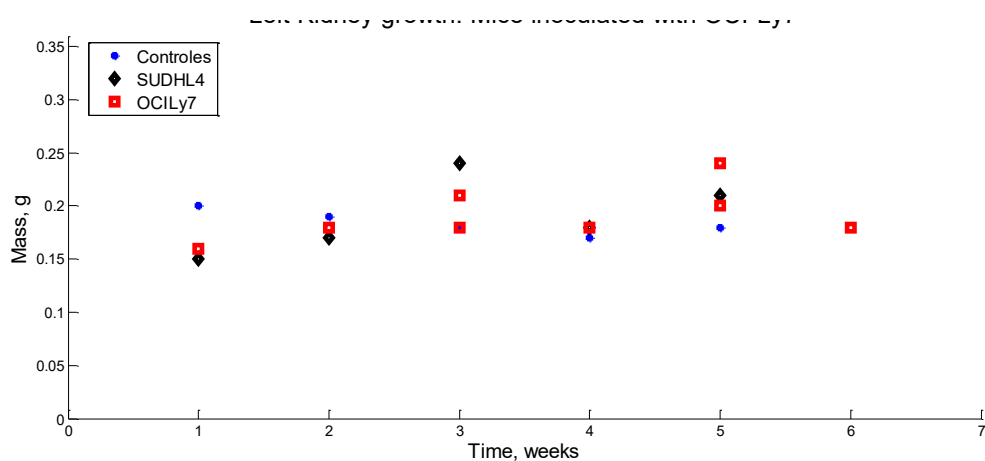


Figure G-4. Comparison of left kidney mass of mice inoculated with OCI-Ly7 (squares), mice inoculated with SU-DHL-4 (rhombus) and mice not inoculated (dots).